

# Correlation Improves Group Testing: Capturing the Dilution Effect

Jiayue Wan\*

School of Operations Research & Information Engineering, Cornell University, NY 14850, jw2529@cornell.edu

Yujia Zhang\*

Center for Applied Mathematics, Cornell University, NY 14850, yz685@cornell.edu

Peter I. Frazier

School of Operations Research & Information Engineering, Cornell University, NY 14850, pf98@cornell.edu

Population-wide screening to identify and isolate infectious individuals is a powerful tool for controlling COVID-19 and other infectious diseases. Group testing can enable such screening despite limited testing resources. Samples' viral loads are often positively correlated, either because prevalence and sample collection are both correlated with geography, or through intentional enhancement, e.g., by pooling samples from people in similar risk groups. Such correlation is known to improve test efficiency in mathematical models with fixed sensitivity. In reality, however, dilution degrades a pooled test's sensitivity by an amount that varies with the number of positives in the pool. In the presence of this dilution effect, we study the impact of correlation on the most widely-used group testing procedure, the Dorfman procedure. We show that correlation's effects are significantly altered by the dilution effect. We prove that under a general correlation structure, pooling correlated samples together (*correlated pooling*) achieves higher sensitivity but can degrade test efficiency compared to independently pooling the samples (*naive pooling*) using the same pool size. We identify an alternative measure of test resource usage, the number of positives found per test consumed, which we argue is better aligned with infection control, and show that correlated pooling outperforms naive pooling on this measure. We build a realistic agent-based simulation to contextualize our theoretical results within an epidemic control framework. We argue that the dilution effect makes it even more important for policy-makers evaluating group testing protocols for large-scale screening to incorporate naturally arising correlation and to intentionally maximize correlation.

*Key words:* COVID-19, group testing, pooled testing, infection control, screening, polymerase chain reaction (PCR)

---

## 1. Introduction

The SARS-CoV-2 virus has killed over 6 million people while causing enormous economic losses. Large-scale screening using polymerase chain reaction (PCR) tests can curb the virus's spread (Mercer and Salit 2021, Xing et al. 2020, Barak et al. 2021) through promptly identifying and isolating infected individuals and their contacts (Cleary et al. 2021, Brault et al. 2021), but it requires a massive amount of chemical reagent and access to many diagnostic testing machines.

\* Equal contribution.

A promising solution is *group testing*. The *Dorfman procedure*, the first group testing protocol proposed in 1943 to screen enlisted soldiers for syphilis (Dorfman 1943), pools multiple samples and tests each pool using a single test. Especially in low-prevalence settings, group testing can save significant test resources compared to individual testing (Kim et al. 2007).

Group testing has proven effective in large-scale community screening worldwide and in controlling the spread of SARS-CoV-2. In May 2020, Wuhan screened nine million people over ten days using pooled testing (Fan 2020). In fall 2020, Cornell University safely reopened its campus by testing 5-7K Cornell students and employees daily in pools of five (Lefkowitz 2020).

Mathematical analysis of group testing’s improved resource utilization has largely assumed independence of pooled samples’ infection status (e.g., Kim et al. 2007, Westreich et al. 2008). Recently, however, several researchers (Barak et al. 2021, Basso et al. 2021, Augenblick et al. 2020, Lin et al. 2020, Comess et al. 2021) have observed that human behavior and the logistics of sample collection naturally lead to correlations. Specifically, when one person is infected, it is more likely that others in their immediate social circles are also infected (Vang et al. 2021, Rader et al. 2020, Lan et al. 2020). Infections transmitted within households, schools, and neighborhoods cause correlation within pools formed from samples collected at the same testing center (Barak et al. 2021).

This literature observes that correlation can significantly affect the performance of pooled testing. Correlation tends to reduce the number of pools with virus-containing samples, which finds support in simulation studies (Lendle et al. 2012, Deckert et al. 2020). Aprahamian et al. (2019) and McMahan et al. (2012a) observe that correlation can be enhanced by pooling people with similar covariates or in similar risk groups together. Mathematical analyses show that when tests are error-free, this causes *test efficiency* (the number of people screened per test) to improve (Augenblick et al. 2020, Lin et al. 2020). This remains true when tests have errors and the *test sensitivity* (the probability that testing a positive sample provides a correct result) is fixed (Basso et al. 2021, Aprahamian et al. 2019, Bilder et al. 2010, Bilder and Tebbs 2012, McMahan et al. 2012a,b).

However, these mathematical analyses of correlation’s effect on pooled testing ignore an important practical aspect of pooled testing: the *dilution effect*. When positive samples are mixed with negatives, the concentration of virus particles (called the *viral load*) in the positive sample is diluted, reducing sensitivity (Wein and Zenios 1996). Analysis of pooled testing assuming samples with independent viral loads (e.g., Kim et al. 2007, Westreich et al. 2008) has found the dilution effect to be critical in understanding the performance of pooled testing, determining optimal pool sizes, and deciding when to employ it over ordinary individual testing. This work has clarified that designing a pooled testing strategy requires consideration of the sensitivity of the test, which may necessitate decreasing the pool size to control the dilution effect.

In this work, we argue that the presence of the dilution effect radically alters the way in which correlation impacts pooled testing. Because correlation tends to increase the number of positive samples in pools with at least one positive sample, it increases the chance that such pools test positive, increasing overall procedure sensitivity. This claimed increase in sensitivity is consistent with a recent experimental study, Barak et al. (2021), which finds that the sensitivity of group testing performed in Israel was higher than independent sampling would suggest. This increase in sensitivity can *decrease* test efficiency, counteracting the increase in test efficiency created by fewer pools with positive samples. We show that correlation can decrease test efficiency overall. Neither effect is present in models without the dilution effect considered in Basso et al. (2021), Augenblick et al. (2020), Lin et al. (2020), Aprahamian et al. (2019).

We support these arguments with theoretical analysis providing significant insight. We prove that, under a general correlation structure in the population and other mild assumptions, pooling correlated samples together (called *correlated pooling*) in the Dorfman procedure yields higher sensitivity compared to independently pooling the samples (called *naive pooling*) with the same pool size. Additionally, we construct a novel metric, the *effective efficiency*, defined as the number of positive cases identified per test consumed. We argue that effective efficiency better captures a procedure’s effectiveness for screening than efficiency, the conventional metric studied in literature, and prove that correlated pooling achieves higher effective efficiency under mild assumptions. We further present an example where correlated pooling has strictly *lower* efficiency than naive pooling, contradicting the prevailing theoretical results in the literature on efficiency (Augenblick et al. 2020, Lin et al. 2020, Basso et al. 2021).

These insights have significant implications for policy-makers, demonstrated in a realistic agent-based simulation. Our simulation models the correlation in viral loads arising naturally from the community and household interactions, which induces correlation within pools. We adopt the perspective of a policy-maker utilizing our simulation to assess various screening policies, including screening frequencies and pool sizes, in response to an emerging pandemic. We draw two primary conclusions. First, policy-makers should incorporate correlation in their modeling effort when choosing a policy that fully utilizes the test capacity. Failure to do so, as in the case of naive pooling, would underestimate screening policies’ true effectiveness and lead to overly cautious policy decisions. Second, enhancing correlation within pools can substantially improve epidemic outcomes. We recommend that policy-makers implement explicit measures to promote household pooling, such as encouraging families or roommates to get tested together and mailing sample collection kits to households (Stanford Medicine 2020).

In an example scenario with a 100-day test supply of  $4 \times 10^4$  for a population of 10,000, a correlation-oblivious policy-maker would deem screening impractical and impose a lockdown. A

correlation-aware policy-maker who does not take further measures to pool households together would opt for screening every five days with pool size 10, incurring 3.2K infections on average. Notably, a policy-maker enhancing correlation by pooling households together would choose to screen every four days with pool size 10, incurring 2.5K infections on average, a 22% reduction compared to one that does not pool households together.

Our work follows one other study with theoretical analysis of a model with correlated pooling in the presence of the dilution effect, Comess et al. (2021). The majority of this study is simulation-based and is consistent with our more general theoretical findings. Their theoretical analysis studies the joint effect of increasing correlation and prevalence on test sensitivity. They find that the combined effect of these two changes increases sensitivity, but does not elucidate whether the effect is due to correlation, increased prevalence, or both.

To summarize, our contributions in this paper are:

- We establish an analytical framework for modeling pooling methods in large populations, formulating a model of correlation in pools derived from an asymptotic analysis of a more general population-level model of infection spread and pool formation.
- We propose a novel metric for test usage called effective efficiency, defined as the number of positives identified per test consumed, and demonstrate its significance in capturing a procedure’s effectiveness for screening in epidemic control.
- We prove that under the general model and other mild assumptions, using correlated pooling in the Dorfman procedure achieves higher sensitivity and effective efficiency than naive pooling. Our work is the first to study sensitivity or efficiency theoretically under a general correlation model in the presence of the dilution effect.

The rest of this paper is organized as follows: Section 2 reviews related work in more detail. Section 3 formulates the model of correlation in pools derived from an asymptotic analysis of a more general population-level model and proves our main theoretical results. Section 4 performs a case study highlighting the importance of correlation for policy-making. Section 5 concludes the paper and discusses future research.

## 2. Related Work

### 2.1. Group Testing and the Dilution Effect

Group testing was proposed by Dorfman (1943) to screen enlisted soldiers for syphilis during World War II. The Dorfman procedure combines multiple samples together and tests the pooled samples, so that samples in a pool testing negative are cleared and samples in a pool testing positive are tested individually for identification. This significantly increases efficiency by screening multiple individuals with a single test. Since then, many generalizations of the Dorfman procedure have

been developed and studied theoretically. Group testing is also widely applied in the surveillance and control of infectious diseases. For a review of recent theory and applications, see Kim et al. (2007) and Aprahamian et al. (2019).

The COVID-19 pandemic has raised further interests in applying group testing to infection control and population-wide surveillance (Mercer and Salit 2021). Multiple studies have used modeling and simulation to explore the value that group testing offers in scaling up testing, such as Cleary et al. (2021), Brault et al. (2021), Pilcher et al. (2020), Eberhardt et al. (2020), and Mutesa et al. (2020). A thorough review of the literature in using group testing for COVID-19 mitigation is provided by Yu et al. (2021).

Despite the extent to which group testing can increase testing capacity, it may have a negative impact on sensitivity. First, the inherent error rate of individual assays, along with the design of the pooling protocol, may lead to failure to detect some positive samples (Graff and Roeloffs 1972, Kim et al. 2007, Westreich et al. 2008). Moreover, sensitivity may decrease due to the dilution effect, that is, a pool dominated by negative samples may test negative, causing its positive members to be missed. The dilution effect was first modeled by Hwang (1976) and subsequently explored by Wein and Zenios (1996), Zenios and Wein (1998), Weusten et al. (2002), Nguyen et al. (2019) for HIV detection and by Hung and Swallow (1999) for prevalence estimation.

Many studies have assessed the dilution effect in SARS-CoV-2 tests from both mathematical and empirical perspectives. Pilcher et al. (2020) assumes a temporal viral load progression in infected individuals, which, together with the detection limit of PCR tests, defines a “window of detection”; under this setting, pooling is equivalent to raising the detection limit of the test and shortening the effective window of detection. Brault et al. (2021) proposes a similar quantification of decrease in sensitivity due to dilution based on a mathematical model for PCR. Some experimental studies (Yelin et al. 2020, Lohse et al. 2020) evidence that pooling up to around 30 samples does not result in a loss of sensitivity, while Bateman et al. (2020) observes an increasing deterioration of sensitivity in pooling 5, 10, and 50 samples.

## 2.2. Correlation in Group Testing

Most of the aforementioned literature assumes that the infection statuses of the samples within a pool, whether binary or not, are independent from each other. However, as we described in the introduction, correlation between samples is often present in reality and can potentially be leveraged for our advantage to combat the dilution effect.

One important cause of correlation is transmission within households. The *secondary attack rate* (SAR), i.e., the probability that an infectious person in a household infects another given household member, is significant for many infectious diseases (Carcione et al. 2011, Whalen et al.

2011, Odaira et al. 2009, Meningococcal Disease Surveillance Group 1976, Glynn et al. 2018). For SARS-CoV-2, a meta-analysis (Madewell et al. 2020) of 40 studies finds an average SAR of 16.6% and a 95% confidence interval of 14.0%-19.3%. Beyond household transmission, correlation in infection statuses among members of the same social group has also been observed among college students belonging to the same fraternity or sorority (Vang et al. 2021), people living in the same neighborhood (Rader et al. 2020), and co-workers (Lan et al. 2020).

Relatively little research explores group testing of correlated samples. Barak et al. (2021), a large-scale observational study, observes that individuals in the same social groups are often pooled together in large-scale screening. It discovers that samples with low viral load, each of which would have likely been missed if it were the only positive sample in the pool, were detected when pooled with high-viral-load samples. This led to higher sensitivity than would have occurred with pools containing independently infected samples. Bilder et al. (2010), Bilder and Tebbs (2012), McMahan et al. (2012a,b) study group testing on samples with similar covariates and derive methods to maximize the number of samples screened per test while pooling samples with similar covariates together. Aprahamian et al. (2019) designs an algorithm to place individuals into pools according to their risk. Augenblick et al. (2020) uses a simple example with pairwise correlation and perfect test accuracy to illustrate reduced test consumption in the Dorfman procedure. Lendle et al. (2012) uses simulations to show that correlation improve the efficiency of hierarchical and matrix-based group testing. Deckert et al. (2020) uses simulation to show that pooling individuals with similar prevalence levels reduces costs. Building on these observations, Lin et al. (2020) models sample collection at a testing site as a regenerative process and calculates the cost efficiency of different testing protocols, while assuming perfect test accuracy. Basso et al. (2021) models a constant pairwise correlation in infections using a Beta-Binomial distribution for the number of positives in a pool, and demonstrates that this correlation improves efficiency. These papers do not study the effect of correlation on sensitivity: they either assume perfect test accuracy or a fixed test sensitivity.

The closest paper in the literature to ours is Comess et al. (2021), which is qualitatively motivated by similar considerations but makes theoretical contributions that are different in nature. There are two major distinctions between our work and Comess et al. (2021).

First, Comess et al. (2021) considers a specific model of correlation in which all participants in a pool are close contacts of each other and infections are acquired in a community infection stage followed by homogeneous secondary infections within the pool. As a result, the prevalence in the correlated pool is *higher* than that in a naive pool (which only assumes community infection). Hence, the model in Comess et al. (2021) is best suited to understanding the joint effect of increasing secondary transmission while pooling related samples together. We argue, however, that the

choice of pooling strategy should be based on a comparison of their properties while holding the population’s prevalence steady. This is the approach we take in our paper.

Second, Comess et al. (2021) theoretically studies a different but related metric of test consumption. A theoretical result therein (Observation 5) defines an efficiency metric that assumes 100% sensitivity of the pooled test and shows that the metric is identical for both pooling methods. This metric, though theoretically tractable, does not fully capture the difference in test consumption in practice, as is reported in their simulation results. Nevertheless, much of the intuition described in Comess et al. (2021) is consistent with our results. In particular, Observation 5 claims that the sensitivity is no worse under correlated pooling than under naive pooling. We prove a similar result in our Theorem 1. In addition, the simulated efficiencies in Figures 6 and 8 of Comess et al. (2021), though not discussed by the authors, indicate that correlated pooling can have lower efficiency than naive pooling, which we demonstrate is possible in Section 3.6.

Beyond viral testing, group testing with correlation has been studied in the signal processing community. For example, graph structures may induce correlation among nodes and edges (Ganesan et al. 2017) or impose constraints on pool formulation (Cheraghchi et al. 2012).

### 3. Theoretical Results

As outlined in Section 1, despite the recognized significance of correlation in analyzing group testing methods in literature, our current theoretical understanding remains limited. Specifically, the existing literature ignores a crucial factor, the dilution effect, when assessing the impact of correlation on pooled testing, thereby yielding inaccurate conclusions. In this section, we aim to bridge this critical knowledge gap by studying how correlation impacts pooled testing in the presence of the dilution effect. We focus on two central metrics, *sensitivity* and *effective efficiency*, which are crucial for evaluating the efficacy of pooling methods. We argue that effective efficiency, a novel metric we introduce, better captures a procedure’s effectiveness for screening compared to the ordinary efficiency metric studied in literature.

#### 3.1. Model Setup

We consider using pooled testing to test a large population of  $N$  individuals whose viral loads are described by random variables  $\{U_i : i = 1, \dots, N\}$ .<sup>1</sup> “Infected” individuals  $i$  are those with  $U_i > 0$ .

We consider the Dorfman procedure, in which samples are placed into non-overlapping, uniformly-sized pools. In the first stage of the Dorfman procedure, each pool is tested. In the second stage, samples from pools testing positive in the first stage are tested individually. A positive sample is correctly declared positive if and only if its pool tests positive *and* it tests positive in the followup

<sup>1</sup>To support arbitrarily large  $N$ , the random variable  $U_i$  is defined for all natural numbers  $i$  and is identically 0 under  $P_{\text{POOL}}^{(N)}$  for  $i > N$ , where POOL is NP or CP.

test. We model the assignments of individuals to pools for testing by  $\mathcal{A} := \{A_j : j = 1, \dots, N/n\}$ , a partition of  $\{1, \dots, N\}$  into  $N/n$  groups of size  $n$ .

We consider  $A_j$  to be a random partition whose distribution depends on the pooling method used. Specifically, under *naive pooling* (NP), each pool is formed by picking  $n$  individuals uniformly at random from the population without replacement. This is not a realistic model for how pooling is done in practice, but we introduce it because it is how pooling is studied in the academic literature. *Correlated pooling* (CP) is a general and more realistic structure that occurs naturally (e.g., because samples are collected from people who live in the same household or neighborhood and are tested together) and can be enhanced by explicit measures. To support analysis of the Dorfman procedure, which depends on the viral loads in one pool, we let  $(V_{j,i} : i = 1, \dots, n) = (U_i : i \in A_j) = U_{A_j}$  indicate the viral loads in pool  $j$ . For both correlated and naive pooling, once the pools are formed, we reorder the samples in each pool by applying independent random permutations of 1 through  $n$ . This simplifies analysis.

To support varying the population size  $N$  and the pooling method, we define a collection of probability measures,<sup>2</sup>  $\mathbb{P}_{\text{NP},\alpha}^{(N)}$  and  $\mathbb{P}_{\text{CP},\alpha}^{(N)}$ , for each pooling method and population size  $N \in \mathbb{N}$ . Let  $\mathbb{E}_{\text{NP},\alpha}^{(N)}[\cdot]$  and  $\mathbb{E}_{\text{CP},\alpha}^{(N)}[\cdot]$  denote the expectations taken under  $\mathbb{P}_{\text{NP},\alpha}^{(N)}$  and  $\mathbb{P}_{\text{CP},\alpha}^{(N)}$ , respectively. We let  $\text{POOL}$  indicate a generic pooling method. Under  $\mathbb{P}_{\text{POOL},\alpha}^{(N)}$ , the expectation of  $\frac{1}{N} \sum_{i=1}^N 1\{U_i > 0\}$  is  $\alpha$  and so  $\alpha$  indicates the prevalence, i.e. the probability that a person chosen uniformly at random has a positive viral load.

*Test outcomes:* We first model the result of a single test. Given an input sample with viral load  $v$ , we assume a test returns a positive result with probability  $p(v) : \mathbb{R}_{\geq 0} \rightarrow [0, 1]$  and a negative result with probability  $1 - p(v)$ . We refer to  $p(v)$  as the *test sensitivity function*. Here we assume  $p(0) = 0$ , i.e., no false positives; later in Appendix F.4.2, we argue that a small individual test false positive rate (FPR), e.g., 0.01% (Public Health Ontario 2020), implies an FPR of correlated pooling low enough for its deployment in repeated large-scale screening. We further assume that  $p(v) > 0$  for  $v > 0$ ,  $p$  is monotone increasing in  $v$ , and that the result of a test, whether individual or pooled, when given its viral load, is conditionally independent from any other test.

We assume a dilution factor equal to the pool size in pooled tests. Consequently, a pooled test with viral loads  $v_1, \dots, v_n$  yields a positive result with probability  $p(\bar{v}_n)$  where  $\bar{v}_n = \frac{1}{n} \sum_{i=1}^n v_i$ . Let  $Y_j = \text{Ber}\left(p\left(\frac{1}{n} \sum_{i=1}^n V_{j,i}\right)\right)$  denote the outcome of the pooled test of pool  $j$  in the first stage. Let  $W_{j,i} = \text{Ber}(p(V_{j,i}))$  denote what the outcome of the individual test for sample  $i$  with viral load  $V_{j,i}$  will be, if it is performed. Let  $S_j = \sum_{i=1}^n 1\{V_{j,i} > 0\}$  denote the number of infected individuals

<sup>2</sup>From a measure theoretic perspective, the random quantities  $\mathcal{A}$ ,  $U_i$ , and others defined below are (measurable) mappings from the event space to the outcome space. The mappings themselves do not depend on  $N$ , but the distributions of these random quantities under  $\mathbb{P}_{\text{POOL},\alpha}^{(N)}$  do because the measure  $\mathbb{P}_{\text{POOL},\alpha}^{(N)}$  itself depends on  $N$ .



and  $D_j = \sum_{i=1}^n Y_j W_{j,i}$  the number of positives identified in pool  $j$ . The conditional independence assumption stated above implies that the pooled and individual tests are conditionally independent given the viral loads of the participating samples.

*Population-level outcomes:* We define three population level averages of pooled outcomes:  $\bar{S} = \frac{1}{|\mathcal{A}|} \sum_{j=1}^{|\mathcal{A}|} S_j$  and  $\bar{D} = \frac{1}{|\mathcal{A}|} \sum_{j=1}^{|\mathcal{A}|} D_j$ , which are the average number of infected individuals present and detected per pool; and  $\bar{Y} = \frac{1}{|\mathcal{A}|} \sum_{j=1}^{|\mathcal{A}|} Y_j$ , which is the fraction of pools testing positive.

### 3.2. Metrics of Interest

We will study two metrics, *sensitivity* and *effective efficiency*, characterizing the performance of a pooling method on a population. They are central to summarizing a pooling method's utility for controlling the spread of infections.

DEFINITION 1 (SENSITIVITY). Let  $\beta$  denote the *overall false negative rate*, or the fraction of positive samples falsely declared negative under the Dorfman procedure. That is,  $\beta = 1 - \frac{\bar{D}}{\bar{S}}$ . Sensitivity is defined as  $1 - \beta$ .

DEFINITION 2 (EFFECTIVE EFFICIENCY). Let  $\gamma$  denote the expected number of positive cases identified per test consumed (including pooled and followup tests). That is,  $\gamma = \frac{\bar{D}}{1 + n\bar{Y}}$ .

Our effective efficiency metric is novel. We offer it as an alternative to the efficiency metric used in the literature to study test consumption.

To see the significance of the metrics described above, consider problem settings such as the ones we study in Section 4 and Appendix F.6, where we select a large-scale screening strategy in a population with large  $N$ . The ability of a testing method to control infections is largely determined by the rate at which it can identify positive individuals in a population and reduce the number of positives missed in screening: when an infected individual is identified, he/she can be isolated, preventing them from infecting other individuals and reducing the number of future infections.

Suppose we have a budget  $bN$  ( $b > 0$ ) for the number of tests available that scales with the population size  $N$ . When  $b$  is large, the rate at which we can test a person is constrained by factors other than the testing budget. Thus, the number of positives found is determined by the sensitivity. When  $b$  is smaller, the rate at which we can test a person is proportional to the testing budget. Therefore, the number of positives found is determined by the product of testing budget and the effective efficiency. We include a more in-depth discussion of these metrics and the ordinary efficiency metric in Section 3.6.

We will show in Section 3.5 that correlated pooling always achieves higher sensitivity and, under a mild condition, has a higher effective efficiency. We illustrate these findings in the context of a realistic epidemic simulation in Section 4.

### 3.3. From Population-Level Model to Single-Pool Model

To support tractable analysis of these metrics, we introduce an analytical framework for modeling pooling strategies in large populations. This framework can be adapted for assessing various test procedures, including but not limited to the Dorfman procedure. We focus on the limit as the population size  $N$  becomes large, enabling us to characterize the population-level outcomes using a more straightforward, simpler-to-analyze *single-pool model*.

The key idea in this analysis is to let  $J$  be a pool chosen uniformly at random from  $\{1, \dots, N/n\}$ . We then define quantities for this single pool that are analogous to the population-level quantities: let  $V_i = V_{J,i}, i = 1, \dots, n$ ;  $S = S_J$ ;  $W_i = W_{J,i}, i = 1, \dots, n$ ;  $Y = Y_J$ ;  $D = D_J$ .

Let  $\mathbb{P}_{\text{POOL},\alpha}$  be the limiting joint distribution of the single-pool quantities  $(V_i : i = 1, \dots, n)$ ,  $S$ ,  $(W_i : i = 1, \dots, n)$ ,  $Y$ , and  $D$  as  $N \rightarrow \infty$ . Such convergence is consistent with the idea that adding one more person to the population should not radically change what happens to a single pool chosen at random from all pools. We refer to this as the *single-pool model*.

We show that with mild assumptions (described in Appendix A.1), the population-level quantities  $(\bar{D}, \bar{S}, \text{ and } \bar{Y})$  converge to constants as  $N \rightarrow \infty$ . The assumption required is phrased in terms of a measure of association between two pools — how much the viral loads in one pool change the expectation of another pool’s test outcomes. Assumption EC.1 assumes that given the sample viral loads in one pool, the number of pool-level quantities with association exceeding a certain threshold exhibit sub-linear scaling relative to the population size.

It follows that as  $N \rightarrow \infty$ , the metrics of interest outlined in Section 3.2 converge in probability to their corresponding single-pool values, as guaranteed by the continuous mapping theorem.

**PROPOSITION 1.** *The metrics  $\beta$  and  $\gamma$  converge in probability to their corresponding single-pool values, i.e.,  $1 - \frac{\mathbb{E}_{\text{POOL},\alpha}[D]}{\mathbb{E}_{\text{POOL},\alpha}[S]}, \frac{\mathbb{E}_{\text{POOL},\alpha}[D]}{1+n\mathbb{E}_{\text{POOL},\alpha}[Y]}$  (denoted  $\beta_{\text{POOL},\alpha}$  and  $\gamma_{\text{POOL},\alpha}$  thereafter), respectively, as  $N \rightarrow \infty$ , for  $\alpha > 0$  and  $\text{POOL} \in \{\text{NP}, \text{CP}\}$ .*

Proposition 1 justifies the analysis of metrics within the single-pool model because they characterize the asymptotic behavior of the population-level metrics of interest.

### 3.4. Properties of the Single-Pool Model

Having justified the use of a single pool selected uniformly at random (i.e., pool  $J$ ) for analyzing the asymptotic performance of a pooling method, we proceed to examine the single-pool values corresponding to the population-level metrics of interest, under probability measure  $\mathbb{P}_{\text{POOL},\alpha}$ , for  $\text{POOL} \in \{\text{NP}, \text{CP}\}$ .

To achieve this, it is essential to understand the fundamental distinction between naive and correlated pooling. In this section, we introduce Propositions 2 and 3, both of which collectively highlight the primary feature differentiating the two pooling methods: as prevalence approaches zero, the

probability that a positive-containing pool contains more than one positive sample diminishes for a randomly selected naive pool (Proposition 2) but persists for a correlated pool (Proposition 3).

Under naive pooling, pools are created by selecting  $n$  individuals uniformly at random without replacement. This pooling method intuitively results in decreasing correlation within pool  $J$  as  $N$  approaches infinity. Indeed, we show that under a mild assumption (Assumption EC.2), samples in pool  $J$  are independent, consistent with the conventional assumption commonly made in pooled testing analyses. Analogous to Assumption EC.1, Assumption EC.2 assumes that for any subset of a pool, the number of individuals in the remaining population with association stronger than some threshold scales sublinearly in population size. This independence result we show aligns with what a policy-maker would assume for a finite population if they do not account for correlation.

**PROPOSITION 2.** *Under Assumption EC.2, the viral loads in pool  $J$  are independent under  $\mathbb{P}_{NP,\alpha}$ .*

Unlike in naive pooling, samples within the correlated pool are expected to display distinct behavior due to their inherent correlation. To quantify such behavior, we characterize the correlation between viral loads in a correlated pool based on the notion of “close contacts”. Specifically, we assume that infected individuals and their close contacts are correlated in infection statuses and are likely to be placed into the same pool under correlated pooling. These assumptions are formalized mathematically in Assumption 1, and we leverage them to derive Proposition 3.

**ASSUMPTION 1.** *For each individual  $i$  in the population, let  $C_i$  denote the set of his/her close contacts. We model  $C_i$  as deterministic. The following conditions hold:*

1. *(Bounded infection risk) For any  $\alpha$ ,  $\mathbb{P}_\alpha^{(N)}(U_i > 0) \in \{0\} \cup [\epsilon_0\alpha, \Pi_0\alpha]$  where  $0 < \epsilon_0 \leq 1 \leq \Pi_0$ .*
2. *(Existence of close contacts for non-isolated individuals)  $C_i \neq \emptyset$  if  $\mathbb{P}_\alpha^{(N)}(U_i > 0) > 0$ .*
3. *(Correlation in infection status) There exists  $c_1 > 0$  such that  $\mathbb{P}_\alpha^{(N)}(U_j > 0 \mid U_i > 0) \geq c_1 \forall j \in C_i$ . This holds for any  $\alpha$  and any  $N$ .*
4. *(Correlated pooling) There exists  $c_2 > 0$  such that  $\mathbb{P}_{CP,\alpha}^{(N)}(j \text{ is in the same pool as } i) \geq c_2 \forall j \in C_i$ . This holds for any  $\alpha$  and any  $N$ .*

Assumption 1 captures important features of the spread of infectious diseases and the correlated pooling method. The first sub-assumption prescribes that each individual in the population either (i) cannot be infected due to social isolation; or (ii) may be infected but the bounds of infection risk fall within the same order as the population-level prevalence. The second sub-assumption is justified because individuals with non-zero infection risk must have some degree of human-to-human contact. The third sub-assumption finds ample support in the literature, regarding transmission between infected individuals and their close contacts (World Health Organization 2020, Madewell et al. 2020). The fourth sub-assumption describes the key feature assumed for correlated pools,

namely that individuals who are close contacts of each other are placed into the same pool with a non-vanishing probability, even as  $N$  goes to infinity. This is justified because in large-scale screening using group testing, correlation either arises naturally or can be enhanced through explicit measures, as discussed later in Section 4.1.

Assumption 1 allows us to derive the following property of pool  $J$  under  $\mathbb{P}_{\text{CP},\alpha}$ .

**PROPOSITION 3.** *Under Assumption 1,  $\lim_{\alpha \rightarrow 0^+} \mathbb{P}_{\text{CP},\alpha}(S > 1 \mid S > 0) > 0$ .*

Propositions 2 and 3 lay the foundation for our main theoretical results discussed in Section 3.5.

### 3.5. Main Theoretical Results

Building upon the properties of the single-pool model outlined above, we establish our primary theoretical findings. Specifically, we prove that correlated pooling attains higher sensitivity and, under a mild condition, achieves higher effective efficiency. To the best of our knowledge, we are the first to (1) theoretically show that correlated pooling has better sensitivity, and (2) theoretically characterize the effect of correlated pooling on test usage while modeling the dilution effect.

First, we show that under a general class of test sensitivity functions, correlated pooling achieves higher sensitivity than naive pooling in the low prevalence setting.

**THEOREM 1.** *If  $p(v)$  is monotone increasing in  $v$ ,  $\lim_{\alpha \rightarrow 0^+} \beta_{\text{NP},\alpha} \geq \lim_{\alpha \rightarrow 0^+} \beta_{\text{CP},\alpha}$ . If, in addition,  $p(v)$  is strictly monotone increasing, then the inequality is strict.*

*Proof sketch of Theorem 1.* For  $\text{POOL} \in \{\text{NP}, \text{CP}\}$ , we can show that the overall false negative rate is given by  $\beta_{\text{POOL},\alpha} = 1 - \mathbb{E}_{\text{POOL},\alpha} [p(\bar{V}_n) p(V_1) \mid V_1 > 0]$ .

For naive pooling, the  $V_i$ 's are i.i.d. As  $\alpha \rightarrow 0^+$ , the probability that a positive pool contains multiple positive samples vanishes, and we can show that  $\lim_{\alpha \rightarrow 0^+} \beta_{\text{NP},\alpha} = 1 - \mathbb{E} [p(\frac{1}{n}V_1) p(V_1) \mid V_1 > 0]$ .

For correlated pooling, a positive pool contains multiple positives with non-negligible probability, so we can write  $\beta_{\text{CP},\alpha} = 1 - \sum_{\ell=1}^n A_\ell \cdot \mathbb{P}_{\text{CP},\alpha}(S = \ell \mid S > 0)$ , where  $A_\ell \triangleq \mathbb{E}_{\text{CP},\alpha} [p(\bar{V}_n) p(V_1) \mid V_1 > 0, S = \ell]$ . When  $\ell = 1$ ,  $A_1 = \mathbb{E}[p(\frac{1}{n}V_1)p(V_1) \mid V_1 > 0] = 1 - \lim_{\alpha \rightarrow 0^+} \beta_{\text{NP},\alpha}$ . When  $\ell \geq 2$ , we have  $\bar{V}_n > \frac{1}{n}V_1$  because there exists at least one other sample with positive viral load. Assuming  $p(v)$  is a monotone increasing function in  $v$ , we obtain  $p(\bar{V}_n) \geq p(\frac{1}{n}V_1)$ , which, combined with  $p(V_1) > 0$  given  $V_1 > 0$ , implies that  $A_\ell \geq A_1$ . Therefore, taking  $\alpha \rightarrow 0^+$  gives  $\lim_{\alpha \rightarrow 0^+} \beta_{\text{CP},\alpha} \leq \lim_{\alpha \rightarrow 0^+} \beta_{\text{NP},\alpha}$ . The inequality is strict if  $p(v)$  is strictly increasing in  $v$ .  $\square$

Second, in Theorem 2, we show that in the low prevalence setting, the Dorfman procedure using correlated pooling achieves no lower effective efficiency than using naive pooling, up to a constant multiplier. This multiplier is determined by the viral load distribution among infected individuals, the test sensitivity function, and the pooling method.

**THEOREM 2.**  $\lim_{\alpha \rightarrow 0^+} \frac{\gamma_{CP,\alpha}}{\gamma_{NP,\alpha}} \geq (1 + \delta)^{-1}$ , where  $\delta = \frac{\mathbb{P}_{CP,\alpha}(Y = 1, S_D = 0 | S > 0)}{\mathbb{P}_{CP,\alpha}(Y = 1, S_D > 0 | S > 0)}$  and  $S_D = \sum_{i=1}^n W_i$ .

In a relatively simple case where a test result deterministically reports whether the sample viral load exceeds a threshold value, correlated pooling consumes no more tests per positive case identified than naive pooling. This is formulated in Corollary 1.

**COROLLARY 1.** *Suppose the sensitivity function is  $p(v) = \mathbb{1}\{v \geq u_0\}$  for some non-negative constant  $u_0$ . Then,  $\lim_{\alpha \rightarrow 0^+} \frac{\gamma_{CP,\alpha}}{\gamma_{NP,\alpha}} \geq 1$ .*

In the real world, the PCR test sensitivity, which directly aligns with our model, albeit not exactly a step function of the viral load  $v$ , closely resembles one in that it increases rapidly from zero to one within a narrow range of  $v$ . (See, e.g., Figure 2b in Section 4.2.3.) Appendix G further shows that, under a realistic sensitivity function, viral load distribution and pool size, the bound in Theorem 2 is almost equal to one.

### 3.6. Revisiting Efficiency

We now revisit the conventional efficiency metric studied in literature, i.e., the number of people screened per test. We make two key arguments. First, correlated pooling can have lower efficiency in reality, contrary to claims in existing studies that do not model the dilution effect. Second, our effective efficiency metric is a better metric than efficiency for evaluating pooling designs for epidemic control.

To support our statements below, observe that efficiency can be expressed for any prevalence  $\alpha$  in terms of  $\beta_{POOL,\alpha}$  and  $\gamma_{POOL,\alpha}$  as follows:

$$\text{efficiency}_{POOL,\alpha} = \frac{n}{1 + n\mathbb{E}_{POOL,\alpha}[Y]} = \frac{\gamma_{POOL,\alpha}}{(1 - \beta_{POOL,\alpha})\alpha}. \quad (1)$$

Existing literature claims that within-pool correlation leads to better efficiency (Comess et al. 2021, Augenblick et al. 2020, Lendle et al. 2012, Deckert et al. 2020, Lin et al. 2020, Basso et al. 2021). The claim is valid under simplified assumptions like noise-free tests but generally does not hold under the dilution effect.

In fact, correlated pooling's improved sensitivity can detract from its efficiency. Correlated pooling can identify positive-containing pools that would have tested negative under naive pooling due to the dilution effect. This results in more followup tests (i.e., a higher  $n\mathbb{E}_{POOL,\alpha}[Y]$  in Equation 1). This effect can outweigh the reduction in the number of positive-containing pools caused by correlation, leading to a lower efficiency than naive pooling. Indeed, Appendix D shows a stylized example where correlated pooling has lower efficiency in pools of size two. The same phenomenon can occur whenever the dilution effect prevents a test from identifying a single positive in a pool, but allows

it to detect two or more positives. Under low prevalence, positives pools created by naive pooling typically have just one positive sample, testing negative. Correlated pooling will create more pools with multiple positives, leading to positive pooled test results and requiring more follow-up tests.

Although correlated pooling can decrease efficiency, we argue that efficiency should not be the sole criterion for evaluating a pooling procedure for epidemic control. A pooling procedure with low sensitivity would incur few followup tests, resulting in high efficiency, but it would miss a large number of positives, failing to control the epidemic. This defies the purpose of epidemic mitigation. However, maximizing sensitivity alone brings us to the opposite extreme of using individual tests, incurring high test consumption. Appendix F.4 dives deeper in to this tradeoff between sensitivity and efficiency.

Our effective efficiency metric precisely balances this tradeoff. In fact, Equation 1 shows that it is proportional to the product of sensitivity and efficiency. As discussed in Section 3.2, effective efficiency quantifies the rate of identifying positives under constraints on test budget. As such, it characterizes the true utility of consuming one test. Therefore, under limited test budget, one should choose the pooling procedure that maximizes the effective efficiency to optimize the epidemic control performance. We contextualize this argument using an SIR model (Kermack and McKendrick 1927) in Appendix F.6.

## 4. Case Study

We conduct a case study to understand the implications that correlated pooling has for decision-making. We mimic the decision-making process of a policy-maker facing an emerging epidemic, who aims to conduct large-scale screening, a proven epidemic control measure adopted by cities (Fan 2020, Barak et al. 2021) and universities (Lefkowitz 2020). The policy-maker uses simulation to evaluate screening policies and select the one that best suits their needs. We show that a policy-maker who does not account for the naturally occurring within-pool correlation would underestimate the power of population-wide screening and make suboptimal policy choices. Moreover, taking measures to enhance within-pool correlation can further improve epidemiological outcomes. Separately, Appendix F uses simulation to study how correlation influences the direct performance characteristics of pooled testing in a simplified setting without epidemic dynamics.

### 4.1. Motivation

Consider a policy-maker facing an emerging epidemic. They would like to use pooled testing followed by isolation of individuals testing positive to curb virus spread.<sup>3</sup> To make this decision, they

<sup>3</sup>In practice, large-scale screening can be complementary to other mitigation measures, such as contact tracing. Positives missed in contact tracing can be found in screening.

will utilize an agent-based simulation. They will vary the *policy* (pool size and testing frequency)<sup>4</sup> in simulation and observe the cumulative number of infections and test consumption, considering a policy feasible if its test consumption is below a threshold. If the best feasible policy results in a cumulative number of infections below a threshold, the policy-maker will implement it, keeping the economy open. Otherwise, they will issue a lockdown.

Some correlation in pools is likely to occur naturally due to community interactions in neighborhoods, schools, and workplaces. As people in the same community tend to frequent the same sampling sites, they tend to be pooled together, creating correlation in the pools. We will show that a policy-maker whose simulation ignores this can make dramatically suboptimal decisions, choosing to issue lockdown when it is not necessary or choosing a poor pool size and testing frequency.

Additionally, members within the same household have an even stronger correlation in infections due to their close and extended daily interactions. Preserving household-induced correlation in pools is more demanding than preserving community-induced correlation. For example, sampling sites would need to add an extra operational step to pool household members together even if they visited at the same time. We show that by intentionally enhancing household-induced correlation, a policy-maker can substantially improve epidemiological outcomes. Possible such measures include encouraging household members to get tested together and mailing test kits to each household for household members to self-collect and pool samples together.

Building on this understanding, we consider three policy-makers with different perceptions of the correlation within pools. The *correlation-oblivious* policy-maker is not aware of the existence of within-pool correlation induced by social interactions. The *correlation-aware* policy-maker is aware of the natural correlation in pools arising from social interactions and reflects it in their modeling. The *correlation-enhancing* policy-maker is aware of the correlation, but they also take further measures to ensure that those from the same household are placed into the same pool.

Mirroring these three policy-making mindsets and in parallel with the theoretical analysis, we simulate three different pooling methods. We assume hereafter that each policy-maker would make decisions based on simulation outcomes from the corresponding pooling method.

- *Naive pooling* (correlation-oblivious policy-maker): pools are formed randomly from the population such that individuals in the same pool are approximately unrelated.
- *Community-correlated pooling* (correlation-aware policy-maker): members of the same pool have some level of social interaction, but they do not necessarily come from the same household.

<sup>4</sup> Within the scope of this paper, we assume the same screening frequency and pool size are used throughout. There are multiple practical constraints that call for a screening policy to remain unchanged over time. For example, it would be hard for labs to change their pooling protocol once it is established. It would also be hard for public health workers to modify their operations to test a population at changing frequencies. An interesting future direction is to study schemes of adaptively choosing the frequency and pool size based on the evolving prevalence and network structure, while still taking correlation into account.

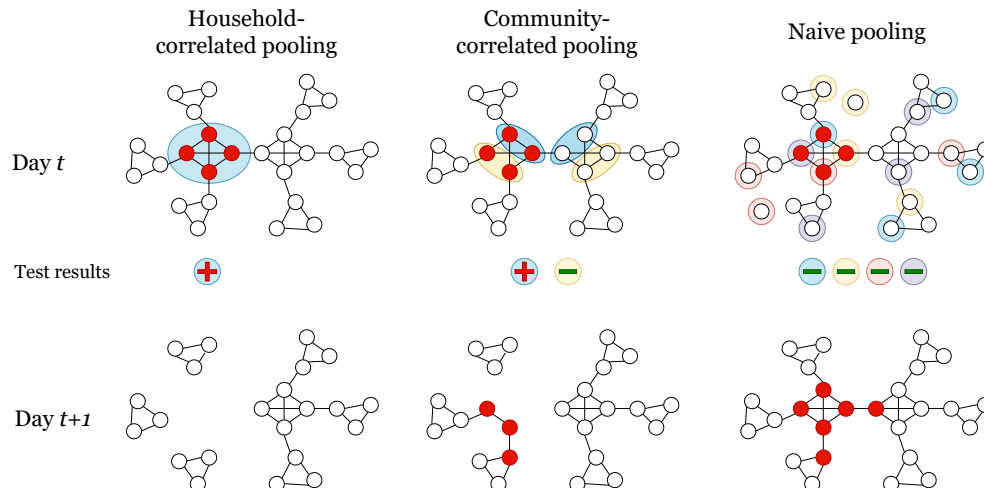


**Figure 1** Schematic illustration of household-correlated pooling, community-correlated pooling, and naive pooling on a simple social network with one infected four-person household, all using pools of size four. Each color represents one pool. Under household-correlated pooling, all four infected individuals are placed into the same pool (blue), identified, and isolated. Under community-correlated pooling, the four infected individuals are placed into two pools (blue and yellow). The blue pool tests positive while the yellow pool does not. The two infected individuals in the yellow pool are not identified and generate one new infection the next day. Under naive pooling, the four infected individuals are placed into four different pools. With none of the pools testing positive, none of them are isolated; they generate two new infections the next day.

- *Household-correlated pooling* (correlation-enhancing policy-maker): individuals from the same household are placed into the same pool.

Though both of the last two pooling methods are a form of correlated pooling, we choose to model community-correlated pooling and household-correlated pooling separately due to their distinct practical implications. The former reflects the naturally induced within-pool correlation and simulates the real-world scenario where pools are formed in large-scale screening. In contrast, the latter assumes additional public-health measures that group members of the same household into the same pool. Figure 1 presents a schematic illustration of the three pooling methods, visualizing disease spread over one day under each pooling method, which we will elaborate on later.

In our simulation, naive pooling is achieved through randomly permuting the individuals and placing them sequentially into pools regardless of household membership. Both correlated pooling methods can be implemented using a node embedding and clustering procedure on the social network. The implementation detail can be found in Appendix E.1.

## 4.2. Simulation Setup

Our simulation reflects realistic features of social networks, viral load progression, and PCR testing.

**4.2.1. Screening and pooling in a social network** We use the SEIRSpplus library (McGee 2021) to simulate an epidemic progression on a realistic social network comprising households of



different sizes and community structure. We simulate 10,000 individuals in households,<sup>5</sup> whose sizes follow the United States’ distribution over household sizes. Each household forms a complete sub-graph, complemented by inter-household edges. We divide the population into equally-sized fixed screening groups, screen one group every day, and rotate through all groups repeatedly. On each day, we allocate the individuals in the screening group into pools using one of the pooling methods and conduct two-stage Dorfman testing. Positive cases are isolated, with isolated individuals excluded from screening and contact with others.

Both the assignment of screening groups and the formation of community and household-correlated pools are implemented using a node embedding and clustering procedure (Appendix E.1.3). We first generate a vector representation for each node using the `node2vec` package (Grover and Leskovec 2016) and use  $k$ -means clustering to allocate individuals to screening groups. This approach tends to assign individuals with close network proximity to the same screening group. For community-correlated pooling and household-correlated pooling, we use the same procedure to allocate individuals within a screening group to pools. We design our algorithm such that household-correlated pools mostly contain members of the same households. This, combined with rapid virus spread within households, results in high within-pool correlation for household-correlated pools. In contrast, community-correlated pools exhibit weaker within-pool correlation. (See Appendix E.1.4 for numerical evidence.)

**4.2.2. Viral load progression** Viral load of an infected individual typically rises then falls during the course of infection (Xu et al. 2020, Liu et al. 2020). Following Brault et al. (2021), we model the log10 viral load of an infected individual as a piecewise linear function over several stages: linear increase, constant peak level, linear decrease, constant tail level, and linear decrease to zero. We assume an individual is infectious when their viral load is above a certain threshold. To account for heterogeneity across infections, we randomly sample the duration of each stage for each infected individual. Figure 2a shows an example log10 viral load trajectory.

**4.2.3. PCR test sensitivity** We develop a realistic model that captures the relationship between PCR test results and sample viral loads. Most existing mathematical models of group testing treat false negatives of PCR tests in an oversimplified way, either assuming a fixed false negative rate or a simple function of the sample viral load (Peng et al. 2021). In practice, before entering the PCR machine, a sample undergoes multiple steps of processing (e.g., subsampling and extraction). Each of these steps introduces stochasticity into the amount of viral RNA that remains. Following the sample handling methodology described in Wyllie et al. (2020) and the mathematical modeling for liquid partitioning in Basu (2017), we outline the steps in a size- $n$

<sup>5</sup> We obtained qualitatively similar results using a network of 5,000 individuals.

pooled test and discuss the randomness associated with each step and its impact on the final test outcome in Appendix E.3. Our modeling of the PCR test is one instantiation of the general test sensitivity function  $p(v)$  discussed in Section 3 (Figure 2b).<sup>6</sup> While our case study focuses on PCR tests, our findings are likely applicable to a range of other tests, such as antibody tests (Zenios and Wein 1998) and various amplification-based tests (Westreich et al. 2008).

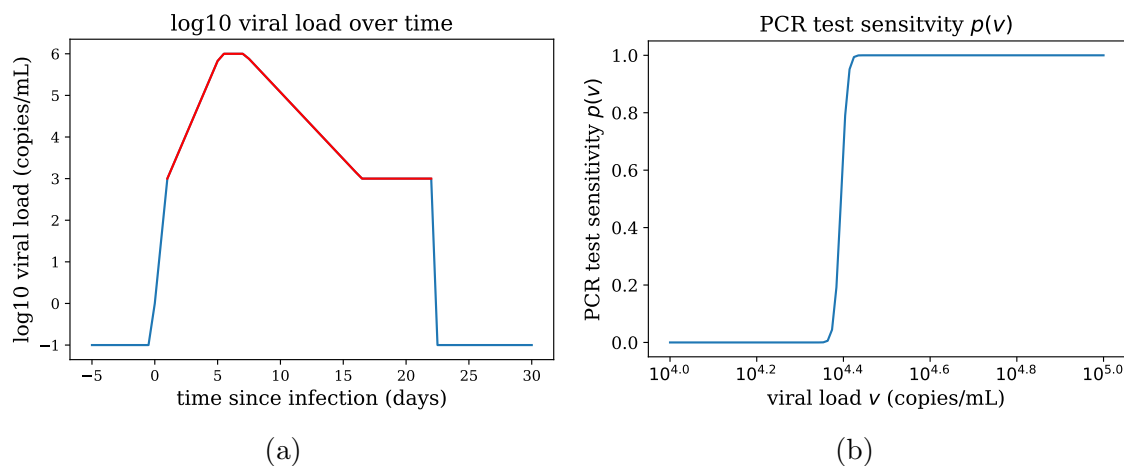


**Figure 2** (a) Example log<sub>10</sub> viral load over time for an infected individual. The period during which the individual is infectious is marked in red. (b) PCR test sensitivity function  $p(v)$ .

### 4.3. Results and Policy Implications

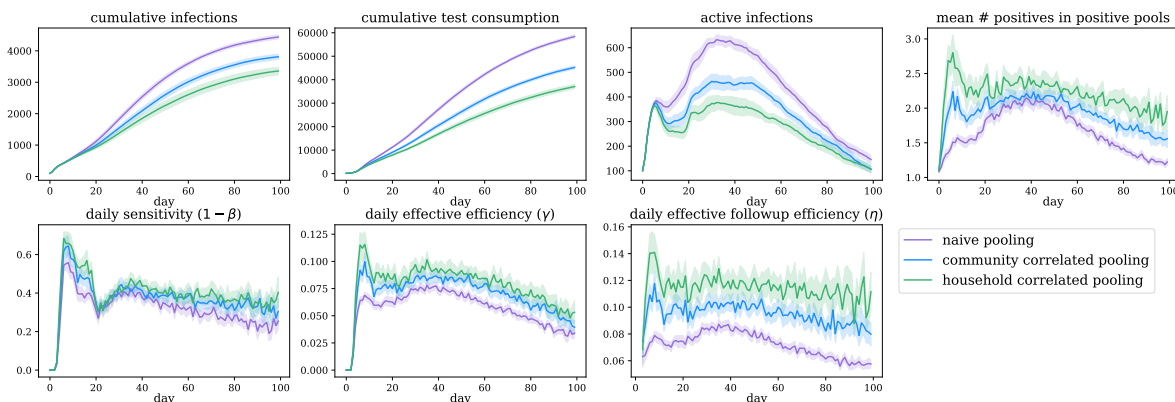


**Figure 3** Simulated epidemic metrics over a 100-day period for naive pooling (purple), community-correlated pooling (blue), and household-correlated pooling (green). The screening policy is to screen every five days using a pool size of 20. Results are averaged over 20 trials, and error bars are two standard errors of the mean (SEM).

<sup>6</sup> In our realistic model,  $p(v) = 0$  for very small  $v$ , while we assume  $p(v) > 0$  for  $v > 0$  in Section 3. Nevertheless, our theoretical and simulation results are still consistent despite this small discrepancy.

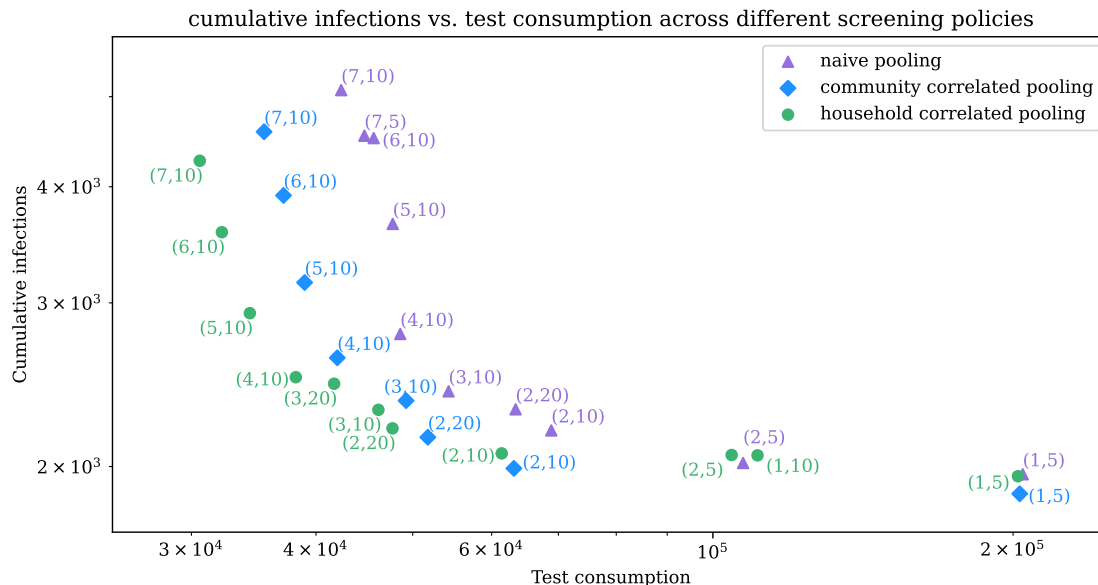


**Figure 4** Total number of infections and total test consumption under Pareto-optimal policy choices for each of naive pooling (purple), community-correlated pooling (blue), and household-correlated pooling (green). Each point corresponds to a choice of screening frequency and pool size, indicated by a tuple in the annotation.

Figure 3 describes the epidemic progression over a 100-day period, during which we employ different pooling methods under a representative scenario of screening every five days using pools of size 20. We highlight two primary performance metrics, namely cumulative number of infections and cumulative test consumption, both of which we aim to minimize. Among the three pooling methods, household-correlated pooling performs better than community-correlated pooling, which performs better than naive pooling. We will see later that this ranking in performance is robust across different pool sizes and testing frequencies, which has profound policy implications. We further report the metrics studied theoretically in Section 3, namely the sensitivity  $1 - \beta$ , effective efficiency  $\gamma$ , and an auxiliary metric, effective followup efficiency  $\eta$  (defined in Appendix C.2). Their behaviors validate our theoretical findings.

Figure 4 presents a landscape of Pareto-optimal screening policies for each pooling method.<sup>7</sup> The order of Pareto dominance aligns with the performance ranking of the three pooling methods in Figure 3. By comparing the cumulative number of infections under different pooling methods in Figure 4 with different test supply, we argue that modeling, if not intentionally enhancing, the correlation is crucial for policy-making. We discuss the implications in more detail.

**4.3.1. Correlation as a modeling choice** First, it is important to reflect the naturally arising within-pool correlation in the modeling; failing to do so may lead to suboptimal decisions.

<sup>7</sup> More infrequent testing would consume fewer tests but would lead to even more infections. Since testing every seven days results in at least 40% of the population infected for all pooling methods, we do not simulate lower frequencies.

*Results* We compare the correlation-oblivious and correlation-aware policy-makers, whose decisions are informed by results from naive pooling and community-correlated pooling, respectively.

In Figure 3, community-correlated pooling (blue) results in fewer infections and test consumption than naive pooling (purple). Notably, the reduced infections demonstrates the importance of accounting for the effect of correlation on sensitivity, a topic not explored in prior literature. When virus starts spreading, mostly in closely-connected parts of the network like households, correlated pooling can more accurately identify these clustered infections early on, preventing the virus from spreading further. On the contrary, the early positives are scattered across different pools in naive pooling, increasing the likelihood of missed cases due to lower sensitivity. The widening gap in cumulative number of infections over time reflects the compounding effect of identifying the positives early on, demonstrating the importance of modeling the true effect of correlation on sensitivity in controlling an epidemic.

The above insight is supported by additional intermediate metrics. First, the behaviors of the metrics studied in Section 3, namely sensitivity  $1 - \beta$  and effective efficiency  $\gamma$ , validate our theoretical results. Second, looking at the average number of positives in positive pools on each day, we observe that positive-containing correlated pools consistently contain more positives than naive pools do, even during the peak of the epidemic, which enhances the sensitivity of correlated pools. Lastly, at the peak of the epidemic (around Day 30), the number of active infections exceeds 600 under naive pooling but is around 450 under community-correlated pooling, demonstrating correlated pooling’s superior power in taming the virus spread.

*Implications for decision-making* The correlation-oblivious policy-maker, informed by analyses ignoring correlation, would make overly conservative decisions compared to the correlation-aware policy-maker. We describe two important classes of such decisions.

**Decision 1: Lockdown or screening.** The first decision for any policy-maker facing an emerging pandemic is whether to issue a lockdown or to keep the society open. Lockdowns incur huge economic losses and are generally undesirable, but the feasibility of keeping the society open depends on resource availability and the policy-maker’s risk tolerance.

Suppose the available PCR testing capacity over 100 days is  $4 \times 10^4$  for pooled and individual tests combined. Assuming naive pooling, the correlation-oblivious policy-maker decides that no screening policy can permit safe reopening and thus issues a lockdown. However, the correlation-aware policy-maker, assuming community-correlated pooling, finds that screening every five, six or seven days with pool size 10 is permitted by the testing capacity. To minimize infections, they choose to screen every five days while keeping the economy open.

Even with a higher test supply that permits naive pooling, naive pooling could overestimate the cumulative infections to be larger than tolerable. Suppose the test supply is about  $4.5 \times 10^4$ .

The optimal naive pooling policies are screening every seven days with pool size five or screening every six days with pool size 10, both giving around  $4.5 \times 10^3$  cumulative infections. On the other hand, the optimal community-correlated pooling policy is screening every four days with pool size 10, resulting in roughly half the cumulative infections,  $2.5 \times 10^3$ . Suppose the policy-makers cannot tolerate more than 30% of the population infected due to resource constraints like ICU availability. The correlation-oblivious policy-maker would choose to issue a lockdown while the correlation-aware policy-maker would keep the economy open while conducting screening.

**Decision 2: Choice of screening frequency and pool size.** When a policy-maker opts for screening, their choice of screening frequency and pool size has a significant impact on the epidemiological outcomes. We argue that the correlation-oblivious policy-maker would choose a suboptimal screening policy compared to the correlation-aware one.

Suppose the test supply is  $4.2 \times 10^4$ . The correlation-oblivious policy-maker chooses to screen every seven days with pool size 10, while the correlation-aware policy-maker decides to screen every four days with pool size 10. Since we assumed community-correlated pooling to closely reflect the reality, the actual outcome for the correlation-oblivious policy-maker would be close to community-correlated pooling’s outcome for the same policy, at about  $4.6 \times 10^3$ , while the correlation-aware policy-maker would get  $2.5 \times 10^3$  infections. Since naive pooling perceives the effective efficiency to be lower than reality (Figure 3, “daily effective efficiency”), the correlation-oblivious policy-maker underestimates the allowed screening frequency, leading to suboptimal epidemic outcomes.

**4.3.2. Correlation as an intervention** If logistically feasible, enhancing correlation by e.g., placing households into the same pool, would further boost epidemic control performance.

*Results* We compare the correlation-aware and correlation-enhancing policy-makers, whose decisions are informed by community-correlated pooling and household-correlated pooling, respectively.

In Figure 3, household-correlated pooling (green) further reduces both the cumulative number of infections and cumulative test consumption compared to community-correlated pooling (blue). On Day 100, household-correlated pooling predicts  $3.4 \times 10^3$  infections on average, which is 11% fewer than community-correlated pooling ( $3.8 \times 10^3$  infections) and 23% fewer than naive pooling ( $4.4 \times 10^3$  infections).

The difference between household-correlated pooling and community-correlated pooling is the same in nature as that between community-correlated pooling and naive pooling: the stronger within-pool correlation improves the overall sensitivity, translating to more effective epidemic mitigation. We refer back to Figure 1 for illustration. When a household with all four members infected is included in the same pool, their chances of being detected together increase. On the other hand, community-correlated pooling reduces this correlation by dividing the household into two separate pools; naive pooling combines each household member with unrelated samples, resulting in failure to identify any positive member.

*Implications for decision-making* If the correlation-enhancing policy-maker executes household-correlated pooling in reality, they would achieve better epidemiological outcomes than the correlation-aware policy-maker, and much better ones than the correlation-oblivious policy-maker. The same arguments regarding decision-making in Section 4.3.1 apply, and the advantage provided by within-pool correlation is even more pronounced if household-correlated pooling is realized.

First, the correlation-enhancing policy-maker could keep the economy open at lower test supply, as shown by the gap between household-correlated pooling (green) and community-correlated pooling (blue) in Figure 4. For example, if test supply is  $3.2 \times 10^4$ , the correlation-aware policy-maker would issue a lockdown while the correlation-enhancing policy-maker would have the option of conducting screening.

Furthermore, the correlation-enhancing policy-maker would be able to achieve better epidemiological outcomes than the correlation-aware counterpart if both conduct screening. For example, given a 100-day test supply of  $4 \times 10^4$ , the correlation-aware policy-maker would choose to screen every five days with pool size 10, incurring in  $3.2 \times 10^3$  infections on average. On the other hand, the correlation-enhancing policy-maker, taking measures to strengthen the correlation in pools, would choose to screen every four days with pool size 10, incurring  $2.5 \times 10^3$  infections on average, a 22% reduction compared to the correlation-aware one.

These results imply that, when feasible, it is worth taking explicit measures to strengthen the correlation within pools. For example, one can encourage individuals from the same household to get tested at the same location and time slot. One can also mail sample collection kits to each household and ask them to self-collect and combine their samples. While we recognize the logistical challenges of implementing these measures, we believe our model can accurately predict their benefits for epidemic control, allowing policy-makers to make informed cost-benefit assessments.

## 5. Conclusion

In this paper, we proved that under a general correlation structure and in the presence of the dilution effect, correlated pooling achieves higher sensitivity but can degrade test efficiency compared to naive pooling using the same pool size. We identified an alternative measure of test resource usage, the number of positives found per test consumed, which we argued is better aligned with infection control, and showed that correlated pooling outperforms naive pooling on this measure. We validated and contextualized our theoretical results in a realistic agent-based epidemic simulation. We argued that the dilution effect makes it even more important for policy-makers evaluating group testing protocols for large-scale screening to account for naturally arising correlation and to intentionally maximize correlation.

Our work can be extended in several directions in future research. First, while we focus on the Dorfman procedure when understanding the impact of correlation on pooled testing in the presence of the dilution effect, similar phenomena likely arise in other testing algorithms. In particular, correlation likely improves the sensitivity of tests within these procedures as well. We anticipate that follow-on work can show that correlation improves the performance of these other test procedures in the presence of the dilution effect. Second, the index case and the secondary cases within the same household could become infected at different times. It would be interesting to explore asynchronous testing protocols that both utilize the correlation and optimize the timing to maximize the overall probability of detecting the infected members. Third, it would be meaningful to incorporate sampling noise, where the sample viral load could be zero for an infected individual. The additional transmission due to undetected individuals may counteract the benefits offered by correlated pooling, and such consideration is of practical interest for large-scale epidemic control. This could be addressed using latent variable models.

## **Acknowledgments**

The authors are grateful to Diego Diel and Jeff Pleiss for conversations on the implementation details of PCR tests. The authors also thank Stephen Chick, Saskia Comess, Claire Donnat, and Susan Holmes for providing valuable feedback. This work was conducted under the support from Cornell University when the authors served in the Cornell COVID mathematical modeling team. Additional support was provided by Air Force Office of Scientific Research FA9550-19-1-0283. J.W. and Y.Z. contributed equally to this paper.

## References

- Aprahamian H, Bish DR, Bish EK (2019) Optimal risk-based group testing. *Management Science* 65(9):4365–4384.
- Augenblick N, Kolstad JT, Obermeyer Z, Wang A (2020) Group testing in a pandemic: The role of frequent testing, correlated risk, and machine learning. Technical report, National Bureau of Economic Research.
- Barak N, Ben-Ami R, Sido T, Perri A, Shtoyer A, Rivkin M, Licht T, Peretz A, Magenheim J, Fogel I, et al. (2021) Lessons from applied large-scale pooling of 133,816 SARS-CoV-2 RT-PCR tests. *Science Translational Medicine* 13(589).
- Basso LJ, Salinas V, Sauré D, Thraves C, Yankovic N (2021) The effect of correlation and false negatives in pool testing strategies for COVID-19. *Health Care Management Science* 1–20.
- Basu AS (2017) Digital assays part I: partitioning statistics and digital PCR. *SLAS Technology: Translating Life Sciences Innovation* 22(4):369–386.
- Bateman AC, Mueller S, Guenther K, Shult P (2020) Assessing the dilution effect of specimen pooling on the sensitivity of SARS-CoV-2 PCR tests. *Journal of Medical Virology* .
- Bilder CR, Tebbs JM (2012) Pooled-testing procedures for screening high volume clinical specimens in heterogeneous populations. *Statistics in Medicine* 31(27):3261–3268.
- Bilder CR, Tebbs JM, Chen P (2010) Informative retesting. *Journal of the American Statistical Association* 105(491):942–955.
- Brault V, Mallein B, Rupprecht JF (2021) Group testing as a strategy for COVID-19 epidemiological monitoring and community surveillance. *PLoS Computational Biology* 17(3):e1008726.
- Carcione D, Giele C, Goggin L, Kwan KS, Smith D, Dowse G, Mak D, Effler P (2011) Secondary attack rate of pandemic influenza A (H1N1) 2009 in Western Australian households, 29 May–7 August 2009. *Eurosurveillance* 16(3):19765.
- Cheraghchi M, Karbasi A, Mohajer S, Saligrama V (2012) Graph-constrained group testing. *IEEE Transactions on Information Theory* 58(1):248–262.
- Cleary B, Hay JA, Blumenstiel B, Harden M, Cipicchio M, Bezney J, Simonton B, Hong D, Senghore M, Sesay AK, et al. (2021) Using viral load and epidemic dynamics to optimize pooled testing in resource-constrained settings. *Science Translational Medicine* 13(589).
- Comess S, Wang H, Holmes S, Donnat C (2021) Statistical modeling for practical pooled testing during the COVID-19 pandemic. *arXiv preprint arXiv:2107.05619* .
- Deckert A, Bärnighausen T, Kyei NN (2020) Simulation of pooled-sample analysis strategies for COVID-19 mass testing. *Bulletin of the World Health Organization* 98(9):590.
- Dorfman R (1943) The detection of defective members of large populations. *Annals of Mathematical Statistics* 14(4):436–440.



- Eberhardt JN, Breuckmann NP, Eberhardt CS (2020) Multi-stage group testing improves efficiency of large-scale covid-19 screening. *Journal of Clinical Virology* 104382.
- Fan W (2020) Wuhan tests nine million people for coronavirus in 10 days. <https://www.wsj.com/articles/wuhan-tests-nine-million-people-for-coronavirus-in-10-days-11590408910>, Accessed: May 18, 2021.
- Ganesan A, Jaggi S, Saligrama V (2017) Learning immune-defectives graph through group tests. *IEEE Transactions on Information Theory* 63(5):3010–3028.
- Glynn JR, Bower H, Johnson S, Turay C, Sesay D, Mansaray SH, Kamara O, Kamara AJ, Bangura MS, Checchi F (2018) Variability in intrahousehold transmission of Ebola virus, and estimation of the household secondary attack rate. *The Journal of Infectious Diseases* 217(2):232–237.
- Graff LE, Roeloffs R (1972) Group testing in the presence of test error; an extension of the Dorfman procedure. *Technometrics* 14(1):113–122.
- Grover A, Leskovec J (2016) node2vec: Scalable feature learning for networks. *Proceedings of the 22nd ACM SIGKDD international conference on Knowledge discovery and data mining*, 855–864.
- Hung M, Swallow WH (1999) Robustness of group testing in the estimation of proportions. *Biometrics* 55(1):231–237.
- Hwang FK (1976) Group testing with a dilution effect. *Biometrika* 63(3):671–680.
- Kermack WO, McKendrick AG (1927) A contribution to the mathematical theory of epidemics. *Proceedings of the Royal Society of London. Series A, Containing papers of a Mathematical and Physical Character* 115(772):700–721.
- Kim HY, Hudgens MG, Dreyfuss JM, Westreich DJ, Pilcher CD (2007) Comparison of group testing algorithms for case identification in the presence of test error. *Biometrics* 63(4):1152–1163.
- Lan FY, Wei CF, Hsu YT, Christiani DC, Kales SN (2020) Work-related COVID-19 transmission in six asian countries/areas: a follow-up study. *PloS One* 15(5):e0233588.
- Lefkowitz M (2020) Robots, know-how drive COVID lab’s massive testing effort. <https://news.cornell.edu/stories/2020/08/robots-know-how-drive-covid-labs-massive-testing-effort>, Accessed: June 23, 2021.
- Lendle SD, Hudgens MG, Qaqish BF (2012) Group testing for case identification with correlated responses. *Biometrics* 68(2):532–540.
- Lin YJ, Yu CH, Liu TH, Chang CS, Chen WT (2020) Positively correlated samples save pooled testing costs. *arXiv preprint arXiv:2011.09794* .
- Liu Y, Yan LM, Wan L, Xiang TX, Le A, Liu JM, Peiris M, Poon LL, Zhang W (2020) Viral dynamics in mild and severe cases of COVID-19. *The Lancet Infectious Diseases* 20(6):656–657.

- Lohse S, Pfuhl T, Berkó-Göttel B, Rissland J, Geißler T, Gärtner B, Becker SL, Schneitler S, Smola S (2020) Pooling of samples for testing for SARS-CoV-2 in asymptomatic people. *The Lancet Infectious Diseases* 20(11):1231–1232.
- Madewell ZJ, Yang Y, Longini Jr IM, Halloran ME, Dean NE (2020) Household transmission of SARS-CoV-2: a systematic review and meta-analysis of secondary attack rate. *medRxiv* .
- McGee RS (2021) SEIRS+ Model Framework. <https://github.com/ryansmcgee/seirsplus>, Accessed: June 1, 2023.
- McMahan CS, Tebbs JM, Bilder CR (2012a) Informative Dorfman screening. *Biometrics* 68(1):287–296.
- McMahan CS, Tebbs JM, Bilder CR (2012b) Two-dimensional informative array testing. *Biometrics* 68(3):793–804.
- Meningococcal Disease Surveillance Group (1976) Meningococcal disease. Secondary attack rate and chemoprophylaxis in the united states, 1974. *Journal of the American Medical Association* 235(3):261–265.
- Mercer TR, Salit M (2021) Testing at scale during the COVID-19 pandemic. *Nature Reviews Genetics* 22(7):415–426.
- Mutesa L, Ndishimye P, Butera Y, Souopgui J, Uwineza A, Rutayisire R, Musoni E, Rujeni N, Nyatanyi T, Ntagwabira E, et al. (2020) A strategy for finding people infected with SARS-CoV-2: optimizing pooled testing at low prevalence. *medRxiv* .
- Nguyen NT, Aprahamian H, Bish EK, Bish DR (2019) A methodology for deriving the sensitivity of pooled testing, based on viral load progression and pooling dilution. *Journal of Translational Medicine* .
- Odaira F, Takahashi H, Toyokawa T, Tsuchihashi Y, Kodama T, Yahata Y, Sunagawa T, Taniguchi K, Okabe N (2009) Assessment of secondary attack rate and effectiveness of antiviral prophylaxis among household contacts in an influenza A(H1N1)v outbreak in Kobe, Japan, May–June 2009. *Eurosurveillance* 14(35):19320.
- Peng B, Zhou W, Pettit RW, Yu P, Matos PG, Greninger AL, McCashin J, Amos CI (2021) Reducing COVID-19 quarantine with SARS-CoV-2 testing: a simulation study. *BMJ open* 11(7):e050473.
- Pilcher CD, Westreich D, Hudgens MG (2020) Group testing for SARS-Cov-2 to enable rapid scale-up of testing and real-time surveillance of incidence. *The Journal of Infectious Diseases* .
- Public Health Ontario (2020) COVID-19 laboratory testing Q&As. <https://www.publichealthontario.ca/-/media/documents/lab/covid-19-lab-testing-faq.pdf?la=en>, Accessed: July 9, 2021.
- Rader B, Scarpino SV, Nande A, Hill AL, Adlam B, Reiner RC, Pigott DM, Gutierrez B, Zarebski AE, Shrestha M, et al. (2020) Crowding and the shape of COVID-19 epidemics. *Nature Medicine* 26(12):1829–1834.
- Stanford Medicine (2020) The vera cloud testing platform, protecting our communities by enabling testing at scale. <https://med.stanford.edu/vera.html>, Accessed: May 18, 2021.

- Vang KE, Krow-Lucal ER, James AE, Cima MJ, Kothari A, Zohoori N, Porter A, Campbell EM (2021) Participation in fraternity and sorority activities and the spread of COVID-19 among residential university communities—Arkansas, August 21–September 5, 2020. *Morbidity and Mortality Weekly Report* 70(1):20.
- Wein LM, Zenios SA (1996) Pooled testing for HIV screening: capturing the dilution effect. *Operations Research* 44(4):543–569.
- Westreich DJ, Hudgens MG, Fiscus SA, Pilcher CD (2008) Optimizing screening for acute human immunodeficiency virus infection with pooled nucleic acid amplification tests. *Journal of Clinical Microbiology* 46(5):1785–1792.
- Weusten JJ, Van Drimmelen HA, Lelie PN (2002) Mathematic modeling of the risk of HBV, HCV, and HIV transmission by window-phase donations not detected by NAT. *Transfusion* 42(5):537–548.
- Whalen CC, Zalwango S, Chiunda A, Malone L, Eisenach K, Joloba M, Boom WH, Mugerwa R (2011) Secondary attack rate of tuberculosis in urban households in Kampala, Uganda. *PloS One* 6(2):e16137.
- World Health Organization (2020) Modes of transmission of virus causing COVID-19: implications for IPC precaution recommendations: scientific brief, 29 March 2020. Technical report, World Health Organization.
- Wyllie AL, Fournier J, Casanovas-Massana A, Campbell M, Tokuyama M, Vijayakumar P, Geng B, Muenker MC, Moore AJ, Vogels CB, et al. (2020) Saliva is more sensitive for SARS-CoV-2 detection in COVID-19 patients than nasopharyngeal swabs. *medRxiv* .
- Xing Y, Wong GW, Ni W, Hu X, Xing Q (2020) Rapid response to an outbreak in Qingdao, China. *New England Journal of Medicine* 383(23):e129.
- Xu T, Chen C, Zhu Z, Cui M, Chen C, Dai H, Xue Y (2020) Clinical features and dynamics of viral load in imported and non-imported patients with covid-19. *International Journal of Infectious Diseases* 94:68–71.
- Yelin I, Aharony N, Tamar ES, Argoetti A, Messer E, Berenbaum D, Shafran E, Kuzli A, Gandali N, Shkedi O, Hashimshony T, Mandel-Gutfreund Y, Halberthal M, Geffen Y, Szwarcwort-Cohen M, Kishony R (2020) Evaluation of COVID-19 RT-qPCR Test in Multi sample Pools. *Clinical Infectious Diseases* ISSN 1058-4838, URL <http://dx.doi.org/10.1093/cid/ciaa531>, ciaa531.
- Yu J, Huang Y, Shen ZJ (2021) Optimizing and evaluating pcr-based pooled screening during COVID-19 pandemics. *Scientific Reports* 11(1):1–14.
- Zenios SA, Wein LM (1998) Pooled testing for HIV prevalence estimation: exploiting the dilution effect. *Statistics in Medicine* 17(13):1447–1467.

# Online Appendix: Correlation Improves Group Testing

## Appendix A: Supplementary Analysis for the Population-Level Model

### A.1. A Model of Association Model

We define a measure of association between the viral loads in  $A_j$  (i.e., the  $j$ th pool by pooling assignment  $\mathcal{A}$ ), and a random variable  $X$  (e.g., a pool-level quantity in a different pool). This measure quantifies the extent to which the viral load in  $A_j$  affects the distribution of random variable  $X$ :

$$\Delta_{\text{POOL},\alpha}^{(N)}(X, k) = \sup_{\mathbf{u} \in \mathbb{R}_{\geq 0}^q} \left| \mathbb{E}_{\text{POOL},\alpha}^{(N)}[X \mid U_{A_k} = \mathbf{u}] - \mathbb{E}_{\text{POOL},\alpha}^{(N)}[X] \right|.$$

For a fixed  $k$ , and a specific pool-level quantity  $Z_j$  (i.e.  $Z_j$  is one of  $S_j$ ,  $Y_j$ , or  $D_j$ , we can define the collection of indices  $j$  ( $j \neq k$ ) such that  $Z_j$  has an association with  $U_{A_k}$  stronger to  $\epsilon$ :

$$\left\{ j : j \neq k, \Delta_{\text{POOL},\alpha}^{(N)}(Z_j, k) > \epsilon \right\}.$$

We denote by  $m_{\text{POOL},\alpha}^{(N)}(\epsilon, Z_{1:|\mathcal{A}|})$  the maximize size of such sets, across  $k \in \{1, \dots, |\mathcal{A}|\}$ :

$$m_{\text{POOL},\alpha}^{(N)}(\epsilon, Z_{1:|\mathcal{A}|}) = \max_{k \in \{1, \dots, |\mathcal{A}|\}} \left| \left\{ j : j \neq k, \Delta_{\text{POOL},\alpha}^{(N)}(Z_j, k) > \epsilon \right\} \right|.$$

Now, we take  $N$  to the asymptotic regime and make the following assumption:

**ASSUMPTION EC.1.** For  $Z_{1:|\mathcal{A}|} \in \{S_{1:|\mathcal{A}|}, Y_{1:|\mathcal{A}|}, D_{1:|\mathcal{A}|}\}$  and  $\text{POOL} \in \{\text{NP}, \text{CP}\}$ , there exists a sequence  $\epsilon_N \downarrow 0$  such that  $\lim_{N \rightarrow \infty} \frac{1}{N} m_{\text{POOL},\alpha}^{(N)}(\epsilon_N, Z_{1:|\mathcal{A}|}) = 0$ .

Assumption EC.1 prescribes that as population size  $N$  goes to infinity, the set of pool-level quantities that have association stronger than  $\epsilon_N$  with the viral loads in pool  $j$  grows slower than linearly in population size. In an epidemic like COVID-19, transmission typically takes place between close contacts (World Health Organization 2020). It is reasonable to assume that for two individuals to be associated in infection statuses, they have to be within a few degrees of contact with each other. Since the duration of the infectious period is finite, and a person's contact rate is typically bounded above by some constant (Hu et al. 2013) even as population size grows large, the number of people connected to any individual in pool  $j$  via within a few degrees of contact grows slower than linearly in population size. Because the pool-level quantities are conditionally independent from viral loads in other pools (given viral loads in the pool), the sub-linearity should be inherited. Hence, this assumption is well-justified.

### A.2. Convergence of Population-Level Metrics

We begin by presenting a lemma which states that under Assumption EC.1, the population-level quantities converge to constants as  $N \rightarrow \infty$ .

**LEMMA EC.1.** Under Assumption EC.1, for  $\alpha > 0$  and  $\text{POOL} \in \{\text{NP}, \text{CP}\}$ , random variables  $\bar{D}$ ,  $\bar{S}$ , and  $\bar{Y}$  under  $\mathbb{P}_{\text{POOL},\alpha}^{(N)}$  converge in probability to  $\mathbb{E}_{\text{POOL},\alpha}[D]$ ,  $\mathbb{E}_{\text{POOL},\alpha}[S]$ , and  $\mathbb{E}_{\text{POOL},\alpha}[Y]$ , respectively, as  $N \rightarrow \infty$ .

*Proof of Lemma EC.1.* For succinctness, we abbreviate  $\mathbb{P}_{\text{POOL},\alpha}^{(N)}(\cdot)$ ,  $\mathbb{E}_{\text{POOL},\alpha}^{(N)}[\cdot]$ ,  $\text{Var}_{\text{POOL},\alpha}^{(N)}(\cdot)$ ,  $\text{Cov}_{\text{POOL},\alpha}^{(N)}(\cdot, \cdot)$  as  $\mathbb{P}^{(N)}(\cdot)$ ,  $\mathbb{E}^{(N)}[\cdot]$ ,  $\text{Var}^{(N)}(\cdot)$  and  $\text{Cov}^{(N)}(\cdot, \cdot)$ , respectively, in this proof. We break down the proof of Lemma EC.1 into two parts, where we first show that  $\text{Var}^{(N)}(\bar{Z}) \rightarrow 0$  for a population-level quantity  $\bar{Z}$ , and then show that  $\bar{Z}$  converges in probability.

1.  $\text{Var}^{(N)}(\bar{Z}) \rightarrow 0$ . Consider a population-level quantity  $\bar{Z}$ , where  $\bar{Z} = \frac{1}{|\mathcal{A}|} \sum_{j=1}^{|\mathcal{A}|} Z_j$ ,  $Z_j$  is one of the pool-level quantities,  $S_j$ ,  $Y_j$  or  $D_j$ . We note that  $Z_j$  is upper bounded by some positive constant  $C_g > 0$  that does not involve  $N$ . We have that

$$\begin{aligned} \text{Var}^{(N)}(\bar{Z}) &= \text{Var}^{(N)}\left(\frac{1}{|\mathcal{A}|} \sum_{j=1}^{|\mathcal{A}|} Z_j\right) \\ &= \frac{1}{|\mathcal{A}|^2} \left( \sum_{j=1}^{|\mathcal{A}|} \text{Var}^{(N)}(Z_j) + \sum_{j=1}^{|\mathcal{A}|} \sum_{k \neq j}^{|\mathcal{A}|} \text{Cov}^{(N)}(Z_j, Z_k) \right). \end{aligned}$$

In order to bound  $\text{Var}(\bar{Z})$  we first provide an upper bound on  $|\text{Cov}(Z_j, Z_k)|$  where  $j \neq k$ . By definition,

$$\begin{aligned} \text{Cov}^{(N)}(Z_j, Z_k) &= \mathbb{E}^{(N)}[Z_j Z_k] - \mathbb{E}^{(N)}[Z_j] \mathbb{E}^{(N)}[Z_k] \\ &= \mathbb{E}^{(N)}[(\mathbb{E}^{(N)}[Z_j | U_{A_k}] - \mathbb{E}^{(N)}[Z_j]) Z_k]. \end{aligned}$$

Now, applying the definition of  $\Delta_{\text{POOL},\alpha}^{(N)}$ , we find that

$$\begin{aligned} |\text{Cov}^{(N)}(Z_j, Z_k)| &\leq \mathbb{E}^{(N)} \left[ Z_k \cdot \Delta_{\text{POOL},\alpha}^{(N)}(Z_j, k) \right] \\ &\leq C_g \cdot \Delta_{\text{POOL},\alpha}^{(N)}(Z_j, k). \end{aligned}$$

This allows us to bound the variance of  $\bar{Z}$ :

$$\begin{aligned} \text{Var}^{(N)}(\bar{Z}) &\leq \frac{1}{|\mathcal{A}|^2} \left( \sum_{j=1}^{|\mathcal{A}|} \text{Var}(Z_j) + \sum_{j=1}^{|\mathcal{A}|} \sum_{k \neq j}^{|\mathcal{A}|} |\text{Cov}(Z_j, Z_k)| \right) \\ &\leq \frac{1}{|\mathcal{A}|^2} \left( |\mathcal{A}| \cdot \frac{1}{4} C_g^2 + \sum_{j=1}^{|\mathcal{A}|} \sum_{k \neq j}^{|\mathcal{A}|} C_g \cdot \Delta_{\text{POOL},\alpha}^{(N)}(Z_j, k) \right). \end{aligned}$$

For any  $\epsilon > 0$ , we have that

$$\begin{aligned} \text{Var}^{(N)}(\bar{Z}) &\leq \frac{1}{|\mathcal{A}|^2} \left( |\mathcal{A}| \cdot \frac{1}{4} C_g^2 + \sum_{j=1}^{|\mathcal{A}|} C_g \cdot \left( (N-1 - m_{\text{POOL},\alpha}^{(N)}(\epsilon, Z_{1:|\mathcal{A}|})) \cdot \epsilon + m_{\text{POOL},\alpha}^{(N)}(\epsilon, Z_{1:|\mathcal{A}|}) \cdot \frac{1}{4} C_g^2 \right) \right) \\ &= \frac{1}{|\mathcal{A}|^2} \left( |\mathcal{A}| \cdot \frac{1}{4} C_g^2 + |\mathcal{A}| \cdot C_g \cdot \left( (N-1 - m_{\text{POOL},\alpha}^{(N)}(\epsilon, Z_{1:|\mathcal{A}|})) \cdot \epsilon + m_{\text{POOL},\alpha}^{(N)}(\epsilon, Z_{1:|\mathcal{A}|}) \cdot \frac{1}{4} C_g^2 \right) \right) \\ &\leq \frac{C_g^2}{4|\mathcal{A}|} + \frac{C_g N \epsilon}{|\mathcal{A}|} + \frac{C_g^3}{4|\mathcal{A}|} \cdot m_{\text{POOL},\alpha}^{(N)}(\epsilon, Z_{1:|\mathcal{A}|}) \\ &= \frac{n C_g^2}{4N} + n C_g \cdot \epsilon + \frac{n C_g^3}{4} \cdot \frac{m_{\text{POOL},\alpha}^{(N)}(\epsilon, Z_{1:|\mathcal{A}|})}{N}. \end{aligned}$$

Let  $\epsilon_N$  be a sequence satisfying Assumption EC.1, i.e.,  $\epsilon_N \downarrow 0$  and  $\lim_{N \rightarrow \infty} \frac{1}{N} m_{\text{POOL},\alpha}^{(N)}(\epsilon, Z_{1:|\mathcal{A}|}) = 0$ . Taking the limit  $N \rightarrow \infty$  of the expression above, we have

$$\lim_{N \rightarrow \infty} \text{Var}(\bar{Z}) \leq \lim_{N \rightarrow \infty} \frac{n C_g^2}{4N} + n C_g \cdot \epsilon_N + \frac{n C_g^3}{4} \cdot \frac{m_{\text{POOL},\alpha}^{(N)}(\epsilon, Z_{1:|\mathcal{A}|})}{N} = 0.$$

2. Proof of convergence. First, it is straightforward that for any  $N$

$$\mathbb{E}^{(N)}[\bar{Z}] = \mathbb{E}^{(N)}\left[\frac{1}{|\mathcal{A}|}Z_j\right] = \mathbb{E}^{(N)}[Z_j] - \mathbb{E}^{(N)}[Z].$$

Because  $\mathbb{E}^{(N)}[Z]$  converges to  $\mathbb{E}[Z]$  as  $N$  goes to infinity, it follows that  $\mathbb{E}^{(N)}[\bar{Z}] \rightarrow \mathbb{E}[Z]$ .

Fix  $\epsilon > 0$ . By definition of limit, there exists some  $N_1 \in \mathbb{N}$  such that for all  $N \geq N_1$ ,

$$|\mathbb{E}^{(N)}[Z] - \mathbb{E}[Z]| < \frac{1}{2}\epsilon.$$

Observing that for all  $N \geq N_1$ ,

$$\begin{aligned} |\bar{Z} - \mathbb{E}[Z]| &= |\bar{Z} - \mathbb{E}^{(N)}[Z] + \mathbb{E}^{(N)}[Z] - \mathbb{E}[Z]| \\ &\leq |\bar{Z} - \mathbb{E}^{(N)}[Z]| + |\mathbb{E}^{(N)}[Z] - \mathbb{E}[Z]| \\ &< |\mathbb{E}^{(N)}[Z] - \mathbb{E}[Z]| + \frac{1}{2}\epsilon, \end{aligned}$$

we have that

$$\begin{aligned} \mathbb{P}^{(N)}(|\bar{Z} - \mathbb{E}[Z]| > \epsilon) &\leq \mathbb{P}^{(N)}\left(|\bar{Z} - \mathbb{E}^{(N)}[Z]| + \frac{1}{2}\epsilon > \epsilon\right) \\ &= \mathbb{P}^{(N)}\left(|\bar{Z} - \mathbb{E}^{(N)}[Z]| > \frac{1}{2}\epsilon\right) \\ &\leq \frac{\text{Var}^{(N)}(\bar{Z})}{\left(\frac{1}{2}\epsilon\right)^2} \end{aligned}$$

by Chebyshev's inequality. Now, in part 1 of the proof, we have shown that  $\text{Var}^{(N)}(\bar{Z}) \rightarrow 0$  as  $N \rightarrow \infty$ . Therefore, for any  $\delta > 0$ , there exists some  $N_2 \in \mathbb{N}$ , such that for all  $N \geq N_2$ ,

$$\text{Var}^{(N)}(\bar{Z}) < \delta \left(\frac{1}{2}\epsilon\right)^2.$$

It follows that for all  $N \geq \max\{N_1, N_2\}$ ,

$$\mathbb{P}^{(N)}(|\bar{Z} - \mathbb{E}[Z]| > \epsilon) \leq \delta.$$

By definition of limit, we have  $\mathbb{P}^{(N)}(|\bar{Z} - \mathbb{E}[Z]| > \epsilon) \rightarrow 0$  as  $N \rightarrow \infty$ . Because this holds true for any  $\epsilon > 0$ , we conclude that  $\bar{Z}$  converges to  $\mathbb{E}[Z]$  in probability.  $\square$

By applying the continuous mapping theorem to Lemma EC.1, we establish that Proposition 1 holds true.

## Appendix B: Proofs of Propositions 2 and 3

For proofs in the section, the subscript **POOL** (or  $\alpha$ ) is dropped when a quantity/operator does not depend on the pooling method (or prevalence level).

We first show that sample viral loads within pool  $J$  are identically distributed, under both  $\mathbb{P}_{\text{NP},\alpha}$  and  $\mathbb{P}_{\text{CP},\alpha}$ .

**LEMMA EC.2.** *The viral loads  $V_i : i = 1, \dots, n$  in pool  $J$  are identically distributed under  $\mathbb{P}_{\text{NP},\alpha}$ . They also follow the same distribution under  $\mathbb{P}_{\text{CP},\alpha}$ .*

It is worth noting that our model does accommodate heterogeneity in viral load across individuals. This property of identical distribution described in Lemma EC.2 arises from applying an independent random permutation to shuffle the samples within each pool after their formation, facilitating the proofs thereafter.

*Proof of Lemma EC.2.* Let  $I$  denote the population index of an arbitrary individual from the naive pool. Because naive pools are formed by picking individuals uniformly at random from the population,  $I \sim U(\{1, \dots, N\})$ . That is,  $\mathbb{P}_{\text{NP},\alpha}^{(N)}(I = i) = \frac{1}{N}$  for all  $i = 1, \dots, N$ . The cdf of the viral load of this sample is

$$\begin{aligned} \mathbb{P}_{\text{NP},\alpha}^{(N)}(V_I \leq v) &= \sum_{i=1}^N \mathbb{P}_{\text{NP}}^{(N)}(I = i) \mathbb{P}_{\alpha}^{(N)}(V_i \leq v) \\ &= \sum_{i=1}^N \frac{1}{N} \mathbb{P}_{\alpha}^{(N)}(V_i \leq v). \end{aligned}$$

Suppose the correlated pool being studied is the  $J$ th of the  $|\mathcal{A}|$  correlated pools. Because the correlated pool we are studying is chosen randomly from the  $|\mathcal{A}|$  pools,  $\mathbb{P}^{(N)}(J = j') = \frac{1}{|\mathcal{A}|}$  for all  $j' = 1, \dots, |\mathcal{A}|$ . Now consider an arbitrary individual from this pool, and suppose this individual is the  $i$ th of this pool. Recall that we reordered samples in each pool by performing an independent random permutation of 1 through  $n$ , denoted by  $\pi$ . Then, the index of  $i$  before the permutation is uniformly distributed over  $\{1, \dots, N\}$ , that is,  $\mathbb{P}^{(N)}(\pi(i') = i) = \frac{1}{n}$  for all  $i' = 1, \dots, n$ . Hence, the cdf of the sample viral load of this arbitrary individual from the correlated pool is given by

$$\begin{aligned} \mathbb{P}_{\text{CP},\alpha}^{(N)}(V_{J,i} \leq v) &= \sum_{j'=1}^{|\mathcal{A}|} \sum_{i'=1}^n \mathbb{P}^{(N)}(J = j') \mathbb{P}^{(N)}(\pi(i') = i) \mathbb{P}_{\alpha}^{(N)}(V_{j',i'} \leq v) \\ &= \frac{1}{|\mathcal{A}|} \frac{1}{n} \sum_{j'=1}^{|\mathcal{A}|} \sum_{i'=1}^n \mathbb{P}_{\alpha}^{(N)}(V_{j',i'} \leq v) \\ &= \frac{1}{N} \sum_{j'=1}^{|\mathcal{A}|} \sum_{i'=1}^n \mathbb{P}_{\alpha}^{(N)}(V_{j',i'} \leq v) \\ &= \sum_{k=1}^N \frac{1}{N} \mathbb{P}_{\alpha}^{(N)}(V_k \leq v), \end{aligned}$$

where the last equality follows from the observation that this double sum is equivalent to summing over all individuals in  $\{1, \dots, N\}$ . This is identical to the cdf of the viral load of an individual chosen uniformly at random from the naive pool.

Because  $\mathbb{P}_{\text{NP},\alpha}^{(N)}(V_{J,i} \leq v) = \mathbb{P}_{\text{CP},\alpha}^{(N)}(V_{J,i'} \leq v)$  for all  $N$  and  $i, i' \in \{1, \dots, n\}$ , taking  $N$  to the limit of infinity keeps the equality, i.e.,

$$\mathbb{P}_{\text{NP},\alpha}^{(N)}(V_{J,i} \leq v) = \mathbb{P}_{\text{CP},\alpha}^{(N)}(V_{J,i'} \leq v), \quad \forall i, i' \in \{1, \dots, n\}.$$

We are done.  $\square$

### B.1. A Second Model of Association

Analogous to the association model introduced in Appendix A.1, we further define a second measure of association, between the viral loads of one individual  $i$  and a group of individuals  $\mathbf{j}$  whose population indices are denoted  $\{j_1, \dots, j_{|\mathbf{j}|}\}$ :

$$\Lambda_{\alpha}^{(N)}(i, \mathbf{j}) = \sup_{\substack{u \in \mathbb{R}_{\geq 0} \\ \mathbf{u} \in \mathbb{R}_{\geq 0}^{|\mathbf{j}|}}} \left| \mathbb{P}_{\alpha}^{(N)}(U_i \leq u \mid U_{\mathbf{j}} = \mathbf{u}) - \mathbb{P}_{\alpha}^{(N)}(U_i \leq u \mid U_{\mathbf{j}} = \mathbf{u}) \right|.$$

where  $U_{\mathbf{j}} = (U_{j_1}, \dots, U_{j_{|\mathbf{j}|}})$ . This measure quantifies the maximize change in the cdf of  $i$ 's viral load with respect to the viral loads of  $\mathbf{j}$ . It reflects the degree to which conditioning on the viral loads of  $\mathbf{j}$  affects the viral load of  $i$ . A larger  $\Lambda_{\alpha}^{(N)}(i, \mathbf{j})$  indicates a stronger association between  $i$  and  $\mathbf{j}$ . The collection of individuals having association with  $\mathbf{j}$  stronger than  $\epsilon$  is

$$\{i : i \notin \mathbf{j}, \Lambda_{\alpha}^{(N)}(i, \mathbf{j}) > \epsilon\}.$$

We denote by  $d_{\alpha}^{(N)}(\epsilon)$  the maximum size of such sets, across any collection  $\mathbf{j}$  of at most  $n - 1$  individuals:

$$d_{\alpha}^{(N)}(\epsilon) = \max_{\mathbf{j} \subset \{1, \dots, N\}, |\mathbf{j}| < n} |\{i : i \notin \mathbf{j}, \Lambda_{\alpha}^{(N)}(i, \mathbf{j}) > \epsilon\}|. \quad (\text{EC.1})$$

When  $d_{\alpha}^{(N)}(\epsilon)$  is small relative to  $N$ , when we add an individual  $i$  to the pool who is chosen uniformly from the larger population, they are unlikely to be in a set with high association  $\Lambda_{\alpha}^{(N)}(i, \mathbf{j}) > \epsilon$  with the individuals already in the pool. This makes the viral loads in the pool unlikely to be strongly correlated.

Now we take  $N$  to the asymptotic regime and make the following assumption.

ASSUMPTION EC.2. *There exists a sequence  $\epsilon_N \downarrow 0$  such that  $\lim_{N \rightarrow \infty} \frac{1}{N} d_{\alpha}^{(N)}(\epsilon_N) = 0$ .*

Assumption EC.2 prescribes that as population size  $N$  goes to infinity, for any collection  $\mathbf{j}$  of individuals of size less than  $n$ , the set of individuals that have association stronger than  $\epsilon_N$  with  $\mathbf{j}$  grows slower than linearly in population size. The same arguments for Assumption EC.1 apply when justifying this assumption.

## B.2. Proof of Proposition 2

*Proof of Proposition 2.* For succinctness, let random variables  $[1], [2], \dots, [n]$  be the population indices of the individuals placed into this randomly chosen naive pool  $J$ .

To prove the proposition, we want to show that the joint cdf of viral loads in a naive pool factors into a product of cdf's of individual viral loads as  $N \rightarrow \infty$ . Let  $\mathbf{u} \in \mathbb{R}_{\geq 0}^n$ . We first use the law of conditional probability to expand the joint cdf:

$$\begin{aligned} & \mathbb{P}_{\text{NP}, \alpha}^{(N)}(U_{[1]} \leq u_1, \dots, U_{[n-1]} \leq u_{n-1}, U_{[n]} \leq u_n) \\ &= \mathbb{P}_{\text{NP}, \alpha}^{(N)}(U_{[1]} \leq u_1, \dots, U_{[n-1]} \leq u_{n-1}) \cdot \mathbb{P}_{\text{NP}, \alpha}^{(N)}(U_{[n]} \leq u_n \mid U_{[1]} \leq u_1, \dots, U_{[n-1]} \leq u_{n-1}). \end{aligned} \quad (\text{EC.2})$$

To analyze the conditional probability in the second term of Equation EC.2, we first make the following claim: For all  $\mathbf{j} \subset \{1, \dots, N\}$  with  $|\mathbf{j}| = n - 1$  and  $i \notin \mathbf{j}$ ,

$$|\mathbb{P}_{\alpha}^{(N)}(U_i \leq u_n \mid U_{j_1} \leq u_1, \dots, U_{j_{n-1}} \leq u_{n-1}) - \mathbb{P}_{\alpha}^{(N)}(U_i \leq u_n)| \leq \Lambda_{\alpha}^{(N)}(i, \mathbf{j}). \quad (\text{EC.3})$$

To prove Claim EC.3, we first expand and bound its conditional probability:

$$\begin{aligned} & \mathbb{P}_{\alpha}^{(N)}(U_i \leq u_n \mid U_{j_1} \leq u_1, \dots, U_{j_{n-1}} \leq u_{n-1}) \\ &= \frac{\mathbb{P}_{\alpha}^{(N)}(U_i \leq u_n, U_{j_1} \leq u_1, \dots, U_{j_{n-1}} \leq u_{n-1})}{\mathbb{P}_{\alpha}^{(N)}(U_{j_1} \leq u_1, \dots, U_{j_{n-1}} \leq u_{n-1})} \\ &= \frac{\int_{\mathbf{z} \in [0, u_1] \times \dots \times [0, u_{n-1}]} \mathbb{P}_{\alpha}^{(N)}(U_i \leq u_n \mid U_{j_1} = z_1, \dots, U_{j_{n-1}} = z_{n-1}) f(U_{j_1} = z_1, \dots, U_{j_{n-1}} = z_{n-1}) \mathbf{d}\mathbf{z}'}{\int_{\mathbf{z} \in [0, u_1] \times \dots \times [0, u_{n-1}]} f(U_{j_1} = z'_1, \dots, U_{j_{n-1}} = z'_{n-1}) \mathbf{d}\mathbf{z}'} \\ &\in \left[ \inf_{\mathbf{z} \in \mathbb{R}_{\geq 0}^{n-1}} \mathbb{P}_{\alpha}^{(N)}(U_i \leq u_n \mid U_{j_1} = z_1, \dots, U_{j_{n-1}} = z_{n-1}), \sup_{\mathbf{z} \in \mathbb{R}_{\geq 0}^{n-1}} \mathbb{P}_{\alpha}^{(N)}(U_i \leq u_n \mid U_{j_1} = z_1, \dots, U_{j_{n-1}} = z_{n-1}) \right]. \end{aligned}$$



Then, the proof of Claim EC.3 becomes straightforward:

$$\begin{aligned}
& \left| \mathbb{P}_\alpha^{(N)}(U_i \leq u_n \mid U_{j_1} \leq u_1, \dots, U_{j_{n-1}} \leq u_{n-1}) - \mathbb{P}_\alpha^{(N)}(U_i \leq u_n) \right| \\
\leq & \max \left\{ \left| \inf_{\mathbf{z} \in \mathbb{R}_{\geq 0}^{n-1}} \mathbb{P}_\alpha^{(N)}(U_i \leq u_n \mid U_{j_1} = z_1, \dots, U_{j_{n-1}} = z_{n-1}) - \mathbb{P}_\alpha^{(N)}(U_i \leq u_n) \right|, \right. \\
& \left. \left| \sup_{\mathbf{z} \in \mathbb{R}_{\geq 0}^{n-1}} \mathbb{P}_\alpha^{(N)}(U_i \leq u_n \mid U_{j_1} = z_1, \dots, U_{j_{n-1}} = z_{n-1}) - \mathbb{P}_\alpha^{(N)}(U_i \leq u_n) \right| \right\} \\
\leq & \sup_{\mathbf{z} \in \mathbb{R}_{\geq 0}^{n-1}} \left| \mathbb{P}_\alpha^{(N)}(U_i \leq u_n \mid U_{j_1} = z_1, \dots, U_{j_{n-1}} = z_{n-1}) - \mathbb{P}_\alpha^{(N)}(U_i \leq u_n) \right| \\
\leq & \sup_{\substack{u_n \in \mathbb{R}_{\geq 0} \\ \mathbf{z} \in \mathbb{R}_{\geq 0}^{n-1}}} \left| \mathbb{P}_\alpha^{(N)}(U_i \leq u_n \mid U_{j_1} = z_1, \dots, U_{j_{n-1}} = z_{n-1}) - \mathbb{P}_\alpha^{(N)}(U_i \leq u_n) \right| \\
= & \Lambda_\alpha^{(N)}(i, \mathbf{j}).
\end{aligned}$$

Claim EC.3 enables a closer analysis of the conditional probability in Equation EC.2. Using the law of iterated expectations where we condition on  $[1], [2], \dots, [n]$  (hereafter abbreviated as  $[1:n]$ ), we have that

$$\begin{aligned}
& \mathbb{P}_{\text{NP},\alpha}^{(N)}(U_{[n]} \leq u_n \mid U_{[1]} \leq u_1, \dots, U_{[n-1]} \leq u_{n-1}) \\
= & \mathbb{E}_{\text{NP},\alpha}^{(N)} \left[ \mathbb{P}_\alpha^{(N)}(U_{[n]} \leq u_n \mid U_{[1]} \leq u_1, \dots, U_{[n-1]} \leq u_{n-1}, [1:n]) \right] \\
\leq & \mathbb{E}_{\text{NP},\alpha}^{(N)} \left[ \mathbb{P}_\alpha^{(N)}(U_{[n]} \leq u_n \mid [n]) + \Lambda_\alpha^{(N)}([n], [1:n-1]) \right] \\
= & \mathbb{P}_{\text{NP},\alpha}^{(N)}(U_{[n]} \leq u_n) + \mathbb{E}_{\text{NP},\alpha}^{(N)} \left[ \Lambda_\alpha^{(N)}([n], [1:n-1]) \right]. \tag{EC.4}
\end{aligned}$$

We consider two cases for the expectation in the second term. For any  $\epsilon > 0$ ,  $\Lambda_\alpha^{(N)}([n], [1:n-1])$  could either be less than  $\epsilon$ , or greater than  $\epsilon$  but upper bounded by 1. That is,

$$\begin{aligned}
\mathbb{E}_{\text{NP},\alpha}^{(N)} \left[ \Lambda_\alpha^{(N)}([n], [1:n-1]) \right] & \leq 1 \cdot \mathbb{P}_{\text{NP},\alpha}^{(N)}(\Lambda_\alpha^{(N)}([n], [1:n-1]) > \epsilon) + \epsilon \cdot \mathbb{P}_{\text{NP},\alpha}^{(N)}(\Lambda_\alpha^{(N)}([n], [1:n-1]) \leq \epsilon) \\
& \leq \mathbb{P}_{\text{NP},\alpha}^{(N)}(\Lambda_\alpha^{(N)}([n], [1:n-1]) > \epsilon) + \epsilon. \tag{EC.5}
\end{aligned}$$

Now, we unpack the first term in this expression.

$$\begin{aligned}
\mathbb{P}_{\text{NP},\alpha}^{(N)}(\Lambda_\alpha^{(N)}([n], [1:n-1]) > \epsilon) & = \mathbb{E}_{\text{NP},\alpha}^{(N)} \left[ \mathbb{P}_{\text{NP},\alpha}^{(N)}(\Lambda_\alpha^{(N)}([n], [1:n-1]) > \epsilon \mid [1:n-1]) \right] \\
& = \mathbb{E}_{\text{NP},\alpha}^{(N)} \left[ \frac{|\{i : \Lambda_\alpha^{(N)}(i, [1:n-1]) > \epsilon\}|}{N - (n-1)} \mid [1:n-1] \right] \\
& \quad \text{because under } \mathbb{P}_{\text{NP},\alpha}^{(N)}, [n] \text{ takes values other than } [1:n-1] \text{ with equal probability} \\
& \leq \mathbb{E}_{\text{NP},\alpha}^{(N)} \left[ \frac{d_\alpha^{(N)}(\epsilon)}{N - (n-1)} \mid [1:n-1] \right] \quad \text{by Equation EC.1} \\
& = \frac{d_\alpha^{(N)}(\epsilon)}{N - (n-1)}.
\end{aligned}$$

Plugging this result back to Equations EC.5 and EC.4, we have the following for each  $\epsilon > 0$ :

$$\begin{aligned}
& \mathbb{P}_{\text{NP},\alpha}^{(N)}(U_{[n]} \leq u_n \mid U_{[1]} \leq u_1, \dots, U_{[n-1]} \leq u_{n-1}) \\
= & \mathbb{P}_{\text{NP},\alpha}^{(N)}(U_{[n]} \leq u_n) + \mathbb{E}_{\text{NP},\alpha}^{(N)} \left[ \Lambda_\alpha^{(N)}([n], [1:n-1]) \right] \\
\leq & \mathbb{P}_{\text{NP},\alpha}^{(N)}(U_{[n]} \leq u_n) + \frac{d_\alpha^{(N)}(\epsilon)}{N - (n-1)} + \epsilon. \tag{EC.6}
\end{aligned}$$

We can apply Bound EC.6 to iteratively decompose and bound the full joint cdf in Equation EC.2.

$$\begin{aligned}
& \mathbb{P}_{\text{NP},\alpha}^{(N)}(U_{[1]} \leq u_1, \dots, U_{[n-1]} \leq u_{n-1}, U_{[n]} \leq u_n) \\
&= \mathbb{P}_{\text{NP},\alpha}^{(N)}(U_{[1]} \leq u_1, \dots, U_{[n-1]} \leq u_{n-1}) \cdot \mathbb{P}_{\text{NP},\alpha}^{(N)}(U_{[n]} \leq u_n \mid U_{[1]} \leq u_1, \dots, U_{[n-1]} \leq u_{n-1}) \\
&\leq \mathbb{P}_{\text{NP},\alpha}^{(N)}(U_{[1]} \leq u_1, \dots, U_{[n-1]} \leq u_{n-1}) \cdot \left( \mathbb{P}_{\text{NP},\alpha}^{(N)}(U_{[n]} \leq u_n) + \frac{d_\alpha^{(N)}(\epsilon)}{N - (n-1)} + \epsilon \right) \\
&\leq \mathbb{P}_{\text{NP},\alpha}^{(N)}(U_{[1]} \leq u_1, \dots, U_{[n-2]} \leq u_{n-2}) \cdot \left( \mathbb{P}_{\text{NP},\alpha}^{(N)}(U_{[n]} \leq u_n) + \frac{d_\alpha^{(N)}(\epsilon)}{N - (n-1)} + \epsilon \right) \\
&\quad \cdot \left( \mathbb{P}_{\text{NP},\alpha}^{(N)}(U_{[n-1]} \leq u_{n-1}) + \frac{d_\alpha^{(N)}(\epsilon)}{N - (n-2)} + \epsilon \right) \\
&\leq \dots \\
&\leq \prod_{k=1}^n \left( \mathbb{P}_{\text{NP},\alpha}^{(N)}(U_{[k]} \leq u_k) + \frac{d_\alpha^{(N)}(\epsilon)}{N - (n-k)} + \epsilon \right) \\
&\leq \prod_{k=1}^n \left( \mathbb{P}_{\text{NP},\alpha}^{(N)}(U_{[k]} \leq u_k) + \frac{d_\alpha^{(N)}(\epsilon)}{N - n} + \epsilon \right).
\end{aligned}$$

Let  $\epsilon_N$  be a sequence satisfying Assumption EC.2, i.e.,  $\epsilon_N \downarrow 0$  and  $\lim_{N \rightarrow \infty} \frac{1}{N} d_\alpha^{(N)}(\epsilon_N) = 0$ . Taking the limit  $N \rightarrow \infty$  of the expression above, we have

$$\begin{aligned}
\lim_{N \rightarrow \infty} \mathbb{P}_{\text{NP},\alpha}^{(N)}(U_{[1]} \leq u_1, \dots, U_{[n-1]} \leq u_{n-1}, U_{[n]} \leq u_n) &\leq \lim_{N \rightarrow \infty} \prod_{k=1}^n \left( \mathbb{P}_{\text{NP},\alpha}^{(N)}(U_{[k]} \leq u_k) + \frac{d_\alpha^{(N)}(\epsilon_N)}{N - n} + \epsilon_N \right) \\
&= \lim_{N \rightarrow \infty} \prod_{k=1}^n \mathbb{P}_{\text{NP},\alpha}^{(N)}(U_{[k]} \leq u_k).
\end{aligned}$$

Similarly, we can use the other direction of Inequality EC.3 to derive a lower bound counterpart to Inequality EC.4:

$$\begin{aligned}
& \mathbb{P}_{\text{NP},\alpha}^{(N)}(U_{[n]} \leq u_n \mid U_{[1]} \leq u_1, \dots, U_{[n-1]} \leq u_{n-1}) \\
&\geq \mathbb{E}_{\text{NP},\alpha}^{(N)} \left[ \mathbb{P}_{\text{NP},\alpha}^{(N)}(U_{[n]} \leq u_n \mid [n]) - \Lambda_\alpha^{(N)}([n], [1 : n-1]) \right] \\
&= \mathbb{P}_{\text{NP},\alpha}^{(N)}(U_{[n]} \leq u_n) - \mathbb{E}_{\text{NP},\alpha}^{(N)} \left[ \Lambda_\alpha^{(N)}([n], [1 : n-1]) \right].
\end{aligned} \tag{EC.7}$$

Applying Inequality EC.7 to Equation EC.2, we derive a lower bound for the joint cumulative distribution function:

$$\mathbb{P}_{\text{NP},\alpha}^{(N)}(U_{[1]} \leq u_1, \dots, U_{[n-1]} \leq u_{n-1}, U_{[n]} \leq u_n) \geq \prod_{k=1}^n \left( \mathbb{P}_{\text{NP},\alpha}^{(N)}(U_{[k]} \leq u_k) - \frac{d_\alpha^{(N)}(\epsilon)}{N - n} - \epsilon \right).$$

For the same sequence of  $\epsilon_N$  satisfying Assumption EC.2, we have

$$\begin{aligned}
\lim_{N \rightarrow \infty} \mathbb{P}_{\text{NP},\alpha}^{(N)}(U_{[1]} \leq u_1, \dots, U_{[n-1]} \leq u_{n-1}, U_{[n]} \leq u_n) &\geq \lim_{N \rightarrow \infty} \prod_{k=1}^n \left( \mathbb{P}_{\text{NP},\alpha}^{(N)}(U_{[k]} \leq u_k) - \frac{d_\alpha^{(N)}(\epsilon_N)}{N - n} - \epsilon_N \right) \\
&= \lim_{N \rightarrow \infty} \prod_{k=1}^n \mathbb{P}_{\text{NP},\alpha}^{(N)}(U_{[k]} \leq u_k).
\end{aligned}$$

Since the lower and upper bounds coincide, we have that

$$\lim_{N \rightarrow \infty} \mathbb{P}_{\text{NP},\alpha}^{(N)}(U_{[1]} \leq u_1, \dots, U_{[n-1]} \leq u_{n-1}, U_{[n]} \leq u_n) = \lim_{N \rightarrow \infty} \prod_{k=1}^n \mathbb{P}_{\text{NP},\alpha}^{(N)}(U_{[k]} \leq u_k),$$

i.e.,

$$\mathbb{P}_{\text{NP},\alpha}(U_{[1]} \leq u_1, \dots, U_{[n-1]} \leq u_{n-1}, U_{[n]} \leq u_n) = \prod_{k=1}^n \mathbb{P}_{\text{NP},\alpha}(U_{[k]} \leq u_k),$$

which concludes the proof.  $\square$

### B.3. Proof of Proposition 3

*Proof of Proposition 3.* For succinctness, we abbreviate the probability operator  $\mathbb{P}_{\text{CP},\alpha}^{(N)}(\cdot)$  and the expectation operator  $\mathbb{E}_{\text{CP},\alpha}^{(N)}[\cdot]$  as  $\mathbb{P}(\cdot)$  and  $\mathbb{E}[\cdot]$  in Appendix B.3.

For a generic pool  $j \in \{1, \dots, |\mathcal{A}|\}$ , let  $I(j)$  be the sample in pool  $A_j$  with nonzero infection probability and the smallest population index,  $I(j) = \min\{i : \mathbb{P}(U_i > 0) > 0, i \in A_j\}$ . If such a sample does not exist in  $A_j$ , then  $I(j) = \infty$ . Let  $C_{I(j)}$  denote the set of  $I(j)$ 's close contacts and  $K(j)$  denote an individual selected uniformly at random from  $C_{I(j)}$ . Let  $S_j = \sum_{i \in A_j} \mathbb{1}\{U_i > 0\}$ . Since the pooling assignment  $\mathcal{A}$  is a random variable,  $A_j$ ,  $I(j)$  and  $C_{I(j)}$  are all random. We make the following observation: if sample  $I(j)$  is positive, sample  $K(j)$  is positive, and  $K(j)$  is also in pool  $j$ , then pool  $j$  must contain more than one positive. Therefore,

$$\begin{aligned} \mathbb{P}(S_j > 1) &= \mathbb{P}(S_j > 1 \mid I(j) < \infty) \cdot \mathbb{P}(I(j) < \infty) \\ &\geq \mathbb{P}(U_{I(j)} > 0, U_{K(j)} > 0, K(j) \in A_j \mid I(j) < \infty) \cdot \mathbb{P}\left(\sum_{i \in A_j} \mathbb{P}(U_i > 0) > 0\right) \\ &= \mathbb{P}(U_{I(j)} > 0 \mid I(j) < \infty) \cdot \mathbb{P}(U_{K(j)} > 0 \mid U_{I(j)} > 0, I(j) < \infty) \\ &\quad \mathbb{P}(K(j) \in A_j \mid U_{I(j)} > 0, U_{K(j)} > 0, I(j) < \infty) \cdot \mathbb{P}\left(\sum_{i \in A_j} \mathbb{P}(U_i > 0) > 0\right) \\ &= \mathbb{P}(U_{I(j)} > 0 \mid I(j) < \infty) \cdot \mathbb{P}(U_{K(j)} > 0 \mid U_{I(j)} > 0, I(j) < \infty) \cdot \mathbb{P}(K(j) \in A_j) \cdot \mathbb{P}\left(\sum_{i \in A_j} \mathbb{P}(U_i > 0) > 0\right) \\ &\quad \text{since pooling assignment is assumed to be independent of viral loads} \\ &\geq \epsilon_0 \alpha \cdot c_1 \cdot c_2 \cdot \mathbb{P}\left(\sum_{i \in A_j} \mathbb{P}(U_i > 0) > 0\right) \quad \text{by Assumption 1.} \end{aligned}$$

We generalize this result to a pool  $J$  selected uniformly at random from all pools.

$$\begin{aligned} \mathbb{P}(S > 1) &= \sum_{j=1}^{|\mathcal{A}|} \mathbb{P}(S_j > 1) \mathbb{P}(J = j) \\ &= \frac{1}{|\mathcal{A}|} \sum_{j=1}^{|\mathcal{A}|} \mathbb{P}(S_j > 1) \\ &\geq \frac{1}{|\mathcal{A}|} \sum_{j=1}^{|\mathcal{A}|} \epsilon_0 \alpha \cdot c_1 \cdot c_2 \cdot \mathbb{P}\left(\sum_{i \in A_j} \mathbb{P}(U_i > 0) > 0\right) \\ &= \epsilon_0 \alpha \cdot c_1 \cdot c_2 \cdot \frac{1}{|\mathcal{A}|} \sum_{j=1}^{|\mathcal{A}|} \mathbb{P}\left(\sum_{i \in A_j} \mathbb{P}(U_i > 0) > 0\right). \end{aligned} \tag{EC.8}$$

On the other hand, for a fixed pooling assignment  $\mathcal{A}$ , the probability that a generic pool  $j$  contains one or more positives can be bounded above:

$$\begin{aligned} \mathbb{P}(S_j > 0 \mid \mathcal{A}) &= \mathbb{P}\left(\bigcup_{i \in A_j} \mathbb{1}\{U_i > 0\} \mid \mathcal{A}\right) \\ &\leq \sum_{i \in A_j} \mathbb{P}(U_i > 0 \mid \mathcal{A}) \quad \text{by the union bound} \end{aligned}$$

$$\begin{aligned}
&= \sum_{i \in A_j} \mathbb{P}(U_i > 0 \mid \mathcal{A}) \cdot \mathbb{1} \left\{ \sum_{i \in A_j} \mathbb{P}(U_i > 0) > 0 \mid \mathcal{A} \right\} \\
&= \sum_{i \in A_j} \mathbb{P}(U_i > 0) \cdot \mathbb{1} \left\{ \sum_{i \in A_j} \mathbb{P}(U_i > 0) > 0 \mid \mathcal{A} \right\} \\
&\quad \text{since viral load does not depend on pooling assignment} \\
&\leq \Pi_0 \alpha \cdot n \cdot \mathbb{1} \left\{ \sum_{i \in A_j} \mathbb{P}(U_i > 0) > 0 \mid \mathcal{A} \right\} \quad \text{by Assumption 1.} \tag{EC.9}
\end{aligned}$$

We now generalize the result in Equation EC.9 to a pool  $J$  selected uniformly at random from all pools and all pooling assignments:

$$\begin{aligned}
\mathbb{P}(S > 0) &= \sum_{j=1}^{|\mathcal{A}|} \mathbb{E}_{\mathcal{A}} [\mathbb{P}(S_j > 0 \mid \mathcal{A})] \cdot \mathbb{P}(J = j) \\
&= \frac{1}{|\mathcal{A}|} \sum_{j=1}^{|\mathcal{A}|} \mathbb{E}_{\mathcal{A}} [\mathbb{P}(S_j > 0 \mid \mathcal{A})] \\
&\leq \frac{1}{|\mathcal{A}|} \sum_{j=1}^{|\mathcal{A}|} \Pi_0 \alpha \cdot n \cdot \mathbb{E}_{\mathcal{A}} \left[ \mathbb{1} \left\{ \sum_{i \in A_j} \mathbb{P}(U_i > 0) > 0 \mid \mathcal{A} \right\} \right] \\
&= \Pi_0 \alpha \cdot n \cdot \frac{1}{|\mathcal{A}|} \sum_{j=1}^{|\mathcal{A}|} \mathbb{P} \left( \sum_{i \in A_j} \mathbb{P}(U_i > 0) > 0 \right). \tag{EC.10}
\end{aligned}$$

Combining Equations EC.8 and EC.10, we find

$$\begin{aligned}
\mathbb{P}(S > 1 \mid S > 0) &= \frac{\mathbb{P}(S > 1)}{\mathbb{P}(S > 0)} \\
&\geq \frac{\epsilon_0 \alpha \cdot c_1 \cdot c_2}{\Pi_0 \alpha \cdot n} \\
&= \frac{\epsilon_0 \cdot c_1 \cdot c_2}{\Pi_0 \cdot n},
\end{aligned}$$

which is a positive constant that does not depend on  $\alpha$  or  $N$ . Taking  $N$  to the limit of infinity proves the proposition.  $\square$

## Appendix C: Proofs of Theorems 1, 2 and Corollary 1

### C.1. Proof of Theorem 1

*Proof of Theorem 1.* For  $\text{POOL} \in \{\text{NP}, \text{CP}\}$ , we have that the overall false negative rate is given by

$$\begin{aligned}
\beta_{\text{POOL}, \alpha} &= 1 - \frac{\mathbb{E}_{\text{POOL}, \alpha} [\# \text{ positives identified in a pool}]}{\mathbb{E}_{\text{POOL}, \alpha} [\# \text{ positives in a pool}]} \\
&= 1 - \frac{\mathbb{E}_{\text{POOL}, \alpha} [D]}{n\alpha} \\
&= 1 - \frac{\mathbb{E}_{\text{POOL}, \alpha} [\sum_{i=1}^n YW_i]}{n\alpha} \\
&= 1 - \frac{1}{n\alpha} \cdot \sum_{i=1}^n \mathbb{E}_{\text{POOL}, \alpha} [YW_i] \\
&= 1 - \frac{1}{n\alpha} \cdot \sum_{i=1}^n \mathbb{E}_{\text{POOL}, \alpha} [\mathbb{E}_{\text{POOL}, \alpha} [YW_i \mid V_{1:n}]] \\
&= 1 - \frac{1}{n\alpha} \cdot \sum_{i=1}^n \mathbb{E}_{\text{POOL}, \alpha} [\mathbb{E}_{\text{POOL}, \alpha} [Y \mid V_{1:n}] \mathbb{E}_{\text{POOL}, \alpha} [W_i \mid V_i]].
\end{aligned}$$

In both correlated pooling and naive pooling, all  $V_i$ 's are identically distributed by Lemma EC.2, which follows that  $(\mathbb{E}_{\text{POOL},\alpha}[Y | V_{1:n}], \mathbb{E}_{\text{POOL},\alpha}[W_i | V_i])$  are also identically distributed. Hence, we obtain that

$$\begin{aligned}\beta_{\text{POOL},\alpha} &= 1 - \frac{1}{n\alpha} \cdot n \cdot \mathbb{E}_{\text{POOL},\alpha}[\mathbb{E}_{\text{POOL},\alpha}[Y | V_{1:n}]\mathbb{E}_{\text{POOL},\alpha}[W_1 | V_1]] \\ &= 1 - \frac{1}{\alpha} \cdot \mathbb{E}_{\text{POOL},\alpha}[p(\bar{V}_n)p(V_1)] \quad \text{where } \bar{V}_n = \frac{1}{n} \sum_{i=1}^n V_i \\ &= 1 - \frac{1}{\alpha} \mathbb{E}_{\text{POOL},\alpha}[p(\bar{V}_n)p(V_1) | V_1 > 0] \mathbb{P}_\alpha(V_1 > 0) \\ &= 1 - \mathbb{E}_{\text{POOL},\alpha}[p(\bar{V}_n)p(V_1) | V_1 > 0].\end{aligned}\tag{EC.11}$$

For naive pooling, the  $V_i$ 's are i.i.d. Hence,

$$\begin{aligned}\beta_{\text{NP},\alpha} &= 1 - \sum_{\ell=1}^n \mathbb{E}_{\text{NP},\alpha}[p(\bar{V}_n)p(V_1) | V_1 > 0, S = \ell] \mathbb{P}_{\text{NP},\alpha}(S = \ell | V_1 > 0) \quad \text{recall that } S = \sum_{i=1}^n \mathbb{1}\{V_i > 0\} \\ &= 1 - \sum_{\ell=1}^n \mathbb{E}_{\text{NP},\alpha}[p(\bar{V}_n)p(V_1) | V_1 > 0, S = \ell] \binom{n-1}{\ell-1} \alpha^{\ell-1} (1-\alpha)^{n-\ell}.\end{aligned}$$

Taking  $\alpha \rightarrow 0^+$  gives

$$\begin{aligned}\lim_{\alpha \rightarrow 0^+} \beta_{\text{NP},\alpha} &= \lim_{\alpha \rightarrow 0^+} \left( 1 - \mathbb{E}_{\text{NP},\alpha}[p(\bar{V}_n)p(V_1) | V_1 > 0, S = 1] \binom{n-1}{1-1} \alpha^{1-1} (1-\alpha)^{n-1} \right) \\ &= 1 - \mathbb{E} \left[ p \left( \frac{1}{n} V_1 \right) p(V_1) | V_1 > 0 \right].\end{aligned}$$

Similarly, we derive  $\beta_{\text{CP},\alpha}$  for correlated pooling. Following Equation EC.11 we have that

$$\begin{aligned}\beta_{\text{CP},\alpha} &= 1 - \sum_{\ell=1}^n \mathbb{E}_{\text{CP},\alpha}[p(\bar{V}_n)p(V_1) | V_1 > 0, S = \ell] \mathbb{P}_{\text{CP},\alpha}(S = \ell | V_1 > 0) \\ &\triangleq 1 - \sum_{\ell=1}^n A_\ell \cdot \mathbb{P}_{\text{CP},\alpha}(S = \ell | S > 0)\end{aligned}$$

where  $A_\ell \triangleq \mathbb{E}_{\text{CP},\alpha}[p(\bar{V}_n)p(V_1) | V_1 > 0, S = \ell]$ .

When  $\ell = 1$ ,  $A_1 = \mathbb{E}[p(\frac{1}{n}V_1)p(V_1) | V_1 > 0]$ . When  $\ell \geq 2$ , we have  $\bar{V}_n > \frac{1}{n}V_1$  because there exists at least one  $i \neq 1$  such that  $V_i > 0$ . Assuming  $p(v)$  is a monotone increasing function in  $v$ , we obtain  $p(\bar{V}_n) \geq p(\frac{1}{n}V_1)$ , which, combined with  $p(V_1) > 0$  given  $V_1 > 0$ , implies that  $A_\ell \geq A_1$ .

Therefore, taking  $\alpha \rightarrow 0^+$  gives

$$\begin{aligned}\lim_{\alpha \rightarrow 0^+} \beta_{\text{CP},\alpha} &= 1 - \lim_{\alpha \rightarrow 0^+} \sum_{\ell=1}^n A_\ell \cdot \mathbb{P}_{\text{CP},\alpha}(S = \ell | S > 0) \\ &= 1 - \sum_{\ell=1}^n A_\ell \cdot \lim_{\alpha \rightarrow 0^+} \mathbb{P}_{\text{CP},\alpha}(S = \ell | S > 0) \quad A_\ell \text{'s do not involve } \alpha \text{ because they condition on } S = \ell \\ &\leq 1 - \sum_{\ell=1}^n A_1 \cdot \lim_{\alpha \rightarrow 0^+} \mathbb{P}_{\text{CP},\alpha}(S = \ell | S > 0) \\ &= 1 - A_1 \\ &= \lim_{\alpha \rightarrow 0^+} \beta_{\text{CP},\alpha}.\end{aligned}$$

If  $p(v)$  is strictly increasing in  $v$ ,  $A_\ell > A_1$  for  $\ell > 1$ . By Proposition 3, there exists  $\ell \geq 2$  such that  $\lim_{\alpha \rightarrow 0^+} \mathbb{P}_{\text{CP},\alpha}(S = \ell | S > 0) > 0$ . It follows that  $\lim_{\alpha \rightarrow 0^+} \beta_{\text{CP},\alpha} < \lim_{\alpha \rightarrow 0^+} \beta_{\text{NP},\alpha}$ .  $\square$

## C.2. Proof of Theorem 2

To prove Theorem 2 we first investigate an auxiliary metric whose structure admits study more easily.

DEFINITION EC.1 (EFFECTIVE FOLLOWUP EFFICIENCY). Let  $\eta$  denote the expected number of positive cases identified per followup test consumed. That is,  $\eta = \frac{\overline{D}}{n\overline{Y}}$ .

To better understand the behavior of  $\gamma$ , we can rewrite the expression of  $\gamma$  in Definition 2 as

$$\gamma = \left( \frac{1}{\overline{D}} + \frac{n\overline{Y}}{\overline{D}} \right)^{-1} = \left( \frac{1}{n\alpha(1-\beta)} + \frac{1}{\eta} \right)^{-1}. \quad (\text{EC.12})$$

Analogous to Proposition 1 we have that  $\eta$  converges in probability to  $\frac{\mathbb{E}_{\text{POOL},\alpha}[D]}{n\mathbb{E}_{\text{POOL},\alpha}[Y]}$  (denoted  $\eta_{\text{POOL},\alpha}$ ), as  $N \rightarrow \infty$ , for  $\alpha > 0$  and  $\text{POOL} \in \{\text{NP}, \text{CP}\}$ .

We present Lemma EC.3, which provides a bound on the ratio of effective followup efficiency under correlated pooling and naive pooling.

LEMMA EC.3.  $\lim_{\alpha \rightarrow 0^+} \frac{\eta_{\text{CP},\alpha}}{\eta_{\text{NP},\alpha}} \geq (1 + \delta)^{-1}$  where  $\delta = \frac{\mathbb{P}_{\text{CP},\alpha}(Y = 1, S_D = 0 \mid S > 0)}{\mathbb{P}_{\text{CP},\alpha}(Y = 1, S_D > 0 \mid S > 0)}$  and  $S_D = \sum_{i=1}^n W_i$ .

*Proof of Lemma EC.3.* We first derive  $\eta_{\text{NP},\alpha}$  for naive pooling. By similar arguments in the Proof of Theorem 1, the denominator of  $\eta_{\text{NP},\alpha}$  is given by

$$\begin{aligned} n\mathbb{E}_{\text{NP},\alpha}[Y] &= n\mathbb{E}_{\text{NP},\alpha} [p(\bar{V}_n)] \\ &= n \sum_{\ell=1}^n \mathbb{E}_{\text{NP},\alpha} [p(\bar{V}_n) \mid S = \ell] \mathbb{P}_{\text{NP},\alpha}(S = \ell) \\ &= n \sum_{\ell=1}^n \mathbb{E}_{\text{NP},\alpha} [p(\bar{V}_n) \mid S = \ell] \binom{n}{\ell} \alpha^\ell (1-\alpha)^{n-\ell} \\ &= n\alpha \cdot \sum_{\ell=1}^n \mathbb{E}_{\text{NP},\alpha} [p(\bar{V}_n) \mid S = \ell] \binom{n}{\ell} \alpha^{\ell-1} (1-\alpha)^{n-\ell}. \end{aligned} \quad (\text{EC.13})$$

The numerator of  $\eta_{\text{NP},\alpha}$  is given by

$$\begin{aligned} \mathbb{E}_{\text{NP},\alpha}[D] &= \mathbb{E}_{\text{NP},\alpha} \left[ \sum_{i=1}^n Y W_i \right] \\ &= n\alpha \cdot \mathbb{E}_{\text{NP},\alpha} [p(\bar{V}_n) p(V_1) \mid V_1 > 0] \\ &= n\alpha \cdot \sum_{\ell=1}^n \mathbb{E}_{\text{NP},\alpha} [p(\bar{V}_n) p(V_1) \mid V_1 > 0, S = \ell] \binom{n-1}{\ell-1} \alpha^{\ell-1} (1-\alpha)^{n-\ell}. \end{aligned} \quad (\text{EC.14})$$

By definition of  $\eta_{\text{NP},\alpha}$  and Equations EC.14 and EC.13, taking  $\alpha \rightarrow 0^+$  gives

$$\begin{aligned} \lim_{\alpha \rightarrow 0^+} \eta_{\text{NP},\alpha} &= \lim_{\alpha \rightarrow 0^+} \frac{\mathbb{E}_{\text{NP},\alpha}[D]}{n\mathbb{E}_{\text{NP},\alpha}[Y]} \\ &= \lim_{\alpha \rightarrow 0^+} \frac{n\alpha \cdot \sum_{\ell=1}^n \mathbb{E}_{\text{NP},\alpha} [p(\bar{V}_n) p(V_1) \mid V_1 > 0, S = \ell] \binom{n-1}{\ell-1} \alpha^{\ell-1} (1-\alpha)^{n-\ell}}{n\alpha \cdot \sum_{\ell=1}^n \mathbb{E}_{\text{NP},\alpha} [p(\bar{V}_n) \mid S = \ell] \binom{n}{\ell} \alpha^{\ell-1} (1-\alpha)^{n-\ell}} \\ &= \frac{\mathbb{E}_{\text{NP},\alpha} [p(\bar{V}_n) p(V_1) \mid V_1 > 0, S = 1]}{\mathbb{E}_{\text{NP},\alpha} [p(\bar{V}_n) \mid S = 1] \cdot \binom{n}{1}} \\ &= \frac{\mathbb{E} [p(\frac{1}{n}V_1) p(V_1) \mid V_1 > 0]}{n \cdot \mathbb{E} [p(\frac{1}{n}V_1) \mid V_1 > 0]} \quad \text{because } V_i\text{'s are iid} \\ &\quad \text{(the denominator is nonzero because } p(v) > 0 \forall v > 0\text{)} \\ &= \frac{\mathbb{E} [p(\frac{1}{n}V_1) W_1 \mid V_1 > 0]}{n \cdot \mathbb{E} [p(\frac{1}{n}V_1) \mid V_1 > 0]} \end{aligned} \quad (\text{EC.15})$$

$$\begin{aligned}
&= \frac{1}{n} \cdot \frac{\mathbb{E}[p(\frac{1}{n}V_1) | V_1 > 0, W_1 = 1] \cdot \mathbb{P}(W_1 = 1 | V_1 > 0)}{\sum_{j=0,1} \mathbb{E}[p(\frac{1}{n}V_1) | V_1 > 0, W_1 = j] \cdot \mathbb{P}(W_1 = j | V_1 > 0)} \\
&= \frac{1}{n} \cdot \left( 1 + \frac{\mathbb{E}[p(\frac{1}{n}V_1) | V_1 > 0, W_1 = 0]}{\mathbb{E}[p(\frac{1}{n}V_1) | V_1 > 0, W_1 = 1]} \cdot \frac{\mathbb{P}(W_1 = 0 | V_1 > 0)}{\mathbb{P}(W_1 = 1 | V_1 > 0)} \right)^{-1}.
\end{aligned} \tag{EC.16}$$

Then, we derive  $\eta_{\text{CP},\alpha}$  for correlated pooling.

$$\begin{aligned}
\eta_{\text{CP},\alpha} &= \frac{\mathbb{E}_{\text{CP},\alpha}[D]}{n\mathbb{E}_{\text{CP},\alpha}[Y]} \\
&= \frac{\mathbb{E}_{\text{CP},\alpha}[\sum_{i=1}^n YW_i]}{n\mathbb{E}_{\text{CP},\alpha}[Y]} \\
&= \frac{1}{n} \cdot \frac{\mathbb{E}_{\text{CP},\alpha}[YS_D | S_D > 0] \mathbb{P}_{\text{CP},\alpha}(S_D > 0)}{\mathbb{E}_{\text{CP},\alpha}[Y | S_D > 0] \mathbb{P}_{\text{CP},\alpha}(S_D > 0)}
\end{aligned} \tag{EC.17}$$

$$\begin{aligned}
&= \frac{1}{n} \cdot \frac{\mathbb{E}_{\text{CP},\alpha}[YS_D | S_D > 0] \mathbb{P}_{\text{CP},\alpha}(S_D > 0 | S > 0)}{\mathbb{P}_{\text{CP},\alpha}(Y = 1 | S_D > 0) \mathbb{P}_{\text{CP},\alpha}(S_D > 0 | S > 0) + \mathbb{P}_{\text{CP},\alpha}(Y = 1 | S_D = 0, S > 0) \mathbb{P}_{\text{CP},\alpha}(S_D = 0 | S > 0)} \\
&\geq \frac{1}{n} \cdot \frac{\mathbb{P}_{\text{CP},\alpha}(Y = 1 | S_D > 0) \mathbb{P}_{\text{CP},\alpha}(S_D > 0 | S > 0)}{\mathbb{P}_{\text{CP},\alpha}(Y = 1 | S_D > 0) \mathbb{P}_{\text{CP},\alpha}(S_D > 0 | S > 0) + \mathbb{P}_{\text{CP},\alpha}(Y = 1 | S_D = 0, S > 0) \mathbb{P}_{\text{CP},\alpha}(S_D = 0 | S > 0)} \\
&\quad \text{because } \mathbb{E}_{\text{CP},\alpha}[YS_D | S_D > 0] \geq \mathbb{E}_{\text{CP},\alpha}[Y | S_D > 0] = \mathbb{P}_{\text{CP},\alpha}(Y = 1 | S_D > 0) \tag{EC.18}
\end{aligned}$$

(both terms in the denominator are nonzero because  $p(v) > 0 \forall v > 0$ )

$$\begin{aligned}
&= \frac{1}{n} \left( 1 + \frac{\mathbb{P}_{\text{CP},\alpha}(Y = 1 | S_D = 0, S > 0)}{\mathbb{P}_{\text{CP},\alpha}(Y = 1 | S_D > 0)} \cdot \frac{\mathbb{P}_{\text{CP},\alpha}(S_D = 0 | S > 0)}{\mathbb{P}_{\text{CP},\alpha}(S_D > 0 | S > 0)} \right)^{-1} \\
&= \frac{1}{n} \left( 1 + \frac{\mathbb{P}_{\text{CP},\alpha}(Y = 1, S_D = 0 | S > 0)}{\mathbb{P}_{\text{CP},\alpha}(Y = 1, S_D > 0 | S > 0)} \right)^{-1}.
\end{aligned} \tag{EC.19}$$

Upper-bounding Equation EC.16 by  $\frac{1}{n}$  and using Equation EC.19 gives the desired result.  $\square$

Then, the proof of Theorem 2 follows Lemma EC.3 in a straightforward manner.

*Proof of Theorems 2.* By Equation EC.12, we have that for  $\text{POOL} \in \{\text{CP}, \text{NP}\}$

$$\gamma_{\text{POOL},\alpha} = \left( \frac{1}{n\alpha(1 - \beta_{\text{POOL},\alpha})} + \frac{1}{\eta_{\text{POOL},\alpha}} \right)^{-1}. \tag{EC.20}$$

Hence, using the results shown in Theorems 1 and 2, we find that

$$\begin{aligned}
\gamma_{\text{CP},\alpha} &= \left( \frac{1}{n\alpha(1 - \beta_{\text{CP},\alpha})} + \frac{1}{\eta_{\text{CP},\alpha}} \right)^{-1} \\
&\geq \left( \frac{1}{n\alpha(1 - \beta_{\text{NP},\alpha})} + \frac{1}{(1 + \delta)^{-1} \eta_{\text{NP},\alpha}} \right)^{-1} \\
&\geq \left( (1 + \delta) \left( \frac{1}{n\alpha(1 - \beta_{\text{NP},\alpha})} + \frac{1}{\eta_{\text{NP},\alpha}} \right) \right)^{-1} \\
&= (1 + \delta)^{-1} \gamma_{\text{NP},\alpha},
\end{aligned}$$

which concludes the proof.  $\square$

### C.3. Proof of Corollary 1

*Proof of Corollary 1.* We apply the threshold sensitivity function to the calculation of  $\lim_{\alpha \rightarrow 0^+} \eta_{\text{NP},\alpha}$  and  $\lim_{\alpha \rightarrow 0^+} \eta_{\text{CP},\alpha}$ . In Equation EC.16, the first term on the numerator in the parenthesis is given by

$$\mathbb{E} \left[ p \left( \frac{1}{n} V_1 \right) | V_1 > 0, W_1 = 0 \right] = \mathbb{E} \left[ \mathbb{1} \left\{ \frac{1}{n} V_1 \geq u_0 \right\} | V_1 > 0, V_1 < u_0 \right] = 0,$$

which implies  $\lim_{\alpha \rightarrow 0^+} \eta_{\text{NP},\alpha} = 1/n$ .

In Equation EC.19, the numerator of the last term is given by

$$\mathbb{P}_{\text{CP},\alpha}(Y = 1, S_D = 0 \mid S > 0) = \mathbb{P}_{\text{CP},\alpha}(\bar{V}_n \geq u_0, V_i < u_0 \ \forall i \text{ s.t. } V_j > 0 \mid S > 0) = 0,$$

which implies  $\eta_{\text{CP},\alpha} \geq \frac{1}{n}$ . Hence,  $\lim_{\alpha \rightarrow 0^+} \frac{\eta_{\text{CP},\alpha}}{\eta_{\text{NP},\alpha}} \geq 1$ , which follows that  $\lim_{\alpha \rightarrow 0^+} \frac{\gamma_{\text{CP},\alpha}}{\gamma_{\text{NP},\alpha}} \geq 1$ .  $\square$

## Appendix D: Example Where Correlated Pooling Has Lower Efficiency

We give an example of sensitivity and viral load distribution under which correlated pooling has lower test efficiency, contrary to the claims in the literature.

Consider a sensitivity function  $p$  such that  $p(0) = 0$ ,  $p(1) = 1$ , and  $p(1/2) = q$  for some  $q \in (0, 1)$ . We examine a correlated pool consisting of two samples with the joint viral load distribution given in Table EC.1. By Lemma EC.2 and Proposition 2, the corresponding naive pool contains two samples whose viral loads are independent with the same marginal distribution as that in Table EC.1.

	$V_2 = 0$	$V_2 = 1$
$V_1 = 0$	$1 - \alpha$	0
$V_1 = 1$	0	$\alpha$

For  $\text{POOL} \in \{\text{NP}, \text{CP}\}$ , referring to naive and correlated pooling respectively, and prevalence  $\alpha$ , we have  $\text{efficiency}_{\text{POOL},\alpha}$ , the number of positives identified per test consumed, given by the following expression:

$$\text{efficiency}_{\text{POOL},\alpha} = \frac{n}{1 + n\mathbb{E}_{\text{POOL},\alpha}[Y]} \quad \text{for } \text{POOL} \in \{\text{NP}, \text{CP}\}. \quad (\text{EC.21})$$

To derive efficiency, we compute the expected value of  $Y$ , the pooled test outcome:

$$\begin{aligned} \mathbb{E}_{\text{NP},\alpha}[Y] &= \alpha^2 \cdot 1 + 2\alpha(1 - \alpha) \cdot q + (1 - \alpha)^2 \cdot 0 = \alpha^2 + 2q \cdot \alpha(1 - \alpha) \\ \mathbb{E}_{\text{CP},\alpha}[Y] &= \alpha \cdot 1 + (1 - \alpha) \cdot 0 = \alpha. \end{aligned} \quad (\text{EC.22})$$

Plugging Equation EC.22 into Equation EC.21 gives the expressions for efficiency under naive and correlated pooling:

$$\begin{aligned} \text{efficiency}_{\text{NP},\alpha} &= \left( \frac{1}{2} + \alpha^2 + 2q \cdot \alpha(1 - \alpha) \right)^{-1} \\ \text{efficiency}_{\text{CP},\alpha} &= \left( \frac{1}{2} + \alpha \right)^{-1}. \end{aligned}$$

We observe that when  $q \in (0, 1/2)$ , for any  $\alpha \in (0, 1)$ ,  $\text{efficiency}_{\text{NP},\alpha} > \text{efficiency}_{\text{CP},\alpha}$ .

## Appendix E: Supplemental Information for the Dynamic Simulation

We provide implementation details for our simulation in Section 4. In Section E.1 we describe the setup of the network-based epidemic simulation with large-scale screening using pooled testing. In Section E.2 we model the viral load progression over time within an infected individual. In Section E.3 we describe a realistic model for PCR testing.



## E.1. Screening and Pooling in a Social Network

**E.1.1. Network generation** We build on the `SEIRSp1us` (McGee 2021) library to simulate generalized SEIRS disease dynamics on a contact network. We generate population-wide contact networks with realistic household and community structures using the library’s built-in implementation of the FARZ algorithm (Fagnan et al. 2018). Given input distributions of age and household size, the FARZ algorithm creates communities within the same age group and households across age groups that comply to the desired distributions. Each household is fully connected. We set the population size to be 10,000 and the household size and age distributions to be those mimicking the United States in `SEIRSp1us` (Tables EC.2 and EC.3). The documentation of `SEIRSp1us` (McGee 2021) provides further details of the FARZ implementation.

**Table EC.2 US household size distribution.**

Household size	1	2	3	4	5	6	7
Weight	0.284	0.345	0.151	0.128	0.058	0.023	0.013

**Table EC.3 US age distribution.**

Age	0-9	10-19	20-29	30-39	40-49	50-59	60-69	70-79	80+
Weight	0.121	0.131	0.137	0.133	0.124	0.131	0.115	0.070	0.038

To mimic a certain level of social distancing amid a pandemic, we downsample the edges generated by the FARZ algorithm. For each node, we sample a number  $n_e$  from  $\text{Exponential}(1/50)$ , select  $n_e$  edges uniformly at random, and discard the rest. We ensure that each household is still fully connected.

**E.1.2. Epidemic Dynamics and Interventions** The epidemic follows the classical SEIR dynamics (Biswas et al. 2014) with additional compartments for isolation. More description can be found in the documentation of `SEIRSp1us` (McGee 2021). We simulate repeated population-wide screening as an intervention. Given a choice of screening frequency, the population is divided into equally sized screening groups. Each individual is assigned to a specific screening group and one group is tested on each day using pooled testing. Positive individuals identified in screening are isolated and isolated individuals do not participate in screening. Isolation lasts for at most 14 days, after which the subject would be released.

We set the simulation parameter `alpha`, governing susceptibility to infection, to be 2, and we increase the intra-household edge weight to 10 to mimic faster transmission within households than between households.

**E.1.3. Pooling based on node clustering** To create screening groups from the population and correlated pools from each screening group, we generate vector representations for each node and cluster similar nodes together.

We use the Python implementation (Cohen 2022) of `node2vec` (Grover and Leskovec 2016) to generate a vector representation (i.e., an *embedding*) for each node that captures the node’s structural position in the network and the communities it belongs to. We use the following parameters in running `node2vec`:

- embedding dimensions: 32
- number of nodes in each walk: 20

- number of walkers per node: 10
- number of workers per node: 1
- window: 10
- min\_count: 1

Furthermore, to emphasize the household structure in learning the embedding, we set a weight  $10^{10}$  of for intra-household edges while keeping the weight to be 1 for other edges. (This modification only affects the learning of node embedding. It does not affect the transmission dynamics on the network.)

Given the learned embeddings, we partition the nodes into smaller, equally-sized clusters using  $k$ -means clustering and minimum weight matching, using L2 as the distance metric. In particular, to partition  $n_N$  nodes into  $n_C$  clusters of size  $s$  within embedding space  $\mathbb{R}^d$  (without loss of generality, assume  $n_N = n_C \cdot s$ ), we perform the following:

- First, we run  $k$ -means clustering to obtain  $n_C$  cluster centroids. They can be represented in a matrix  $C \in \mathbb{R}^{n_C \times d}$  where each row is a centroid. The clusters formed from  $k$ -means are not necessarily equally-sized.
- Let  $\tilde{C} \in \mathbb{R}^{n_N \times d}$  be the matrix obtained from repeating  $C$  for  $s$  times along the row dimension. Mathematically,  $\tilde{C} = (\mathbf{1}_s \otimes I_{n_C})C$ , where  $\mathbf{1}_s$  is the all-1 column vector in  $\mathbb{R}^s$ ,  $I_{n_C}$  is the identity matrix in  $\mathbb{R}^{n_C}$ , and  $\otimes$  denotes the Kronecker product.
- Compute  $L \in \mathbb{R}^{n_N \times n_N}$  such that  $L_{ij}$  is the L2 distance between the  $i$ th node embedding and the  $j$ th row in  $\tilde{C}$ .
- Solve the minimum weight matching problem using  $L$  as the cost matrix, such that each node is matched to one row in  $\tilde{C}$  and the total cost is minimized:

$$\min \sum_{i=1}^{n_N} \sum_{j=1}^{n_N} L_{ij} X_{ij}, \quad X_{ij} \in \{0, 1\}.$$

Denote the solution as  $X^*$ . By construction, only one entry is 1 and the rest are 0 in each row and each column of  $X^*$ .

- For each node  $i$ , let  $J(i)$  denote the location of 1 in the  $i$ th row of  $X^*$ . Assign node  $i$  to the cluster  $(J(i) \bmod n_C)$ . It can be shown that the clusters assigned this way are all equally sized.

In our simulation, suppose we screen the size- $N$  population every  $k$  days using pools of size  $n$ . The above procedure has three use cases:

- Generating screening groups from the population: partition  $N$  nodes into size- $N/k$  clusters.
- Generating community-correlated pools: partition the screening group into size- $2n$  clusters; within each cluster, divide them randomly into two size- $n$  pools. We use this to simulate community-induced correlation.
- Generating household-correlated pools: partition the screening group directly into size- $n$  clusters. This simulates household-induced correlation.

Finally, naive pooling is implemented by reordering the entire screening group and forming pools sequentially from the permuted group members.

**E.1.4. Validation of pooling implementation** We present numerical evidence that validates the implementation of community and household-correlated pooling. We work with a setting similar to Figure 3 in the main text of screening every five days on a population of size 10,000 using pools of size 20.

First, we validate that the household-correlated pools are more closely connected than the community-correlated pools, and community-correlated pools are more closely connected than naive pools. We quantify the closely-connectedness using a simple metric, namely the number of edges on the subgraph induced by members of a pool. In Figure EC.1a, we plot the distribution of the number of edges within a pool over all realized pools under each pooling method. The median is 15 for community-correlated pools and 25 for household-correlated pools. On the other hand, naive pools mostly have 1-2 edges. This stark difference among pooling methods implies that the possibility of a pool containing multiple positives would be significantly higher in correlated pools than in naive pools, especially under low prevalence.

Moreover, Figure EC.1b presents the distribution of the number of pools each household is allocated to. The majority of households are allocated to only one pool.

Therefore, the evidence presented in Figure EC.1 validates our pooling implementation using node embedding and clustering.

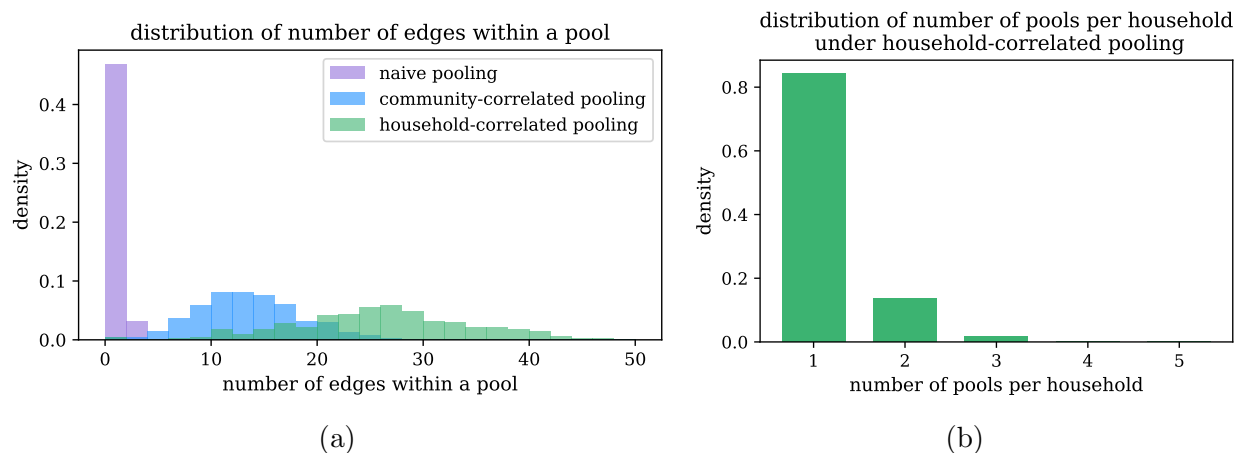


**Figure EC.1 Validation of pooling implementation. (a) Distribution of the number of edges within a pool under each pooling method. A larger number implies that the members of the pool are more closely connected. (b) Distribution of the number of pools that each household is allocated to under household-correlated pooling. The majority of households are placed into the same pool.**

## E.2. Realistic Viral Load Progression

We follow Brault et al. (2021) and model the viral load of an infected individual as a piecewise log-linear function. A similar pattern has been discussed in other studies, such as Cleary et al. (2021).

In particular, we assume the  $\log_{10}$  viral load rises, reaches a plateau value of 6, drops, remain at 3 for a while, then drops to -1. We further assume that the individual is infectious whenever their  $\log_{10}$  viral load is at least 3.

For each infected individual, assuming their infection starts at time 0, the viral load progression is parameterized by the following critical time points:

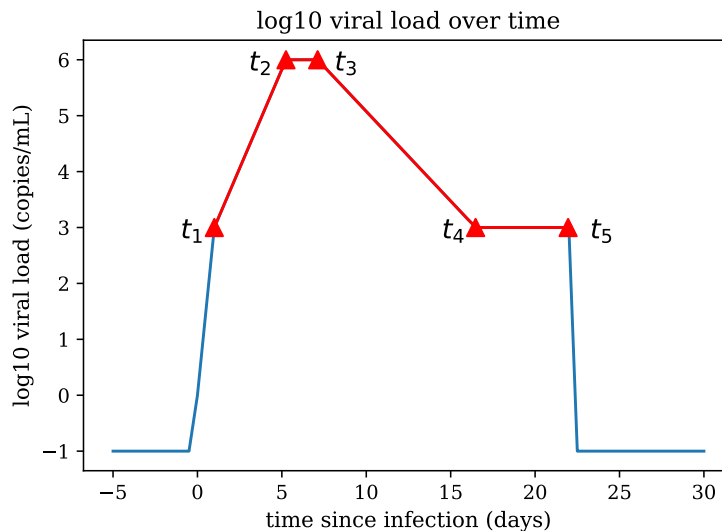


**Figure EC.2** Example log10 viral load progression for an infected individual. The critical time points are marked and annotated. The individual is assumed infectious when their log10 viral load is at least 3 (red).

- $t_1$ , the time at which the log10 viral load reaches 3;
- $t_2$ , the time at which the log10 viral load reaches 6;
- $t_3$ , the time at which the log10 viral load starts declining from 6;
- $t_4$ , the time at which the log10 viral load reaches 3;
- $t_5$ , the time at which the log10 viral load drops to  $-1$ .

Figure EC.2 shows an example progression of log10 viral load. We set  $t_1 = 1$  for all infected individuals. To create heterogeneity, we sample the duration of each subsequent piece uniformly from an interval, specified in Table EC.4.

**Table EC.4** Parameter values for viral load progression.  $\text{Unif}[\cdot, \cdot]$  denotes a continuous uniform distribution.

	sample range
$t_1$	1
$t_2 - t_1$	$\text{Unif}[3, 5]$
$t_3 - t_2$	$\text{Unif}[1, 3]$
$t_4 - t_3$	$\text{Unif}[7, 10]$
$t_5 - t_4$	$\text{Unif}[5, 6]$

Among the initial infections at the start of the simulation, we let half of them be at the start of infectivity (i.e., at  $t_1$ ) and the other half to be at the start of the peak (i.e., at  $t_2$ ).

### E.3. PCR Modeling

We describe a realistic sensitivity function for the PCR test that captures the randomness in the subsampling and pooling processes, an aspect overlooked by most existing literature studying group testing protocols.

The first step in a pooled PCR test is the collection of samples from each subject. For SARS-CoV-2 testing, the most common sample types include nasopharyngeal swabs, anterior nares swabs, and saliva. We assume

the raw volume of the samples is the same across all subjects, denoted by  $V_{sample}$ . (Nasopharyngeal and anterior nares swabs can be transported in a fixed amount of viral transport media; saliva samples, whether self-collected or not, can require a prescribed volume.)

Once the  $n$  samples are collected, they are transported to the lab to be prepared for pooling. Let  $V_i$  denote the viral load (i.e., the number of viral RNA copies per unit volume) of the  $i$ th sample in the pool. If the  $i$ th sample is negative, then  $V_i = 0$ . A pipetting robot fetches a volume of  $V_{subsample}$  from each sample for pooling, so the number of RNA copies selected for pooling is  $N_i \sim \text{Binom}\left(V_{sample} \cdot V_i, \frac{V_{subsample}}{V_{sample}}\right)$  for the  $i$ th sample. We assume that, compared to an individual test, pooling reduces the subsampling volume by a multiplicative factor of  $n$ . (That is, the  $n$  subsamples, when pooled together, have the same volume as an individual test in the same step.) Then, all  $n$  subsamples are pooled together and go through an RNA extraction step using glass fiber plates. Assuming that each RNA copy attaches to the glass fiber plates independently with probability  $\xi$ , the number of eluted RNA copies used as templates that enter the PCR machine follows a binomial distribution  $M \sim \text{Binom}\left(\sum_{i=1}^n N_i, \xi\right)$ . Aggregating the binomial subsampling in these steps, we find that  $M$  follows a binomial distribution:  $M \sim \text{Binom}\left(V_{sample} \cdot \sum_{i=1}^n V_i, \frac{V_{subsample}}{V_{sample}} \cdot \xi\right)$ .<sup>8</sup> Finally, we assume the PCR test has a detection threshold  $\tau$ , a positive integer, such that if  $M \geq \tau$ , the test returns a positive result; otherwise, negative.<sup>9</sup> (As a result, a negative sample is always classified as negative.)

**Table EC.5** Parameter values used in the realistic PCR model.

Parameter name	Symbol	Parameter value
Sample volume	$V_{sample}$	1 mL
Subsample volume	$V_{subsample}$	100/pool size (pooled); 100 (individual) $\mu\text{L}$
Glass fiber binding efficiency	$\xi$	0.5
Detection threshold	$\tau$	calibrated to population-average individual test FNR

This PCR model enables us to simulate the test outcome given the sample viral loads in a pooled test. Table EC.5 gives the parameter values we use in simulation. Among them, the detection threshold  $\tau$  is a key quantity that affects the test outcome. Since it varies for different approved assays (US Food and Drug Administration 2020), we choose to not set a single value for it. Instead, we utilize its correspondence with the false negative rate (FNR) of a PCR test: a higher detection threshold leads to a higher false negative rate when testing the same sample, and vice versa. In particular, while keeping the other parameters in Table EC.5 fixed, we use simulation to calibrate  $\tau$  to different values of *population-average individual test FNR*  $\bar{\beta}$ , i.e., the expected false negative probability of a PCR test on an individual positive sample whose viral load follows the viral load distribution in the population. We use a viral load distribution calibrated from a large real-world dataset of infected individuals from Brault et al. (2021) (see Table EC.8 in Section F.1).

<sup>8</sup> The proof of this relation is straightforward, based on two identities: (i) If  $X_i \sim \text{Binom}(n_i, p)$  are independent, then  $\sum_i X_i \sim \text{Binom}(\sum_i n_i, p)$ ; (ii) If  $X \sim \text{Binom}(n, p)$  and  $Y | X \sim \text{Binom}(X, q)$ , then  $Y \sim \text{Binom}(n, pq)$ .

<sup>9</sup> The detection threshold  $\tau$  is not to be confused with the limit of detection (LoD), i.e., the lowest concentration of the target (in copies per volume) that a PCR assay can detect at least 95% of the time (Burns and Valdivia 2008). In our model, a higher  $\tau$  corresponds to a higher LoD. The way we model the subsampling steps using binomial random variables captures the randomness associated with the definition of LoD.

Table EC.6 describes the calibrated values of  $\tau$  corresponding to  $\bar{\beta}$  values of 2.5%, 5%, 10% and 20%. We use  $\tau = 1240$  in our simulation.

**Table EC.6** Population-average individual test FNRs  $\bar{\beta}$  and their corresponding calibrated values of  $\tau$  in the PCR model.

$\bar{\beta}$	Calibrated value of $\tau$
2.5%	108
5%	174
10%	342
20%	1240

## Appendix F: Static Simulation

In addition to our dynamic simulation, we thoroughly study how different factors (prevalence, pool size, household size distribution, PCR test sensitivity, and strength of correlation) affect the test performance of naive pooling and correlated pooling in more controlled settings. We call these the “static simulation”. The results from the static simulation offer important insights into decision-making similar to those from the dynamic simulation.

We do not explicitly model community-correlated pooling here. Instead, we assume the within-pool correlation arises only due to transmission within households and we tune a parameter governing the strength of household transmission to vary the within-pool correlation.

We demonstrate that correlated pooling consistently outperforms naive pooling in terms of both sensitivity and efficiency. Based on an SIR model (Kermack and McKendrick 1927) that incorporates repeated large-scale screening, we show that correlated pooling can stabilize or decrease the number of active infections using fewer tests than naive pooling.

### F.1. Viral Load Distribution

We use the viral load distribution calibrated on a large collection of infected individuals in Brault et al. (2021). We acknowledge that this distribution is different from the one induced by viral load progression and epidemic dynamics in our dynamic simulation. We opt to use it here because it is well-specified.

We first specify a probability distribution governing viral loads across infected individuals. One way to quantify the viral load in a sample is with the so-called Ct value. A PCR test amplifies the viral RNA copies in a sample by approximately doubling them in each cycle of the reaction. The minimum number of cycles required for the RNA copies to reach a detectable threshold is called the *cycle threshold*, denoted Ct (Heid et al. 1996). The lower the initial viral load in the sample, the more duplicating cycles it requires to become detectable, and the larger its Ct value is.

Jones et al. (2020) obtains empirically measured  $C_t$  values from asymptomatic screening conducted in Germany. Brault et al. (2021) fits a censored Gaussian mixture model (GMM) to the distribution of  $C_t$  values in Jones et al. (2020):

$$f(x) = \sum_{k=1}^3 \pi_k \frac{f_{\mu_k, \sigma_k}(x)}{F_{\mu_k, \sigma_k}(d_{cens})} \cdot \mathbb{1}\{x \leq d_{cens}\}. \quad (\text{EC.23})$$

In Equation EC.23,  $f_{\mu_k, \sigma_k}$  and  $F_{\mu_k, \sigma_k}$  denote the probability density function and cumulative density function of the  $k^{\text{th}}$  component with mean  $\mu_k$  and standard deviation  $\sigma_k$ , respectively. The censoring threshold  $d_{cens}$  represents the limit of detection of the PCR assay, such that a sample with  $C_t$  value exceeding it is not observed. Brault et al. (2021) obtains  $d_{cens} = 35.6$  and GMM parameter values in Table EC.7.

**Table EC.7** Gaussian mixture model parameters for the distribution of  $C_t$  values.

	$\pi_k$	$\mu_k$	$\sigma_k$
$k = 1$	0.33	20.13	3.60
$k = 2$	0.54	29.41	3.02
$k = 3$	0.13	34.81	1.31

*Note:* Here,  $\pi_k$ ,  $\mu_k$ ,  $\sigma_k$  are the weight, mean and standard deviation of the  $k^{\text{th}}$  component, respectively.

The associated *uncensored* GMM model represents the true  $C_t$  distribution of the entire population, including those that may not be detected through individual PCR tests.

Moreover, since  $C_t$  value is a measurement of the viral load, and viral load is the quantity directly of interest to our simulation, we use a formula given in Jones et al. (2020) to convert this distribution to that of the  $\log_{10}$  of viral load (copies/mL):<sup>10</sup>

$$\begin{aligned} \log_{10} VL &= \log_{10}(1.105 \cdot 10^{14} \cdot e^{-0.681C_t}) \\ &= (14 + \log_{10} 1.105) - \frac{0.681}{\ln 10} C_t. \end{aligned}$$

This results in a GMM on the  $\log_{10}$  of the viral load with parameters shown in Table EC.8. A normally-distributed mixture component on the  $C_t$  value is equivalent to a normally-distributed mixture component with a different mean and variance on the  $\log_{10}$  viral load.

**Table EC.8** Gaussian mixture model parameters for the distribution of  $\log_{10}$  viral load (copies/mL) among infected individuals.

	$\pi_k$	$\mu_k$	$\sigma_k$
$k = 1$	0.33	8.09	1.06
$k = 2$	0.54	5.35	0.89
$k = 3$	0.13	3.75	0.39

*Note:* Here,  $\pi_k$ ,  $\mu_k$ ,  $\sigma_k$  are the weight, mean and standard deviation of the  $k^{\text{th}}$  component, respectively.

In our simulation, we assume the viral load of any individual is independent from the viral loads of all other individuals given his/her infection status. This assumption is mild given the heterogeneity in the individual biological response to the virus, which we consider independent. Hence, for each infected individual, we can sample his/her viral load from the distribution specified in Table EC.8.

<sup>10</sup> The data reported in Jones et al. (2020) are based on two PCR assays, the cobas system and the LC480 system, each of which has a conversion formula between  $C_t$  and viral load. Since over 60% of the positives in their screened population were identified with the cobas system and the two conversion formulae are approximately the same, we use the formula for the cobas system here.

## F.2. Household Size Distribution

Tables EC.9 and EC.10 describe the household size distribution of four different countries from census data, and variants of the U.S. household size distribution.

	1	2	3	4	5	6+
United States (US)	0.284	0.345	0.151	0.127	0.058	0.035
China (CN)	0.156	0.272	0.247	0.171	0.089	0.065
Australia (AUS)	0.244	0.334	0.162	0.159	0.067	0.034
France (FR)	0.364	0.327	0.136	0.115	0.042	0.016

*Source:* U.S. (Duffin 2020), China (National Bureau of Statistics of China 2018), Australia (.idcommunity 2016), and France (Institut National d'études Démographiques 2017).

Household size	1	2	3	4	5	6+
US+1	0.209	0.36	0.166	0.142	0.073	0.05
US+2	0.134	0.375	0.181	0.157	0.088	0.065
US-1	0.359	0.33	0.136	0.112	0.043	0.020
US-2	0.434	0.315	0.121	0.097	0.028	0.005

*Note:* US±1, US±2 are household distributions with weights ±0.075, ±0.15 respectively uniformly allocated to household sizes > 1 from the weight of household size 1. For example, US+1 has weight 0.284 − 0.075 on households of size 1, weight 0.345 + 0.075/5 on households of size 2, weight 0.151 + 0.075/5 on households of size 3, etc.

## F.3. Experiment Setup

**F.3.1. Correlated Infections in Households** We model the population as consisting of households with size  $H$  ranging from one to six (since households of size larger than six are rare). We gather the household size distributions of four countries from census data and assume that all probability mass on  $H > 6$  is allocated to  $H = 6$  (Table EC.9). We also explore variants of the U.S. census data, in which we either add to or subtract from the weight on household size of one and adjust the weights on other household sizes accordingly (Table EC.10).

A household is said to be infected if one person is infected as the index case in the household. We assume different households are infected independently with probability  $p_h$ , i.e., correlation through other social groups is considered negligible. Within each infected household, we assume transmissions occur independently with secondary attack rate (SAR)  $q$ . That is, given a positive index case in a size- $h$  household, the remaining  $h - 1$  members become infected independently with probability  $q$ . We consider the following possible values for  $q$ : [0.166, 0.140, 0.193, 0.005, 0.446]. These are the estimated mean, 95% CI lower and upper bounds, minimum and maximum values of household SAR from 40 studies, respectively, reported by a meta-analysis (Madewell et al. 2020).

The distribution of household size  $H$ , probability that a household is infected  $p_h$ , and secondary attack rate  $q$  together yield an expected prevalence in the population, which matches the overall population-level prevalence  $\alpha$ :

$$p_h \cdot \mathbb{E}_H[(1 + (H - 1)q)] = \alpha. \quad (\text{EC.24})$$



We now describe the steps for simulating correlated infections within households, given a fixed population-level prevalence, SAR, and household size distribution:

1. Compute the household infection probability  $p_h$  using Equation EC.24.
2. Generate households with sizes drawn from the household size distribution.
3. Let each household be infected independently with probability  $p_h$ , with one member selected uniformly at random as the index case.
4. In each infected household, generate secondary infections.
5. Assign to each infection a viral load sampled from the distribution described in Table EC.8.

**F.3.2. Pooling Assignment** Having developed a model for correlated infections in households, we now describe how we allocate samples into pools when using naive pooling and correlated pooling, under the Dorfman procedure:

- Naive pooling: we perform an independent random permutation on all the individual samples from the population and place them sequentially into pools regardless of household membership.
- Correlated pooling: we aim to place samples of individuals from the same household in the same pool. A collection of partially full pools are maintained and households are added sequentially. To add a household, we look for the first unfinished, capacity-permitting pool and place all samples of the household into this pool. If this is infeasible, we split the household across two or more pools.

Per the Dorfman procedure, samples in the same pool undergo one pooled test. All individuals in the pools testing positive take followup tests. We assume the amount of sample collected from each individual is enough so that no re-sampling is required if the followup test is necessary. This implies that the viral loads in the subsamples used for the pooled test and followup test are equal. The subsample for the pooled test is smaller than that for an individual test by a factor of the pool size, which results in dilution in the pooled sample.

#### F.4. Simulation Results

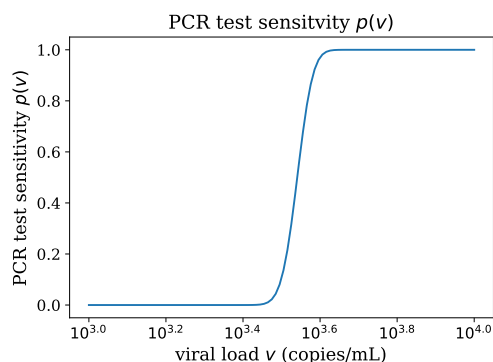
We demonstrate the advantage of correlated pooling over naive pooling through numerical results under different sets of parameters. First, we pick a set of parameters as the baseline setting, shown in Table EC.11. We consider this to be a representative setting for a medium-sized town in the early stage of an epidemic. The choice of pool size is informed by empirical implementations of group testing for COVID-19 (Fan 2020, Lefkowitz 2020, Barak et al. 2021). We set the detection threshold  $\tau = 174$ , corresponding to a population-average individual test FNR of 5% (Table EC.6). The test sensitivity function  $p(v)$  is shown in Figure EC.3.<sup>11</sup> In Section F.5, we vary these parameters to show that the advantage is robust.

We focus on two metrics to evaluate the performance of a group testing protocol, namely sensitivity (i.e.,  $1 - \text{FNR}$ ) and efficiency, the number of individual screened per test. Both are important for epidemic mitigation, as high sensitivity helps identify the positives accurately, while high efficiency permits more frequent screening under limited resources. Here we present efficiency as the metric for test consumption

<sup>11</sup> Here we use a different detection threshold  $\tau$  than in the dynamic simulation. We would like our static simulation to approximate the stylized setting with high sensitivity while the dynamic simulation would allow more test errors. However, the same insights hold if  $\tau$  is varied.

**Table EC.11** Baseline parameter values in the static simulation.

Parameter	Value
Population level prevalence	1%
Pool size	6
SAR	16.6%
Household distribution	US
Population-average individual test FNR	5%
Population size	12000

**Figure EC.3** PCR test sensitivity  $p(v)$  used in the static simulation.

because it is most widely used. The performance in the metric  $\gamma_{\text{POOL},\alpha}$  proposed in Section 3.2, the number of positive cases identified per PCR test, can be inferred by taking the product of sensitivity and efficiency.

The performance of naive pooling and correlated pooling under the baseline setting over 2000 iterations is shown in Table EC.12. As a reference, only using individual testing has a sensitivity of 95% and an efficiency of 1. Correlated pooling has better performance in terms of both sensitivity and efficiency than naive pooling. This is because correlated pooling in general has more positive cases in a positive-containing pool (due to correlation among samples from the same household). As a result, a sample with low viral load, which might otherwise be missed in naive pooling, is more likely to be “rescued” by other positive samples in the same pool in correlated pooling, leading to higher sensitivity. (This is referred to as the “hitchhiker effect” in Barak et al. (2021).) Meanwhile, the clustering of more positive cases in the same pool also implies a smaller number of pools that contain positive samples and require followup tests, resulting in a higher efficiency of correlated pooling.

**Table EC.12** Performance of naive and correlated pooling in the Dorfman procedure under the baseline parameter setting, averaging over 2000 iterations.

Pooling method	Sensitivity	Efficiency
Naive pooling (NP)	81.9%	4.67
Correlated pooling (CP)	86.0%	4.83
Percent advantage of CP over NP	5.02%	3.51%

*Note:* The standard errors for the sensitivity and efficiency are within 0.1% and 0.01, respectively.

Such improvement has a significant impact on real world policy making. We will show in Section F.6 that, when pool size is optimized for both pooling methods separately, correlated pooling enables more effective epidemic control than naive pooling.

**F.4.1. Sensitivity Versus Efficiency Across Pool Sizes** Under the same population-level prevalence, we anticipate test accuracy and efficiency will vary when we choose different pool sizes. Figure EC.4 reveals the tradeoff between sensitivity and efficiency using the two pooling methods under different prevalence levels. All parameters other than the prevalence level and the pool size take the values given in Table EC.11. In most scenarios (except when under high prevalence *and* large pool size), correlated pooling outperforms naive pooling in both sensitivity and efficiency.

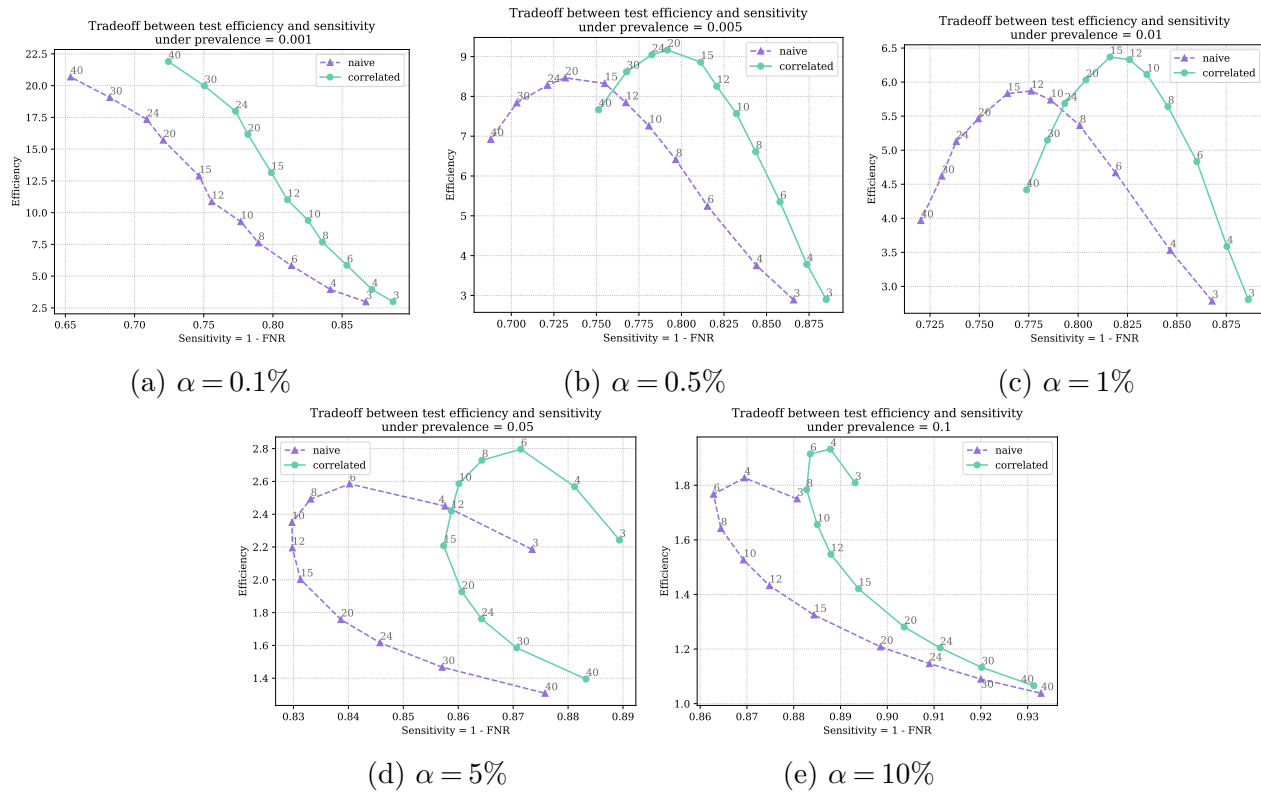


**Figure EC.4 Tradeoff between sensitivity and efficiency for correlated pooling and naive pooling under different prevalence levels. As we prefer both higher sensitivity and higher efficiency, a point in the upper right corner of the plot is more preferable. Each point is obtained by taking the average outcome over 2000 simulation runs using a pool size annotated next to the point.**

When prevalence is low (e.g., 0.1%, Figure EC.4a), as pool size increases, sensitivity decreases and efficiency increases. Under low prevalence, most of the pools have either zero or one positive sample even when the pool size is large. A larger pool size causes a stronger dilution effect which lowers the pooled test sensitivity. Meanwhile, efficiency increases with pool size because fewer pools are needed, and under low prevalence not many pools require followup tests even if they are large.

When prevalence is intermediate (e.g., 0.5% or 1%, Figures EC.4b or EC.4c), as pool size increases, sensitivity decreases because of the dilution effect. Efficiency, however, reaches a peak first before declining. This is because large pool size under intermediate prevalence results in many positive pools. The heightened demand for followup tests offsets the savings in the number of pooled tests.

When prevalence is high (e.g., 5% or 10%, Figures EC.4d or EC.4e), as pool size increases, sensitivity first decreases and then increases. This is because a larger pool size under high prevalence leads to multiple positive samples in the same pool, offsetting the dilution effect. Efficiency drops dramatically as pool size increases, since a majority of pools test positive and most samples require followup tests. The efficiency of large pools under 10% prevalence, for example, is close to 1, indicating little reduction in test consumption compared to individual tests. In this scenario, one should consider using individual testing instead of group testing, as is also suggested in Eberhardt et al. (2020).

Figure EC.5 visualizes the advantage of correlated pooling over naive pooling under different prevalence levels and pool sizes. Except when prevalence  $\alpha = 10\%$ , pool size  $n = 40$ , correlated pooling is more advantageous. The advantages in sensitivity and efficiency are both more significant under low prevalence and when the pool size is large.

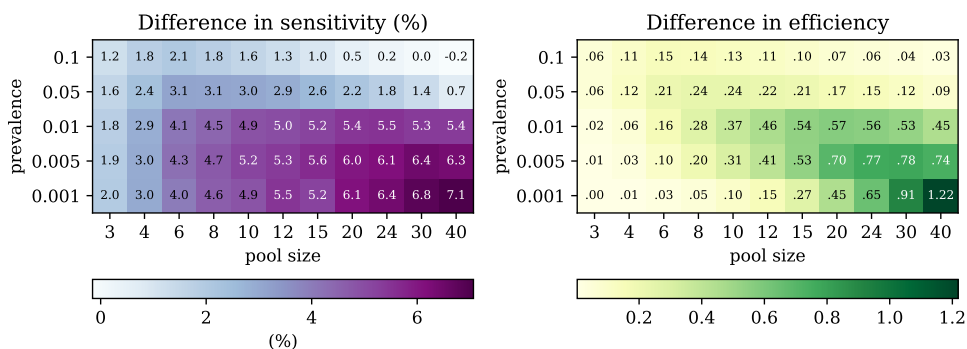


**Figure EC.5** The advantage of correlated pooling in (left) sensitivity and (right) efficiency, over naive pooling. In both heatmaps, the value in the cell is the metric value of correlated pooling minus that of naive pooling; a positive value implies that correlated pooling is more advantageous.

**F.4.2. Test Specificity** As discussed in Section 1, false positives pose challenges to large-scale screening, including waste of public health and economic resources, disruption of personal lives, and increased exposure risk during unnecessary treatment. Though false positives are not explicitly included in our modeling, here we argue that they are not a significant concern if pooling is used. In particular, we demonstrate that group testing has substantially lower false positive rate (FPR) than individual testing, and, moreover, correlated pooling achieves a lower FPR than naive pooling.

For our discussion, we start by assuming that false positives originate mainly from lab contamination that occurs independently across tests. We assume any PCR test on a negative sample has a small constant FPR (e.g., 0.01% as reported in Public Health Ontario (2020)), which is much smaller than the probability that a typical positive-containing pool tests positive. Under these assumptions, the probability that a negative sample in an all-negative pool is declared positive is negligible (e.g.,  $10^{-8}$ ) compared to when it is in a positive-containing pool. Hence, we estimate the FPR of a testing protocol by the fraction of negative samples that receive individual tests, assuming they are all in positive-containing pools. This can be directly inferred from our simulation results.

First, we compute the fraction of samples in the population receiving individual tests using  $\text{frac}_{\text{indiv}} = \text{efficiency}^{-1} - \frac{1}{n}$ . Second, we estimate  $\text{frac}_{\text{pos, indiv}}$ , the fraction of samples that are positive *and* receive individual tests, using  $\alpha \cdot \text{sensitivity}$ .<sup>12</sup> We take the difference of the above two quantities to estimate  $\text{frac}_{\text{neg, indiv}}$ , the fraction of samples that are negative *and* receive individual tests. Multiplying this difference by 0.01% then gives  $\text{frac}_{\text{neg, indiv pos}}$ , the fraction of samples that are negative *and* test positive in individual tests. Finally, we divide the  $\text{frac}_{\text{neg, indiv pos}}$  by  $1 - \alpha$ , the fraction of samples that are negative, to obtain the estimate for FPR.

We summarize the above calculations for correlated pooling and naive pooling in Table EC.13 based on the simulation results for the baseline setting in Table EC.12. We see that both pooling methods achieve an FPR on the order of  $10^{-6}$ , with correlated pooling slightly outperforming naive pooling. In our regime of discussion, the FPR roughly scales linearly with pool size and prevalence. Hence, for a prevalence of up to 1% and a pool size of up to 20, we expect the FPR of either pooling method to be at least as good as  $10^{-5}$ . This is a ten-fold reduction from the FPR of individual testing. Such specificity is sufficiently high in many uses of repeated screening for infection control.

**Table EC.13** FPR estimates for naive and correlated pooling under the baseline setting.

Quantity	Correlated pooling	Naive pooling
$\text{frac}_{\text{indiv}}$	4.03%	4.75%
$\text{frac}_{\text{pos, indiv}}$	0.86%	0.82%
$\text{frac}_{\text{neg, indiv}}$	3.17%	3.93%
$\text{frac}_{\text{neg, indiv pos}}$	3.17E-6	3.93E-6
FPR estimate	3.20E-6	3.97E-6

We also argue that false positives from PCR tests have little impact on efficiency, i.e., they incur only a small number of extra tests. In the pooled stage, 0.01% of the all-negative pools are expected to test positive and require follow-up tests for their samples. As the number of samples in all-negative pools is upper bounded by  $N$ , the extra tests due to PCR false positives translate to a less than  $10^{-4}$  increment in the number of tests per person. Besides, sensitivity is not affected by false positives of PCR tests.

### F.5. Robustness Analysis

We demonstrate that the advantage of correlated pooling over naive pooling is robust across different parameter values. In Figure EC.6, we show the performance of naive and correlated pooling when varying the population-level prevalence, pool size, population-average individual test FNR, SAR, and household size distribution respectively, while keeping others at the baseline setting. Each bar/point in the plots is obtained by taking the average outcome over 2000 simulation runs. In all plots, correlated pooling consistently performs better than naive pooling in terms of both sensitivity and efficiency.

Figure EC.6a shows that smaller prevalence leads to lower sensitivity but higher efficiency. This is due to the existence of fewer positive samples in a positive pool, which results in larger FNR because of the dilution

<sup>12</sup> Note that not all positives receiving individual tests test positive. Hence, this estimate is an underestimate, which eventually leads to an upper bound on FPR.

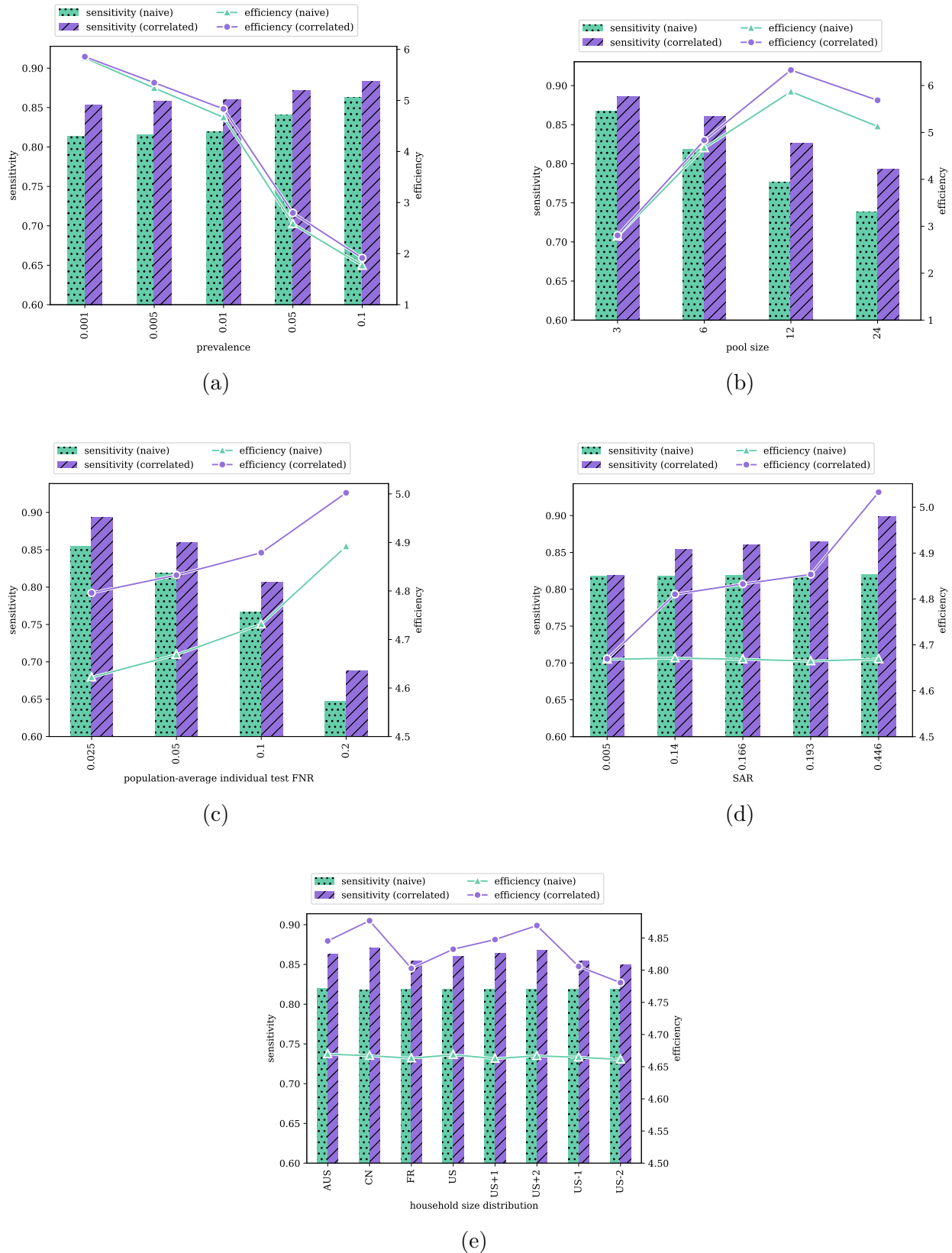


**Figure EC.6** Sensitivity and efficiency for varying (a) prevalence, (b) pool size, (c) population-average individual test FNR, (d) SAR and (e) household size distribution, under correlated pooling and naive pooling. Bars and points are obtained by taking the average outcome over 2000 simulation runs.

effect. Smaller prevalence also implies fewer positive pools, leading to fewer followup tests and therefore higher overall efficiency.

Figure EC.6b shows that a larger pool size typically implies a stronger dilution effect, which causes sensitivity to decline. Efficiency increases with pool size initially because for smaller pools the number of pooled tests is the dominating factor in determining the efficiency. On the other hand, a larger pool (e.g., size of 24) is more likely to contain a positive, which requires more individual tests once the pool tests positive. This causes the efficiency to decline for larger pools.

In Figure EC.6c, sensitivity decreases and efficiency increases as the population-average individual test FNR,  $\bar{\beta}$ , rises. A higher  $\bar{\beta}$  also implies a higher FNR of the pooled test, which explains the drop in sensitivity. Efficiency increases because a higher detection threshold causes more cases to be missed by the pooled tests and therefore fewer followup tests are required.

Figure EC.6d shows that the change in SAR does not affect the performance of naive pooling, as the protocol does not benefit from the correlation structure in the population. Meanwhile, correlated pooling achieves a better sensitivity and efficiency under larger SAR values. This is because a larger SAR creates a stronger correlation among household members, causing positive samples to be clustered in fewer pools. This in turn raises the probability of detecting positive pools and simultaneously lowers the number of followup tests needed. This aligns with the advantage of household-correlated pooling over community-correlated pooling in the dynamic simulation.

In Figure EC.6e, the change in household size distribution does not affect the performance of naive pooling, but it does affect that of correlated pooling. Under household size distributions that have larger weights on larger household sizes (e.g., CN, US+1, US+2), positive pools under correlated pooling tend to contain a larger number of positives, which implies improvement in both sensitivity and efficiency.

While the results above are based on the baseline setting, we do expect the sensitivity analysis based on other parameter settings to show similar patterns.

## F.6. Implication of Correlation for Decision-making

In this section, we show that correlated pooling enables more powerful epidemic control than naive pooling based on a deterministic SIR model (Kermack and McKendrick 1927), which translates to important implications for policy-making similar to those derived from the dynamic simulation in Section 4.3.1.

We let  $S$ ,  $I$ ,  $R$  denote the fractions of susceptible, actively infected, removed (due to either natural recovery or being detected and isolated in screening followed by recovery) individuals in the population, respectively.<sup>13</sup> We assume a constant fraction of the non-isolated population is screened every day. The disease dynamics can be represented by a set of three discrete-time equations, where a time step corresponds to a day:

$$\begin{aligned} S(t+1) - S(t) &= -b_I \cdot S(t)I(t) \\ I(t+1) - I(t) &= b_I \cdot S(t)I(t) - (b_R + f \cdot \text{sensitivity}) \cdot I(t) \\ R(t+1) - R(t) &= (b_R + f \cdot \text{sensitivity}) \cdot I(t), \end{aligned} \tag{EC.25}$$

<sup>13</sup> We assume, for simplicity, that an infected individual is infectious and a recovered individual does not become susceptible again.

where  $b_I$ ,  $b_R$  are the rates of transmission and recovery, respectively;<sup>14</sup>  $f$  is the frequency of screening for non-isolated individuals, i.e, those in the  $S$  and  $I$  groups.

We first derive the critical screening frequency required to control the epidemic, i.e., stabilize or reduce the number of active infections. To quantify the epidemic growth, we define the *growth factor*  $\lambda$  at time  $t$  as the ratio of the number of new cases at time  $t$  to the number of cases removed at time  $t$ :  $\lambda(t) = \frac{b_I \cdot S(t)I(t)}{(b_R + f \cdot \text{sensitivity}) \cdot I(t)}$ .

According to Equation EC.25, the number of infected individuals grows when  $\lambda(t) > 1$  and declines when  $\lambda(t) < 1$ . We further construct a time-invariant upper bound on  $\lambda(t)$  by setting  $S(t) = 1$ :  $\lambda' = \frac{b_I}{b_R + f \cdot \text{sensitivity}}$ .<sup>15</sup> Since  $\lambda(t) \leq \lambda'$  for all  $t$ , any screening frequency  $f$  that results in a  $\lambda'$  less than 1 also implies  $\lambda(t) < 1$  for all  $t$ . Therefore, we use  $\lambda' = 1$  as a threshold that characterizes whether the epidemic is brought under control. At this threshold, the screening frequency has a critical value  $f^*$  satisfying  $f^* \times \text{sensitivity} = b_I - b_R$ , which implies that

$$f^* \propto \text{sensitivity}^{-1}. \quad (\text{EC.26})$$

A larger value of  $f$  would reduce  $\lambda'$  even further, but it would increase test consumption, a key quantity of practical concern. Hence, we next use  $f^*$  to derive the *minimum* test consumption required for epidemic control. For a screening frequency  $f$ , test consumption per day satisfies:

$$\begin{aligned} \text{test consumption per day} &\propto \text{screening frequency} \times \# \text{ tests consumed per person} \\ &= f \times \text{efficiency}^{-1}. \end{aligned} \quad (\text{EC.27})$$

By Equations EC.26 and EC.27,

$$\begin{aligned} \text{minimum test consumption per day} &\propto f^* \times \text{efficiency}^{-1} \\ &\propto \text{sensitivity}^{-1} \times \text{efficiency}^{-1}. \end{aligned} \quad (\text{EC.28})$$

That is, the minimum test consumption per day is directly proportional to  $\text{sensitivity} \times \text{efficiency}$ , which manifests the significance of having both higher sensitivity and efficiency in group testing. In fact, this product is precisely the effective efficiency metric  $\gamma$  studied in Section 3.2.

By Equations EC.26 and EC.27,

$$\begin{aligned} \text{minimum test consumption per day} &\propto f^* \times \text{efficiency}^{-1} \\ &\propto \text{sensitivity}^{-1} \times \text{efficiency}^{-1}, \end{aligned} \quad (\text{EC.29})$$

where we recall that both sensitivity and efficiency depend on the pool size, prevalence level, and pooling choice. Therefore, one should maximize  $\text{sensitivity} \times \text{efficiency}$  when optimizing the pool size for a group testing protocol in real-world decision making.

Table EC.14 compares the optimal naive pooling and correlated pooling policies (by choosing a pool size that maximizes  $\text{sensitivity} \times \text{efficiency}$ ) under different prevalence levels. The last column of Table EC.14



**Table EC.14** Comparison of optimal correlated pooling and naive pooling policies in terms of sensitivity  $\times$  efficiency under different prevalence levels.

Prevalence	Optimal naive pooling		Optimal correlated pooling		Reduction in test consumption when using correlated pooling
	Pool size	Sensitivity $\times$ Efficiency	Pool size	Sensitivity $\times$ Efficiency	
0.1%	40	13.52	40	15.86	14.8%
0.5%	15	6.29	20	7.26	13.4%
1%	12	4.56	12	5.23	12.9%
5%	6	2.17	6	2.44	10.9%
10%	4	1.59	4	1.72	7.4%

illustrates the reduction in minimum test consumption required for epidemic control using the optimal correlated pooling policy relative to the optimal naive pooling policy.

For example, when prevalence is 1%, a pool size of 12 is optimal for both naive pooling and correlated pooling in terms of maximizing sensitivity  $\times$  efficiency. Using Equation EC.29, we derive the optimal naive pooling policy uses  $\frac{1/4.56 - 1/5.23}{1/5.23} = 14.7\%$  more tests than the optimal correlated pooling policy.

Such a difference has a substantial impact on real-world policy-making. As correlated pooling accounts for the naturally arising within-pool correlation, it is a more accurate model for reality than naive pooling. Hence, policies informed by models ignoring the correlation tends to overestimate the test consumption necessary for controlling the epidemic. This leads to two insights similar to those derived in Section 4.3.1:

- If the available testing capacity meets the minimum test consumption required by the optimal correlated pooling policy but not the optimal naive pooling policy, a correlation-oblivious policy-maker would decide that no screening policy can permit safe reopening and thus issue a lockdown. However, a correlation-aware policy maker could have kept the economy open with a feasible screening policy.
- If the available testing capacity of the city meets the minimum test consumption required by the optimal naive pooling policy, the correlation-oblivious policy-maker would decide to conduct screening. However, they would choose a lower screening frequency than allowed in reality because naive pooling underestimates the actual efficiency. On the other hand, a correlation-aware policy-maker would choose a higher screening frequency and achieve better epidemic mitigation.

Furthermore, if the naturally-induced within-pool correlation is weak, explicit measures can be taken to facilitate correlated pooling. For example, one can mandate that individuals from the same household get tested together so that their samples can be placed in the same pool without many logistical difficulties. For a city with limited resources, such measures could enable a safe reopen with population-wide screening, while it may not be feasible otherwise.

## Appendix G: Quantifying the $(1 + \delta)$ Bound in Theorem 2

In Appendix G, we numerically investigate the bound  $1 + \delta$  derived in Theorem 2 and show that it is consistently close to one under various conditions. We first derive an upper bound  $\delta'$  for  $\delta$  and then provide 95% confidence interval for  $\delta'$  under various pool sizes and detection thresholds. Appendix G.1 lays out

<sup>14</sup> We assume  $b_I > b_R$ , since the epidemic dies out naturally even without intervention if  $b_I \leq b_R$

<sup>15</sup> Alternatively,  $\lambda'$  can be interpreted as the growth factor in the early stage of the epidemic, where the majority of the population is susceptible, i.e.,  $S(t) \approx 1$ .

the conditional independence relations necessary for the upper bound derivation. Appendix G.2 derives the upper bound  $\delta'$  for  $\delta$ . Appendix G.3 presents the point estimate and 95% confidence interval for  $\delta'$  under various pool sizes and detection thresholds. Appendix G.4 discusses the implications of Theorem 2 for test Consumption in practice.

For succinctness, we abbreviate the probability operator  $\mathbb{P}_{\text{CP},\alpha}(\cdot)$  and the expectation operator  $\mathbb{E}_{\text{CP},\alpha}[\cdot]$  as  $\mathbb{P}(\cdot)$  and  $\mathbb{E}[\cdot]$  in Appendix G.

### G.1. Conditional Independence Relations

We rely on two conditional independence assumptions discussed previously in Section 3 to derive an upper bound  $\delta'$  for  $\delta$ , which we formulate again below.

ASSUMPTION EC.3. *For all  $i = 1, \dots, n$ ,  $W_i$  is independent of  $\{V_j\}_{j \neq i}$  and  $\{W_j\}_{j \neq i}$  given  $V_i$ .*

ASSUMPTION EC.4. *For all  $i = 1, \dots, n$ ,  $V_i$  is independent of  $\{V_j\}_{j \neq i}$  given  $E_i$  where  $E_i = \mathbb{1}\{V_i > 0\}$ .*

Assumptions EC.3 and EC.4 also imply a sequence of conditional independence results, which we use in the derivation of an upper bound for  $\delta$  in Appendix G.2.

First, we show that Assumption EC.3 implies a weaker conditional independence relation, namely  $\{W_i\}_{i=1}^n$  are independent given all  $\{V_i\}_{i=1}^n$ .

LEMMA EC.4.  *$\{W_i\}_{i=1}^n$  are conditionally independent given  $\{V_i\}_{i=1}^n$ .*

*Proof of Lemma EC.4.* Starting from the joint conditional density, we have that

$$\begin{aligned} f(w_{1:n} | v_{1:n}) &= \frac{f(w_{1:n}, v_{2:n} | v_1)}{f(v_{2:n} | v_1)} \\ &= \frac{f(w_1 | v_1) f(w_{2:n}, v_{2:n} | v_1)}{f(v_{2:n} | v_1)} \quad \text{by Assumption EC.3} \\ &= f(w_1 | v_1) f(w_{2:n} | v_{1:n}) \\ &= \dots \quad \text{repeat the above calculations for } n-1 \text{ times} \\ &= \prod_{i=1}^{n-1} f(w_i | v_i) \cdot f(w_n | v_{1:n}) \\ &= \prod_{i=1}^{n-1} f(w_i | v_{1:n}) \cdot f(w_n | v_{1:n}) \quad \text{by Assumption EC.3} \\ &= \prod_{i=1}^n f(w_i | v_{1:n}). \end{aligned}$$

□

Then, we derive a similar conditional independence relation that  $\{V_i\}_{i=1}^n$  are independent given  $\{E_i\}_{i=1}^n$ . To see this, we first note that by the definition of independence, it immediately follows from Assumption EC.4 that given  $E_i$ ,  $V_i$  is also independent of the indicators  $E_j$  where  $j \neq i$ .

LEMMA EC.5. *For all  $i = 1, \dots, n$ ,  $V_i$  is conditionally independent of  $\{E_j\}_{j \neq i}$  given  $E_i$ .*

Lemma EC.5, together with Assumption EC.4, implies that given all indicator variables  $\{E_i\}_{i=1}^n$ ,  $\{V_i\}_{i=1}^n$  are independent.

LEMMA EC.6.  $\{V_i\}_{i=1}^n$  are conditionally independent given  $\{E_i\}_{i=1}^n$ .

*Proof of Lemma EC.6.* The proof technique is the same as that of Lemma EC.4. Starting from the joint conditional density, we have that

$$\begin{aligned}
f(v_{1:n} | e_{1:n}) &= \frac{f(v_{1:n}, e_{2:n} | e_1)}{f(e_{2:n} | e_1)} \\
&= \frac{f(v_1 | e_1) f(v_{2:n}, e_{2:n} | e_1)}{f(e_{2:n} | e_1)} \quad \text{by Assumption EC.4 and Lemma EC.5} \\
&= f(v_1 | e_1) f(v_{2:n} | e_{1:n}) \\
&= \dots \quad \text{repeat the above calculations for } n-1 \text{ times} \\
&= \prod_{i=1}^{n-1} f(v_i | e_i) \cdot f(v_n | e_{1:n}) \\
&= \prod_{i=1}^{n-1} f(v_i | e_{1:n}) \cdot f(v_n | e_{1:n}) \quad \text{by Lemma EC.5} \\
&= \prod_{i=1}^n f(v_i | e_{1:n}).
\end{aligned}$$

Hence, given  $E_{1:n}, V_1, \dots, V_n$  are independent.  $\square$

It follows from Lemmas EC.4 and EC.6 that  $(V_i, W_i), i = 1, \dots, n$  are also conditionally independent, given the indicators  $\{E_i\}_{i=1}^n$ .

LEMMA EC.7.  $\{V_i, W_i\}_{i=1}^n$  are conditionally independent given  $\{E_i\}_{i=1}^n$ .

*Proof of Lemma EC.7.* We consider the joint conditional density of  $(V_i, W_i)_{i=1}^n$  given  $\{E_i\}_{i=1}^n$ :

$$\begin{aligned}
f((v_i, w_i)_{i=1}^n | e_{1:n}) &= f(w_{1:n} | v_{1:n}, e_{1:n}) f(v_{1:n} | e_{1:n}) \\
&= f(w_{1:n} | v_{1:n}) f(v_{1:n} | e_{1:n}) \\
&= \prod_{i=1}^n f(w_i | v_{1:n}) \prod_{i=1}^n f(v_i | e_{1:n}) \quad \text{by Lemma EC.4 and EC.6} \\
&= \prod_{i=1}^n f(w_i | v_i) \prod_{i=1}^n f(v_i | e_i) \quad \text{by Assumptions EC.3 and EC.4} \\
&= \prod_{i=1}^n f(w_i, v_i | e_i) \\
&= \prod_{i=1}^n f(w_i, v_i | e_{1:n}) \quad \text{by Lemma EC.4 and EC.6.}
\end{aligned}$$

We are done.  $\square$

## G.2. Deriving an Upper Bound for $\delta$

Now we are equipped with the tools needed to provide an upper bound for  $\delta$ . Recall that

$$\delta = \frac{\mathbb{P}(Y = 1, S_D = 0 | S > 0)}{\mathbb{P}(Y = 1, S_D > 0 | S > 0)} = \frac{\mathbb{P}(Y = 1 | S_D = 0, S > 0) \mathbb{P}(S_D = 0 | S > 0)}{\mathbb{P}(Y = 1 | S_D > 0) \mathbb{P}(S_D > 0 | S > 0)}. \quad (\text{EC.30})$$

To bound  $\delta$  from above, we provide upper and lower bounds for the terms in the numerator and denominator in Equation EC.30, respectively. We start by proving an upper bound for the second term in the numerator. It also implies that  $\mathbb{P}(S_D > 0 | S > 0) \geq \mathbb{P}(S_D > 0 | S = 1)$  for the second term in the denominator.

PROPOSITION EC.1.  $\mathbb{P}(S_D = 0 \mid S > 0) \leq \mathbb{P}(S_D = 0 \mid S = 1)$ .

*Proof of Proposition EC.1.* We consider  $\mathbb{P}(S_D = 0 \mid S = k)$  for any  $k \in \{1, 2, \dots, n\}$ . Since  $S_D = \sum_{i=1}^n W_i$ , we have that

$$\begin{aligned}
\mathbb{P}(S_D = 0 \mid S = k) &= \mathbb{P}\left(\bigcap_{i=1}^n \{W_i = 0\} \mid S = k\right) \\
&= \mathbb{E}\left[\mathbb{P}\left(\bigcap_{i=1}^n \{W_i = 0\} \mid E_{1:n}, S = k\right) \mid S = k\right] \\
&= \mathbb{E}\left[\prod_{i=1}^n \mathbb{P}(W_i = 0 \mid E_{1:n}) \mid S = k\right] \quad \text{by Lemma EC.7} \\
&= \mathbb{E}\left[\prod_{i=1}^n \mathbb{E}[1 - p(V_i) \mid E_{1:n}] \mid S = k\right] \\
&= \mathbb{E}\left[\prod_{i=1}^n \mathbb{E}[1 - p(V_i) \mid E_i] \mid S = k\right] \quad \text{by Lemma EC.5.} \tag{EC.31}
\end{aligned}$$

Note that for  $i = 1, 2, \dots, n$ , we have

$$\begin{aligned}
\mathbb{E}[1 - p(V_i) \mid E_i] &= \mathbb{P}(W_i = 0 \mid E_i) \\
&= \begin{cases} 1 & E_i = 0 \\ \bar{\beta} & E_i = 1 \end{cases} \\
&= \bar{\beta}^{E_i}. \tag{EC.32}
\end{aligned}$$

where  $\bar{\beta}$  is the *population-average individual test FNR*, i.e.,  $\bar{\beta} = \mathbb{E}[1 - p(V) \mid V > 0]$ .<sup>16</sup>

Recall that  $S = \sum_{i=1}^n \mathbb{1}\{V_i > 0\} = \sum_{i=1}^n E_i$ . Combining Equations EC.31 and EC.32, we find that

$$\begin{aligned}
\mathbb{P}(S_D = 0 \mid S = k) &= \mathbb{E}\left[\prod_{i=1}^n \bar{\beta}^{E_i} \mid S = k\right] \\
&= \mathbb{E}\left[\bar{\beta}^{\sum_{i=1}^n E_i} \mid S = k\right] \\
&= \bar{\beta}^k.
\end{aligned}$$

Since  $\bar{\beta} \in [0, 1]$ , we find  $\mathbb{P}(S_D = 0 \mid S = k) \leq \mathbb{P}(S_D = 0 \mid S = 1)$  for all  $k \in \{1, 2, \dots, n\}$ . By the law of iterated expectations, it follows that  $\mathbb{P}(S_D = 0 \mid S > 0) \leq \mathbb{P}(S_D = 0 \mid S = 1)$ .  $\square$

Second, we provide a lower bound for the first term in the denominator in Equation EC.30. To achieve this, we characterize a first-order stochastic dominance relation, given in Lemmas EC.8.

LEMMA EC.8.  $\mathbb{P}(V_i \geq v \mid W_i = 1) \geq \mathbb{P}(V_i \geq v \mid W_i = 0)$  for all  $i \in \{1, 2, \dots, n\}$ .

*Proof of Lemma EC.8.* Recall that  $W_i = \text{Ber}(p(V_i))$  where  $p(\cdot) : \mathbb{R}_{\geq 0} \rightarrow [0, 1]$  is monotone increasing.

By Bayes rule, we have that

$$\begin{aligned}
\mathbb{P}(V_i \geq v \mid W_i = 1) &= \frac{\mathbb{P}(W_i = 1 \mid V_i \geq v)\mathbb{P}(V_i \geq v)}{\mathbb{P}(W_i = 1)} \\
\mathbb{P}(V_i \geq v \mid W_i = 0) &= \frac{\mathbb{P}(W_i = 0 \mid V_i \geq v)\mathbb{P}(V_i \geq v)}{\mathbb{P}(W_i = 0)} = \frac{(1 - \mathbb{P}(W_i = 1 \mid V_i \geq v))\mathbb{P}(V_i \geq v)}{1 - \mathbb{P}(W_i = 1)}.
\end{aligned}$$

<sup>16</sup> Note that  $\bar{\beta}$  is not to be confused with  $\beta_{\text{POOL}, \alpha}$  ( $\text{POOL} \in \{\text{NP}, \text{CP}\}$ ) introduced in Section 3 which represents the overall FNR of a specific group testing protocol.

Then,

$$\begin{aligned}
& \mathbb{P}(V_i \geq v \mid W_i = 1) \geq \mathbb{P}(V_i \geq v \mid W_i = 0) \\
\iff & \frac{\mathbb{P}(W_i = 1 \mid V_i \geq v)}{\mathbb{P}(W_i = 1)} \geq \frac{1 - \mathbb{P}(W_i = 1 \mid V_i \geq v)}{1 - \mathbb{P}(W_i = 1)} \\
\iff & \mathbb{P}(W_i = 1 \mid V_i \geq v) \geq \mathbb{P}(W_i = 1) \\
\iff & \mathbb{P}(W_i = 1 \mid V_i \geq v)(1 - \mathbb{P}(V_i \geq v)) \geq \mathbb{P}(W_i = 1 \mid V_i < v)(1 - \mathbb{P}(V_i \geq v)).
\end{aligned}$$

If  $\mathbb{P}(V_i \geq v) = 1$ , then the inequality holds; otherwise, by monotonicity of  $p(v)$  we have

$$\mathbb{P}(W_i = 1 \mid V_i \geq v) \geq p(v) \geq \mathbb{P}(W_i = 1 \mid V_i < v).$$

We are done.  $\square$

PROPOSITION EC.2.  $\mathbb{P}(Y = 1 \mid S_D > 0) \geq \mathbb{P}(Y = 1 \mid S_D > 0, S = 1)$ .

*Proof of Proposition EC.2.* We consider  $\mathbb{P}(Y = 1 \mid S_D = k, S = s)$  for any  $0 \leq k \leq s \leq n$  and show that it is increasing in both  $k$  and  $s$ . We have that

$$\begin{aligned}
\mathbb{P}(Y = 1 \mid S_D = k, S = s) &= \mathbb{E}[\mathbb{P}(Y = 1 \mid W_{1:n}, E_{1:n}) \mid S_D = k, S = s] \\
&= \mathbb{E} \left[ \mathbb{E} \left[ p \left( \frac{1}{n} \sum_{i=1}^n V_i \right) \mid W_{1:n}, E_{1:n} \right] \mid S_D = k, S = s \right].
\end{aligned}$$

To derive the inner expectation, we study the joint conditional density of  $V_1, \dots, V_n$  given  $W_{1:n}$  and  $E_{1:n}$ .

We have that

$$\begin{aligned}
f(v_{1:n} \mid w_{1:n}, e_{1:n}) &= \frac{f(v_{1:n}, w_{1:n} \mid e_{1:n})}{f(w_{1:n} \mid e_{1:n})} \\
&= \prod_{i=1}^n \frac{f(v_i, w_i \mid e_{1:n})}{f(w_i \mid e_{1:n})} \quad \text{by Lemma EC.7} \\
&= \prod_{i=1}^n f(v_i \mid w_i, e_{1:n}) \\
&= \prod_{i=1}^n \frac{f(w_i \mid v_i) f(v_i \mid e_{1:n})}{\int f(w_i \mid v_i) f(v_i \mid e_{1:n}) dv_i} \\
&= \prod_{i=1}^n \frac{f(w_i \mid v_i) f(v_i \mid e_i)}{\int f(w_i \mid v_i) f(v_i \mid e_i) dv_i} \quad \text{by Assumption EC.4} \\
&= \prod_{i=1}^n f(v_i \mid w_i, e_i).
\end{aligned}$$

Hence, given  $W_{1:n}$  and  $E_{1:n}$ ,  $\{V_i\}_{i=1}^n$  are independent, with the distribution of  $V_i$  given by  $V_i \mid W_i, E_i$ . Since  $V_1, \dots, V_n$  are identically distributed, we have that  $\{V_i \mid W_i = 1, E_i = 1\}_{i=1}^n$  and  $\{V_i \mid W_i = 0, E_i = 1\}_{i=1}^n$  are also identically distributed, respectively. Denote the distributions for  $V_i \mid W_i = 1, E_i = 1$  and  $V_i \mid W_i = 0, E_i = 1$  by  $F_{V \mid W=1}$  and  $F_{V \mid W=0}$ , respectively. Then,  $\sum_{i=1}^n V_i$  is the sum of  $S_D$  i.i.d random variables with distribution  $F_{V \mid W=1}$  and  $S - S_D$  i.i.d random variables with distribution  $F_{V \mid W=0}$ . That is, the distribution of  $\sum_{i=1}^n V_i$  only depends on  $\{E_i\}_{i=1}^n$  and  $\{W_i\}_{i=1}^n$  through their respective sums,  $S$  and  $S_D$ . Hence, since  $p(v)$  is monotone increasing,  $\mathbb{P}(Y = 1 \mid S_D = k, S = s)$  is increasing in  $s$ . Moreover, since  $F_{V \mid W=1}$  first-order

stochastic dominates  $F_{V|W=0}$  by Lemma EC.8,  $\mathbb{P}(Y = 1 | S_D = k, S = s)$  is also increasing in  $k$ . Therefore, we have

$$\begin{aligned} \mathbb{P}(Y = 1 | S_D > 0) &= \mathbb{E}[\mathbb{P}(Y = 1 | S_D, S) | S_D > 0] \\ &\geq \mathbb{E}[\mathbb{P}(Y = 1 | S_D = 1, S = 1) | S_D > 0] \\ &= \mathbb{P}(Y = 1 | S_D = 1, S = 1). \end{aligned}$$

We are done.  $\square$

PROPOSITION EC.3.  $\mathbb{P}(Y = 1 | S_D = 0, S > 0) \leq \mathbb{P}(Y = 1 | S_D = 0, S = n)$ .

*Proof of Proposition EC.3.* As shown in the proof of Proposition EC.2, we have that  $\mathbb{P}(Y = 1 | S_D = k, S = s)$  is increasing in  $s$ . Hence,

$$\begin{aligned} \mathbb{P}(Y = 1 | S_D = 0, S > 0) &= \mathbb{E}[\mathbb{P}(Y = 1 | S_D, S) | S_D = 0, S > 0] \\ &\leq \mathbb{E}[\mathbb{P}(Y = 1 | S_D, S = n) | S_D = 0, S > 0] \\ &= \mathbb{P}(Y = 1 | S_D = 0, S = n), \end{aligned}$$

which concludes the proof.  $\square$

Combining Propositions EC.1, EC.2 and EC.3, we find that

$$\begin{aligned} \delta' &= \frac{\mathbb{P}(Y = 1 | S_D = 0, S = n)\mathbb{P}(S_D = 0 | S = 1)}{\mathbb{P}(Y = 1 | S_D = S = 1)\mathbb{P}(S_D = 1 | S = 1)} \\ &= \frac{\mathbb{P}(Y = 1 | S_D = 0, S = n)}{\mathbb{P}(Y = 1 | S_D = S = 1)} \cdot \frac{\bar{\beta}}{1 - \bar{\beta}}, \end{aligned} \tag{EC.33}$$

is an upper bound for  $\delta$ .

### G.3. Confidence Interval for $\delta'$

In this section we provide a point estimate and 95% confidence interval for  $\delta'$  under different pool sizes and detection thresholds. We show that  $\delta'$  is consistently small under various conditions. Below we describe the methodology in details.

We use Monte Carlo simulation to estimate  $\mathbb{P}(Y = 1 | S_D = 0, S = n)$  and  $\mathbb{P}(Y = 1 | S_D = S = 1)$  separately. Let  $V_1, \dots, V_n \stackrel{i.i.d.}{\sim} F_{V|W=0}$  where  $F_{V|W=0}$  is the distribution for  $V_i | W_i = 0, E_i = 1$ . Then, as shown in the proof of Proposition EC.2,  $X = \mathbb{P}(Y = 1 | V_{1:n}) = p\left(\frac{1}{n} \sum_{i=1}^n V_i\right)$  is an unbiased estimator for  $\mathbb{P}(Y = 1 | S_D = 0, S = n)$ , i.e.  $\mathbb{P}(Y = 1 | S_D = 0, S = n) = \mathbb{E}[X]$ . To sample from  $F_{V|W=0}$ , we first sample  $V$  from  $V | V > 0$ , the viral load distribution described in Table EC.8, then we sample  $W \sim \text{Ber}(p(V))$ . We keep the sampled  $V$  if the sampled  $W$  is equal to zero and discard  $V$  otherwise. We generate  $B = 10^6$  samples  $X_1, \dots, X_B$  for estimating  $\mathbb{P}(Y = 1 | S_D = 0, S = n)$ .

Similarly, let  $V \sim F_{V|W=1}$  where  $F_{V|W=1}$  is the distribution for  $V_i | W_i = 1, E_i = 1$ . Then,  $Z = \mathbb{P}(Y = 1 | V, 0, \dots, 0) = p(V/n)$  is an unbiased estimator for  $\mathbb{P}(Y = 1 | S_D = S = 1)$ , i.e.  $\mathbb{P}(Y = 1 | S_D = S = 1) = \mathbb{E}[Z]$ . Sampling from  $F_{V|W=1}$  follows a similar procedure as sampling from  $F_{V|W=0}$ . We generate  $B = 10^6$  samples  $Z_1, \dots, Z_B$  for estimating  $\mathbb{P}(Y = 1 | S_D = S = 1)$ .

Hence, the point estimate for  $\delta'$  is given by

$$\hat{\delta}' = \frac{\bar{X}}{\bar{Z}} \cdot \frac{\bar{\beta}}{1 - \bar{\beta}}.$$

To provide a confidence interval for  $\delta'$ , we first find confidence intervals for the  $\mathbb{E}[X]$  and  $\mathbb{E}[Z]$  separately. We derive the confidence interval for  $\mathbb{E}[Z]$  based on central limit theorem. Using normal approximation, the  $q = 99.99\%$  confidence interval for  $\mathbb{E}[Z]$  is given by  $[L_Z, U_Z] = [\bar{Z} - 3.891 \cdot \sigma_{\bar{Z}}, \bar{Z} + 3.891 \cdot \sigma_{\bar{Z}}]$ . On the other hand,  $\mathbb{E}[X]$  is close to zero in the regime we consider, and the samples  $X_i$  can differ by several orders of magnitude. Thus, instead of using the normal approximation, we employ bootstrapping (Efron and Tibshirani 1993) with  $10^4$  replications to construct the  $\frac{95}{q}\%$  confidence interval for  $\mathbb{E}[X]$ , denoted by  $[L_X, U_X]$ .

Because the samples  $X_i$ 's and  $Z_i$ 's are independent, the Cartesian product  $[L_X, U_X] \times [L_Z, U_Z]$  is a  $(\frac{95}{q} \cdot q)\% = 95\%$  confidence interval for  $(\mathbb{E}_{1,\alpha}[X], \mathbb{E}_{1,\alpha}[Z])$ . It follows that  $[\frac{L_X}{U_Z}, \frac{U_X}{L_Z}]$  (assuming that  $0 < L_Z \leq U_Z$  and  $0 \leq L_X \leq U_X$ ) is a 95% confidence interval for  $\delta'$ .

Table EC.15 summarizes the point estimate and 95% confidence interval for  $\delta'$  under different pool sizes and detection thresholds. We see that under all conditions,  $\hat{\delta}'$  is consistently small, with the maximum  $\hat{\delta}'$  achieved at  $n = 2$  and  $\bar{\beta} = 2.5\%$ .

**Table EC.15** Point estimate and 95% confidence interval for  $\delta'$  under different pool sizes  $n$  and population-average individual test FNR  $\bar{\beta}$ .

$n$	$\bar{\beta}$	$\bar{X}$	$\bar{Z}$	$\hat{\delta}'$	95% CI for $\delta'$ (lb)	95% CI for $\delta'$ (ub)
2	0.025	3.35E-02	0.960	8.96E-04	8.90E-04	9.02E-04
2	0.05	1.35E-02	0.946	7.51E-04	7.44E-04	7.59E-04
2	0.1	2.94E-03	0.938	3.48E-04	3.41E-04	3.55E-04
2	0.2	1.73E-04	0.932	4.64E-05	4.26E-05	5.03E-05
4	0.025	1.00E-02	0.903	2.84E-04	2.81E-04	2.86E-04
4	0.05	1.94E-03	0.888	1.15E-04	1.13E-04	1.17E-04
4	0.1	1.06E-04	0.881	1.33E-05	1.25E-05	1.42E-05
4	0.2	6.49E-07	0.853	1.90E-07	3.70E-08	4.34E-07
6	0.025	4.48E-03	0.871	1.32E-04	1.31E-04	1.33E-04
6	0.05	4.82E-04	0.856	2.96E-05	2.89E-05	3.03E-05
6	0.1	7.98E-06	0.846	1.05E-06	8.84E-07	1.23E-06
6	0.2	2.53E-11	0.802	7.89E-12	2.87E-14	2.32E-11
12	0.025	1.12E-03	0.817	3.51E-05	3.47E-05	3.55E-05
12	0.05	3.34E-05	0.801	2.20E-06	2.12E-06	2.28E-06
12	0.1	1.57E-08	0.779	2.24E-09	1.48E-09	3.13E-09
12	0.2	1.73E-26	0.710	6.08E-27	7.34E-35	1.83E-26

#### G.4. Implications of Theorem 2 for Test Consumption in Practice

We show that in this setting, correlated pooling consumes no more followup tests per positive identified than naive pooling for a wide range of pool sizes and PCR test sensitivities (80% – 97.5%).

Using Monte Carlo simulation with  $10^6$  replications, we find that across a wide range of  $\bar{\beta}$  and pool sizes,  $\delta'$  is consistently close to zero (Table EC.15). The maximum value of  $\delta'$  is  $8.96 \times 10^{-5}$  (95% CI:  $(8.90 \times 10^{-4}, 9.02 \times 10^{-5})$ ), obtained when  $n = 2$  and  $\bar{\beta} = 2.5\%$ . As  $n$  increases, the relaxed bound converges to 1.

Now we provide intuition for why  $\delta'$  is small. We first examine a representative curve of PCR test sensitivity versus sample viral load under  $\bar{\beta} = 5\%$ . Based on the viral load distribution among infected individuals given in Table EC.8, when  $\bar{\beta} = 5\%$ , the PCR test sensitivity grows rapidly from 0 to 1 over a narrow range of log viral load in the sample (as shown in Figure EC.3).

Specifically, a  $\log_{10}$  viral load of 3.45 gives a PCR test sensitivity of 0.3%, while a  $\log_{10}$  viral load of 3.65 gives a PCR test sensitivity of 99.8%. The fraction of infected individuals that have  $\log_{10}$  viral load between 3.45 and 3.65 is only 2.8%, indicating that the majority of positive samples either test positive with high probability (if the  $\log_{10}$  viral load is above 3.65) or test positive with low probability (if the  $\log_{10}$  viral load is below 3.45). Though not depicted here, the  $p(v)$  curves corresponding to different  $\bar{\beta}$  follow the same pattern.

Based on the above observations, we argue that correlated pooling's test consumption per positive identified nearly meets or exceeds that of naive pooling in practice. We first observe that  $\mathbb{P}_{1,\alpha}(Y = 1 \mid S_D = 0, S = n)$ , which is in the numerator of  $\delta'$ , is small. If a pool contains only  $n$  positives that would all test negative individually, i.e.,  $S_D = 0$ , then they likely all have viral loads below the narrow region where an individual test's sensitivity rises. Thus, the viral load in the pool, which is the average of the viral loads of these positive samples, is likely also below the narrow region, making it likely to test negative, i.e.,  $Y = 0$ .

On the other hand, we argue that  $\mathbb{P}(Y = 1 \mid S_D = S = 1)$ , which is in the denominator of  $\delta'$ , is reasonably large. In other words, if a pool contains only one positive sample and it would test positive individually, then the pool is likely to test positive. With its viral load drawn from the distribution described in Table EC.8, a positive sample that would test positive individually has its viral load way above the narrow region with a reasonably large probability. Hence, even when such a sample is diluted by a factor equal to the pool size, the pooled sample likely still has its viral load above the narrow region and is likely to test positive, i.e.,  $Y = 1$ .



## References for the Appendices

- Barak N, Ben-Ami R, Sido T, Perri A, Shtoyer A, Rivkin M, Licht T, Peretz A, Magenheim J, Fogel I, et al. (2021) Lessons from applied large-scale pooling of 133,816 SARS-CoV-2 RT-PCR tests. *Science Translational Medicine* 13(589).
- Biswas MHA, Paiva LT, de Pinho MDR, et al. (2014) A SEIR model for control of infectious diseases with constraints. *Mathematical Biosciences and Engineering* 11(4):761–784.
- Brault V, Mallein B, Rupprecht JF (2021) Group testing as a strategy for COVID-19 epidemiological monitoring and community surveillance. *PLoS Computational Biology* 17(3):e1008726.
- Burns M, Valdivia H (2008) Modelling the limit of detection in real-time quantitative PCR. *European Food Research and Technology* 226(6):1513–1524.
- Cleary B, Hay JA, Blumenstiel B, Harden M, Cipicchio M, Bezney J, Simonton B, Hong D, Senghore M, Sesay AK, et al. (2021) Using viral load and epidemic dynamics to optimize pooled testing in resource-constrained settings. *Science Translational Medicine* 13(589).
- Cohen E (2022) Node2Vec. <https://github.com/eliorc/node2vec/tree/master>, Accessed: September 25, 2023.
- Duffin E (2020) Distribution of U.S. households by size 1970-2020. <https://www.statista.com/statistics/242189/distribution-of-households-in-the-us-by-household-size/>, Accessed: May 18, 2021.
- Eberhardt JN, Breuckmann NP, Eberhardt CS (2020) Multi-stage group testing improves efficiency of large-scale covid-19 screening. *Journal of Clinical Virology* 104382.
- Efron B, Tibshirani RJ (1993) *An Introduction to the Bootstrap*. Number 57 in Monographs on Statistics and Applied Probability (Boca Raton, Florida, USA: Chapman & Hall/CRC).
- Fagnan J, Abnar A, Rabbany R, Zaiane OR (2018) Modular networks for validating community detection algorithms. *arXiv preprint arXiv:1801.01229* .
- Fan W (2020) Wuhan tests nine million people for coronavirus in 10 days. <https://www.wsj.com/articles/wuhan-tests-nine-million-people-for-coronavirus-in-10-days-11590408910>, Accessed: May 18, 2021.
- Grover A, Leskovec J (2016) node2vec: Scalable feature learning for networks. *Proceedings of the 22nd ACM SIGKDD international conference on Knowledge discovery and data mining*, 855–864.
- Heid CA, Stevens J, Livak KJ, Williams PM (1996) Real time quantitative PCR. *Genome Research* 6(10):986–994.
- Hu H, Nigmatulina K, Eckhoff P (2013) The scaling of contact rates with population density for the infectious disease models. *Mathematical Biosciences* 244(2):125–134.
- idcommunity (2016) Australia community profile. <https://profile.id.com.au/australia/household-size#:~>, Accessed: May 18, 2021.

- Institut National d'études Démographiques (2017) Households in France. [https://www.ined.fr/en/everything\\_about\\_population/data/france/couples-households-families/households](https://www.ined.fr/en/everything_about_population/data/france/couples-households-families/households), Accessed: May 18, 2021.
- Jones TC, Mühlemann B, Veith T, Biele G, Zuchowski M, Hoffmann J, Stein A, Edelman A, Corman VM, Drosten C (2020) An analysis of SARS-CoV-2 viral load by patient age. *medRxiv* .
- Kermack WO, McKendrick AG (1927) A contribution to the mathematical theory of epidemics. *Proceedings of the Royal Society of London. Series A, Containing papers of a Mathematical and Physical Character* 115(772):700–721.
- Lefkowitz M (2020) Robots, know-how drive COVID lab's massive testing effort. <https://news.cornell.edu/stories/2020/08/robots-know-how-drive-covid-labs-massive-testing-effort>, Accessed: June 23, 2021.
- Madewell ZJ, Yang Y, Longini Jr IM, Halloran ME, Dean NE (2020) Household transmission of SARS-CoV-2: a systematic review and meta-analysis of secondary attack rate. *medRxiv* .
- McGee RS (2021) SEIRS+ Model Framework. <https://github.com/ryansmcgee/seirsplus>, Accessed: June 1, 2023.
- National Bureau of Statistics of China (2018) China statistical yearbook 2018. <http://www.stats.gov.cn/tjsj/ndsj/2018/indexeh.htm>, Accessed: May 18, 2021.
- Public Health Ontario (2020) COVID-19 laboratory testing Q&As. <https://www.publichealthontario.ca/-/media/documents/lab/covid-19-lab-testing-faq.pdf?la=en>, Accessed: July 9, 2021.
- US Food and Drug Administration (2020) SARS-CoV-2 reference panel comparative data. <https://www.fda.gov/medical-devices/coronavirus-covid-19-and-medical-devices/sars-cov-2-reference-panel-comparative-data>, Accessed: May 18, 2021.
- World Health Organization (2020) Modes of transmission of virus causing COVID-19: implications for IPC precaution recommendations: scientific brief, 29 March 2020. Technical report, World Health Organization.